Criticality Analysis of the R. E. Ginna Nuclear Power Plant Fresh and Spent Fuel Racks, and Consolidated Rod Storage Canisters

June, 1994

S. Srinilta
T. P. Phelps
C. S. Erwin
W. D. Newmyer

Verified: _____

M. Corum
Core Design C

Approved: C. R. Savage

C. R. Savage, Manager
Core Design B

Table of Contents

List of Tables

List of Figures

1.0 Introduction

This report presents the results of a criticality analysis of the R. E. Ginna Nuclear Power Plant (Ginna) fresh and spent fuel storage racks, and the consolidated rod canisters in Region 2 spent fuel racks. The fresh and spent designs considered herein are existing arrays of fuel racks, previously qualified for storage of various 14x14 fuel assembly types with maximum enrichments up to 4.25 w/o U^{235}.

The Ginna fresh fuel storage racks are being reanalyzed to allow storage of the Westinghouse 14x14 OFA fuel assembly type with nominal enrichments up to 5.0 w/o U^{235}. The Ginna spent fuel racks are being reanalyzed to allow storage of the Westinghouse 14x14 OFA fuel assembly type and all other 14x14 fuel assembly types currently being stored in the Ginna spent fuel racks. The following storage configurations and enrichment limits are considered in this analysis:

Fresh Fuel Racks	Storage of fresh fuel assemblies with nominal enrichments up to 5.0 w/o U^{235} utilizing all available storage cells.
Spent Fuel Racks Region 1	Storage of fuel assemblies with nominal enrichments up to 4.0 w/o U^{235} utilizing two out of four checkerboard arrangement. Fresh fuel assemblies with higher initial enrichments up to 5.0 w/o U^{235} can also be stored in these racks provided a minimum number of IFBAs are present in each fuel assembly. IFBAs consist of neutron absorbing material applied as a thin ZrB_2 coating on the outside of the UO_2 fuel pellet. As a result, the neutron absorbing material is a non-removable or integral part of the fuel assembly once it is manufactured.
Spent Fuel Racks Region 2	Storage of Westinghouse 14x14 OFA, Westinghouse 14x14 STD and Exxon 14x14 fuel assemblies utilizing all available storage cells. The Westinghouse 14x14 STD fuel assemblies must have an initial enrichment up to 1.85 w/o U^{235} (nominal) or satisfy a minimum burnup requirement. The Westinghouse 14x14 OFA and the Exxon 14x14 fuel assemblies must have an initial enrichment up to 1.95 w/o U^{235} (nominal) or satisfy the minimum burnup requirement. Storage of Region 2 assemblies in Region 1 spent fuel racks is allowed since Region 2 is the enrichment limiting region.
Consolidated Rod Canisters in Spent Fuel Racks	Storage of future consolidated Westinghouse 14x14 STD fuel rods at a nominal enrichment of 1.85 w/o U^{235}, and Westinghouse 14x14 OFA and Exxon 14x14 fuel rods at a nominal enrichment of 1.95 w/o U^{235} in storage canisters in Region 1 and Region 2 are acceptable provided that the number of consolidated rods is not greater than 144 or no less than 256 rods. Enrichments higher than the nominal values are allowed provided that the minimum burnup requirements are satisfied. Storage of existing consolidated rod storage canisters is acceptable in Region 1 and Region 2 spent fuel racks.

The Ginna fresh and spent fuel rack analyses are based on maintaining a $K_{eff} \leq 0.95$ for storage of

14x14 fuel assemblies under full water density conditions and ≤ 0.98 under low water density (optimum moderation) conditions. The optimum moderation condition applies only to the fresh fuel racks since these racks are used to store fuel in a dry environment.

1.1 Design Description

The Ginna fresh fuel rack layout is shown in Figure 1 on page 37. The Ginna fresh fuel rack storage cell design is shown in Figure 2 on page 38. The Ginna spent fuel storage rack layout is depicted in Figure 3 on page 39. The spent fuel rack storage cells for Region 1 and Region 2 are shown in Figure 4 on page 40 and Figure 5 on page 41, respectively, with nominal dimensions provided on each figure. The schematic for consolidated rod storage canister is shown in Figure 6 on page 42.

The fuel parameters relevant to this analysis are given in Table 1 on page 27. The Westinghouse 14x14 OFA fuel is the only fuel type considered for storage in the Ginna fresh fuel racks. For the Ginna spent fuel rack calculations, three different fuel assembly types were considered. They include: Westinghouse 14x14 OFA assembly, Westinghouse 14x14 STD or HIPAR, and Exxon 14x14. Of the three types, the Westinghouse 14x14 OFA at a nominal enrichment of 4.0 w/o U^{235} is the most reactive fuel type for storage in spent fuel rack Region 1, and the Westinghouse 14x14 STD at a nominal enrichment of 1.85 w/o U^{235} is the most reactive fuel type for storage in spent fuel rack Region 2. Since only Westinghouse 14x14 OFA fresh fuel is currently used at Ginna, the Region 1 and Region 2 spent fuel rack calculations will use the Westinghouse 14x14 OFA fuel type as the base case. For Region 2 spent fuel racks, a burnup credit curve will be generated to cover the more reactive Westinghouse 14x14 STD fuel and other fuel types currently stored in Ginna Region 2 spent fuel racks.

1.2 Design Criteria

Criticality of fuel assemblies in a fuel storage rack is prevented by the design of the rack which limits fuel assembly interaction. This is done by fixing the minimum separation between fuel assemblies and inserting neutron poison between them.

The design basis for preventing criticality outside the reactor is that, including uncertainties, there is a 95 percent probability at a 95 percent confidence level that the effective neutron multiplication factor, K_{eff}, of the fuel assembly array will be less than 0.95 as recommended by ANSI 57.2-1983, ANSI 57.3-1983 and NRC guidance[1], and less than 0.98 under low water density (optimum moderation) conditions as recommended by NUREG-0800. The optimum moderation condition applies only to the fresh fuel racks since these racks are used to store fuel in a dry environment.

2.0 Analytical Methods

2.1. Criticality Calculation Methodology

The criticality calculation method and cross-section values are verified by comparison with critical experiment data for fuel assemblies similar to those for which the racks are designed. This benchmarking data is sufficiently diverse to establish that the method bias and uncertainty will apply to rack conditions which include strong neutron absorbers, large water gaps and low moderator densities.

The design method which insures the criticality safety of fuel assemblies in the fuel storage rack uses the AMPX[2,3] system of codes for cross-section generation and KENO Va[4] for reactivity determination.

The 227 energy group cross-section library that is the common starting point for all cross-sections used for the benchmarks of KENO Va and the KENO Va storage rack calculations is generated from ENDF/B-V[2] data. The NITAWL[3] program includes, in this library, the self-shielded resonance cross-sections that are appropriate for each particular geometry. The Nordheim Integral Treatment is used. Energy and spatial weighting of cross-sections is performed by the XSDRNPM[3]program which is a one-dimensional S_n transport theory code. These multigroup cross-section sets are then used as input to KENO Va[4] which is a three dimensional Monte Carlo theory program designed for reactivity calculations.

A set of 44 critical experiments[5,6,7,8,9] has been analyzed using the above method to demonstrate its applicability to criticality analysis and to establish the method bias and uncertainty. The benchmark experiments cover a wide range of geometries, materials, and enrichments, ranging from relatively low enriched (2.35, 2.46, and 4.31 w/o), water moderated, oxide fuel arrays separated by various materials (B_4C, aluminum, steel, water, etc.) that simulate LWR fuel shipping and storage conditions to dry, harder spectrum, uranium metal cylinder arrays at high enrichments (93.2 w/o) with various interspersed materials (Plexiglass and air). Comparison with these experiments demonstrates the wide range of applicability of the method. Table 2 on page 28 summarizes these experiments.

The highly enriched benchmarks show that the criticality code sequence can correctly predict the reactivity of a hard spectrum environment, such as the optimum moderation condition often considered in fresh rack and shipping cask analyses. However, the results of the 12 highly enriched benchmarks are not incorporated into the criticality method bias because the enrichments are well above any encountered in commercial nuclear power applications. Basing the method bias solely on the 32 low enriched benchmarks results in a more appropriate and more conservative bias.

The 32 low enriched, water moderated experiments result in an average KENO Va K_{eff} of 0.9930. Comparison with the average measured experimental K_{eff} of 1.0007 results in a method bias of 0.0077. The standard deviation of the bias value is 0.0014 ΔK. The 95/95 one-sided tolerance limit factor for 32 values is 2.20. Thus, there is a 95 percent probability with a 95 percent confidence level that the uncertainty in reactivity, due to the method, is not greater than 0.0030

ΔK. This KENO Va bias and uncertainty are consistent with the previous Westinghouse bias and uncertainty calculated for KENO IV[10].

Material and construction tolerance reactivity effects and reactivity sensitivities are determined using the transport theory computer code, PHOENIX[11]. PHOENIX is a depletable, two-dimensional, multigroup, discrete ordinates, transport theory code which utilizes a 42 energy group nuclear data library.

The agreement between reactivities computed with PHOENIX and the results of 81 critical benchmark experiments is summarized in Table 3 on page 29. Key parameters describing each of the 81 experiments are given in Table 4 on pages 30 & 31. These reactivity comparisons again show good agreement between experiment and PHOENIX calculations.

2.2 Reactivity Equivalencing for Burnup and IFBA Credit

Storage of spent fuel assemblies with initial enrichments higher than that allowed by the methodology described in Section 2.1 is achievable by means of the concept of reactivity equivalencing. Reactivity equivalencing is predicated upon the reactivity decrease associated with fuel depletion or the addition of IFBA fuel rods. A series of reactivity calculations is performed to generate a set of enrichment-burnup or enrichment-IFBA ordered pairs which all yield an equivalent K_{eff} when the fuel is stored in the Ginna spent fuel racks. The data points on the reactivity equivalence curve are generated with the transport theory computer code, PHOENIX.

A study was done to examine fuel reactivity as a function of time following reactor shutdown. Fission product decay was accounted for using CINDER[12]. CINDER is a point-depletion computer code used to determine fission product activities. The fission products were permitted to decay for 30 years after shutdown. The fuel reactivity was found to reach a maximum at approximately 100 hours after shutdown. At this time, the major fission product poison, Xe^{135}, has nearly completely decayed away. Furthermore, the fuel reactivity was found to decrease continuously from 100 hours to 30 years following shutdown. Therefore, the most reactive time for a fuel assembly after shutdown of the reactor can be conservatively approximated by removing the Xe^{135}.

The PHOENIX code has been validated by comparisons with experiments where the isotopic fuel composition has been examined following reactor shutdown. In addition, an extensive set of benchmark critical experiments has been analyzed with PHOENIX. Comparisons between measured and predicted uranium and plutonium isotopic fuel compositions are shown in Table 5 on page 32. The measurements were made on fuel discharged from Yankee Core 5[13]. The data in Table 5 on page 32 shows that the agreement between PHOENIX predictions and measured isotopic compositions is good.

Uncertainties associated with the burnup and IFBA dependent reactivities computed with PHOENIX are accounted for in the development of the individual reactivity equivalence limits. For burnup credit, an uncertainty is applied to the PHOENIX calculational results which starts at zero for zero burnup and increases linearly with burnup, passing through 0.01 ΔK at 30,000 MWD/MTU. This bias is considered to be very conservative and is based on consideration of the good agreement between PHOENIX predictions and measurements and on conservative estimates

of fuel assembly reactivity variances with depletion history. For IFBA credit applications, an uncertainty of approximately 10% of the total number of IFBA rods is accounted for in the development of the IFBA requirements. Additional information concerning the specific uncertainties included in each of the Ginna burnup credit and IFBA credit limits is provided in the individual sections of this report.

2.3 Boraflex Shrinkage And Gap Methodology

As a result of blackness testing measurements performed at other storage rack facilities, the presence of shrinkage and gaps in some of the Boraflex absorber panels has been noted. The effects of Boraflex shrinkage and gaps will be considered in the Region 2 spent fuel rack criticality evaluations performed for this report.

Previous generic studies of Boraflex shrinkage and reactivity effects have been performed[14] for storage rack geometries which resemble the Ginna Region 2 spent fuel racks. The results of these studies (and experience gained in performing similar studies for other rack geometries) indicate that:

- When absorber panel shrinkage occurs evenly and uniformly (equal pull-back is experienced at both ends and the panel remains axially centered and intact), meaningful increases in rack reactivity will not occur until more than 7.0 inches of total active fuel length is exposed (3.5 inches on each end). Assuming a conservative 4% shrinkage scenario, combined top and bottom fuel exposure will reach 3.16 inches given the initial Ginna Boraflex panel length of 144 inches. For this level of uniform top and bottom exposure, generic study[14] data indicates that reactivity will not increase.
- When absorber panel shrinkage occurs all at one end, experience has shown that the reactivity impact will remain approximately constant even when an identical length of exposure is added to the opposite end. For the one-end scenario, generic data indicates that reactivity will not increase by more than 0.02 delta-k when 4% uniform, one-end shrinkage is assumed in the Ginna racks.
- When absorber panel shrinkage is assumed to result in the formation of a single large gap in every panel, and all panel gaps are conservatively positioned at the vertical centerline of the active fuel, generic study data indicates that reactivity will increase dramatically once a gap size of 1 inch has been exceeded. For an assumed 4% shrinkage at Ginna, the data indicates that reactivity will increase by more than 0.06 delta-k if all shrinkage is modeled as a single, large (5.76 inch) gap at the centerline.

These generic study results indicate that Boraflex shrinkage and gap formation will result in extremely large reactivity impacts for the conservative scenarios of single-end exposure and mid-plane gap development. Accommodating this level of impact in the Ginna rack limits would cause an unreasonable and unacceptable loss of enrichment storage capability. Therefore, a conservative, but more realistic treatment of shrinkage and gap formation will be considered in this criticality evaluation.

To conservatively bound the current and future development of shrinkage and gaps, the following assumptions will be employed in the criticality evaluations performed for each of the Ginna

storage regions which utilize Boraflex absorbers:

1. All absorber panels will be modeled with 4% width shrinkage.
2. All absorber panels will modeled with 4% length shrinkage (5.76 inches) which will be assumed to occur either uniformly (where the panel remains intact over its entire length) or non-uniformly (where a conservative, single 4 inch gap develops somewhere along the panel length).
3. For those panels which are modeled with a gap, the remainder of the 4% length shrinkage not accounted for by the single 4 inch gap will be conservatively applied as bottom end shrinkage.
4. Gaps will be distributed randomly with respect to axial position for the absorber panels which are modeled with gaps.
5. Shrinkage will be conservatively applied to the bottom end for those absorber panels which are modeled with uniform shrinkage (the bottom end results in more active fuel exposure than the top end). Applying all shrinkage to the bottom is very conservative since it ignores the realistic possibilities of uniform top/bottom shrinkage or random distribution of top or bottom shrinkage among the many absorber panels.
6. Determination of which panels experience shrinkage and which experience gaps will be based on random selection. Several scenarios will be considered to cover the complete spectrum of shrinkage and gap combinations:
   - 100% of the panels experience non-uniform shrinkage (random gaps).
   - 75% of the panels experience non-uniform shrinkage (random gaps) and the remaining 25% of panels experience uniform shrinkage (pull-back) from the bottom-end.
   - 50% of the panels experience non-uniform shrinkage (random gaps) and the remaining 50% of panels experience uniform shrinkage (pull-back) from the bottom-end.
   - 25% of the panels experience non-uniform shrinkage (random gaps) and the remaining 75% of panels experience uniform shrinkage (pull-back) from the bottom-end.
   - 100% of the panels experience uniform shrinkage (pull-back) from the bottom-end.
7. A criticality model which simulates 16 storage cells and 32 individual absorber panels will be employed to provide sufficient problem size and flexibility for considering gaps and shrinkage on a random basis.
8. All absorber material which is lost to shrinkage or gaps will be conservatively removed from the model. In reality, the absorber material is not lost -- it is simply repositioned by shrinkage to the remaining intact areas of the panel.

The above assumptions are conservative and bounding with respect to the upper bound values for shrinkage and gaps recommended by EPRI.

3.0 Criticality Analysis of Fresh Fuel Racks

This section describes the analytical techniques and models employed to perform the criticality analysis for the storage of fresh fuel in the Ginna fresh fuel storage racks.

Since the fresh fuel racks are normally maintained in a dry condition, the criticality analysis will show that the rack K_{eff} is less than 0.95 for the accidental full water density flooding scenario and less than 0.98 for the accidental low water density (optimum moderation) flooding scenario. The criticality methodology employed in this analysis is discussed in Section 2 of this report.

The following assumptions were used to develop the KENO model for the storage of fresh fuel in the Ginna Fresh Fuel Storage Rack under full density and low density optimum moderation conditions:

1. The fuel assembly parameters relevant to the criticality analysis are based on the Westinghouse 14x14 OFA design (see Table 1 on page 27 for fuel parameters).
2. All fuel rods contain uranium dioxide at a maximum enrichment of 5.05 w/o (both full density flood and optimum moderation flood) over the entire length of each rod.
3. The fuel pellets under full density and optimum moderation density water flooded conditions are modeled assuming values of 96% theoretical density and no dishing fraction.
4. No credit is taken for any natural or reduced enrichment axial blankets.
5. No credit is taken for any U^{234} or U^{236} in the fuel.
6. No credit is taken for any spacer grids or spacer sleeves.
7. No credit is taken for any burnable absorber in the fuel rods for the KENO models.
8. No credit is taken for PVC corners which are present to guide the fuel assembly into the storage cell. The presence of PVC lowers rack reactivity by reducing neutron reflection and increasing neutron absorption.
9. For both the full density and optimum moderation cases, there is no boron in the water.
10. Fuel rods are modeled with a fuel stack height which is infinitely long for the full density moderation scenario and 141.4 inches long for the optimum moderation scenario.

3.1 Full Density Moderation Analysis

In the KENO model for the full density moderation analysis, the moderator is pure water at a temperature of 68°F. A conservative value of 1.0 gm/cm^3 is used for the density of water. The fuel array is infinite in lateral (x and y) and axial (vertical) extent which precludes any neutron leakage from the array.

The fuel assembly parameters assumed in the full density analysis are based on the Westinghouse 14x14 OFA design (see Table 1 on page 27). Under fully flooded conditions and at the enrichment level considered in this evaluation, the OFA is the most reactive fuel type in use at Ginna.

The maximum K_{eff} under normal conditions arises from consideration of mechanical and material

thickness tolerances resulting from the manufacturing process in addition to asymmetric positioning of fuel assemblies within the storage cells. Studies of asymmetric positioning of fuel assemblies within the storage cells have shown that symmetrically placed fuel assemblies yield conservative results in rack K_{eff}. Due to the relatively large cell spacing, the small tolerance on the cell center-to-center spacing is not considered since it will have an insignificant effect on the fuel rack reactivity. However, the stainless steel cell wall thickness is reduced to its minimum tolerance. The most conservative, or "worst case", KENO model of the fresh fuel storage racks assumes minimum steel thickness with symmetrically placed 14x14 OFA assemblies. Furthermore, the fuel enrichment is assumed to be a maximum of 5.05 w/o U^{235} to conservatively account for enrichment reliability.

The KENO calculation for the worst case resulted in a K_{eff} of 0.9018 with a 95 percent probability/95 percent confidence level uncertainty of 0.0041 ΔK.

Based on the analysis described above, the following equation is used to develop the maximum K_{eff} for Ginna fresh fuel storage racks:

$$K_{eff} = K_{worst} + B_{method} + \sqrt{ks_{worst}^2 + ks_{method}^2}$$

where:

K_{worst}	=	maximum KENO K_{eff} that includes material, mechanical and enrichment tolerances
B_{method}	=	method bias determined from benchmark critical comparisons
ks_{worst}	=	95/95 uncertainty in the worst case KENO K_{eff}
ks_{method}	=	95/95 uncertainty in the method bias

Substituting calculated values in the order listed above, the result is:

$$K_{eff} = (0.9018) + (0.0077) + \sqrt{0.0041^2 + 0.0030^2} = 0.9146$$

Since K_{eff} is less than 0.95 including uncertainties at a 95/95 probability/confidence level, the acceptance criteria for criticality is met for the Ginna fresh fuel storage rack under full density water flooding conditions for storage of Westinghouse 14x14 OFA fuel assemblies with nominal enrichments up to 5.0 w/o U^{235}.

3.2 Low Density Optimum Moderation Analysis

For the low density optimum moderation analysis, the fuel array is finite in all directions. "Worst case" assumptions on UO_2 material properties are used in modeling the entire fresh fuel rack array. All available fresh fuel storage cells are utilized as depicted in Figure 1 on page 37. Fuel rods are modeled with a nominal active fuel length of 141.4 inches. Concrete walls and floor are

modeled. Under low water density conditions, the presence of concrete is conservative because neutrons are reflected back into the fuel array more efficiently than they would be with just low density water. The area above the fresh fuel racks is filled with water at the optimum moderation density.

Analysis of the Ginna fresh fuel racks shows that the maximum rack K_{eff} under low density moderation conditions occurs at 0.06 gm/cm^3 water density. The K_{eff} of the fresh rack at 0.06 gm/cm^3 water density is 0.6535 with a 95 percent probability and 95 percent confidence level uncertainty of ±0.0045 ΔK. Figure 7 on page 43 shows the fresh fuel rack reactivity as a function of water density in the range where the optimum moderation peak occurs. Over the remainder of the density range between 0.10 gm/cm^3 and 1.00 gm/cm^3 (fully flooded), the rack reactivity will be less than the values calculated for the optimum moderation peak and for the full density condition.

The following equation is used to develop the maximum K_{eff} for the Ginna fresh fuel storage racks under low water density optimum moderation conditions:

$$K_{eff} = K_{optimum} + B_{method} + \sqrt{ks_{optimum}^2 + ks_{method}^2}$$

where:

$K_{optimum}$ = maximum KENO K_{eff} with low density optimum moderation

B_{method} = method bias determined from benchmark critical comparisons

$ks_{optimum}$ = 95/95 uncertainty in the low density optimum moderation KENO K_{eff}

ks_{method} = 95/95 uncertainty in the method bias

Substituting calculated values in the order listed above, the result is:

$$K_{eff} = (0.6535) + (0.0077) + \sqrt{0.0045^2 + 0.0030^2} = 0.6666$$

Since K_{eff} is less than 0.98 including uncertainties at a 95/95 probability/confidence level, the acceptance criteria for criticality is met.

4.0 Criticality Analysis of Region 1 Spent Fuel Racks

This section describes the analytical techniques and models employed to perform the criticality analysis and reactivity equivalencing evaluations for the Ginna Region 1 spent fuel storage racks.

Section 4.1 describes the reactivity calculations performed for Region 1 with the nominal enrichment up to 4.0 w/o U^{235}. Section 4.2 describes the analysis which allows for storage of assemblies with nominal enrichments above 4.0 w/o U^{235} and up to 5.0 w/o U^{235} by taking credit for Integral Fuel Burnable Absorbers (IFBAs). Section 4.3 presents the results of calculations performed to show the reactivity sensitivity of variations in enrichment, center-to-center spacing, and wall thickness.

4.1 Reactivity Calculations

To show that storage of burned and fresh 14x14 fuel assemblies in the Region 1 spent fuel racks satisfies the 0.95 K_{eff} criticality acceptance criteria, KENO is used to establish a nominal reference reactivity and PHOENIX is used to assess the effects of material and construction tolerance variations. The nominal temperature range of 50°F to 180°F is considered in the analysis. A final 95/95 K_{eff} is developed by statistically combining the individual tolerance impacts with the calculational and methodology uncertainties and summing this term with the nominal KENO reference reactivity.

The following assumptions are used to develop the nominal case KENO model for storage of fuel assemblies in the Ginna Region 1 spent fuel rack:

1. The fuel assembly parameters relevant to the criticality analysis are based on the Westinghouse 14x14 OFA design (see Table 1 on page 27 for fuel parameters).
2. All fuel assemblies contain uranium dioxide at a nominal enrichment of 4.0 w/o over the entire length of each rod.
3. The fuel pellets are modeled assuming nominal values for theoretical density and dishing fraction.
4. No credit is taken for any natural or reduced enrichment axial blankets.
5. No credit is taken for any U^{234} or U^{236} in the fuel, nor is any credit taken for the buildup of fission product poison material.
6. No credit is taken for any spacer grids or spacer sleeves.
7. No credit is taken for any burnable absorber in the fuel rods.
8. The moderator is pure water (no boron) at a temperature of 68°F. A limiting value of 1.0 gm/cm^3 is used for the density of water to conservatively bound the range of normal (50°F to 180°F) spent fuel pool water temperatures.
9. The array is infinite in lateral (x and y) extent and infinite in axial (vertical) extent.
10. The assemblies are arranged in the two out of four checkerboard pattern as depicted in Figure 4 on page 40.

With the above assumptions, the KENO calculation for the nominal case results in a K_{eff} of 0.9271 with a 95 percent probability/95 percent confidence level uncertainty of ±0.0041 ΔK. This K_{eff} will be used as the reference reactivity for the Region 1 storage configuration.

Calculational and methodology biases must be considered in the final K_{eff} summation prior to comparing against the 0.95 K_{eff} limit. The following biases are included:

Methodology: As discussed in Section 2 of this report, benchmarking of the Westinghouse KENO Va methodology resulted in a method bias of 0.0077 ΔK.

Water Temperature: To account for the effect of the normal range of spent fuel pool water temperatures (50°F to 180°F) on water cross section properties, a reactivity bias of 0.0073 ΔK is applied. The reactivity effect of spent fuel pool water temperature on water density was considered in assumption 8 above.

To evaluate the reactivity effects of possible variations in material characteristics and mechanical/ construction dimensions, PHOENIX perturbation calculations are performed. For the Ginna Region 1 spent fuel rack configuration, UO_2 material tolerances are considered along with construction tolerances related to the cell I.D., cell pitch, and stainless steel thickness. Uncertainties associated with calculation and methodology accuracy are also considered in the statistical summation of uncertainty components.

The following tolerance and uncertainty components are considered in the total uncertainty statistical summation:

U^{235} Enrichment: The standard DOE enrichment tolerance of ±0.05 w/o U^{235} about the nominal 4.0 w/o U^{235} reference enrichment was evaluated with PHOENIX and resulted in a reactivity increase of 0.0024 ΔK.

UO_2 Density: A ±2.0% variation about the nominal 95% reference theoretical density was evaluated with PHOENIX and resulted in a reactivity increase of 0.0027 ΔK.

Fuel Pellet Dishing: A variation in fuel pellet dishing fraction from 0.0% to 2.0% (about the nominal 1.1926% reference value) was evaluated with PHOENIX and resulted in a reactivity increase of 0.0015 ΔK.

Storage Cell I.D., Storage Cell Pitch, and Stainless Steel Thickness: The +0.06 inch tolerance about the nominal 8.25 inch reference cell I.D., the +0.06 inch tolerance about the nominal 8.43 inch reference storage cell pitch, and the ±0.004 inch tolerance about the nominal 0.09 inch reference stainless steel thickness for all rack structures was evaluated with PHOENIX and resulted in a reactivity increase of 0.0017 ΔK.

Assembly Position: The KENO reference reactivity calculation assumes fuel assemblies are symmetrically positioned within the storage cells since experience has shown that centered fuel assemblies yield equal or more conservative results in rack K_{eff} than non-centered (asymmetric) positioning. Therefore, no reactivity uncertainty needs to be applied for this tolerance since the most reactive configuration is considered in the calculation of the reference K_{eff}.

Calculation Uncertainty: The KENO calculation for the nominal reference reactivity resulted in a K_{eff} with a 95 percent probability/95 percent confidence level uncertainty of ±0.0041 ΔK.

Methodology Uncertainty: As discussed in Section 2 of this report, comparison against benchmark experiments showed that the 95 percent probability/95 percent confidence uncertainty in reactivity, due to method, is not greater than 0.0030 ΔK.

The maximum K_{eff} for the Ginna alternating rows storage configuration is developed by adding the calculational and methodology biases and the statistical sum of independent uncertainties to the nominal KENO reference reactivity. The summation is shown in Table 6 on page 33 and results in a maximum K_{eff} of 0.9487.

Since K_{eff} is less than 0.95 including uncertainties at a 95/95 probability/confidence level, the acceptance criteria for criticality is met for storage of 14x14 fuel assemblies with nominal enrichment up to 4.0 w/o U^{235} in the Ginna Region 1 spent fuel racks.

4.2 IFBA Credit Reactivity Equivalencing

Storage of fuel assemblies with nominal enrichments greater than 4.0 w/o U^{235} in the Region 1 spent fuel storage racks is achievable by means of the concept of reactivity equivalencing. The concept of reactivity equivalencing is predicated upon the reactivity decrease associated with the addition of Integral Fuel Burnable Absorbers (IFBA)[15]. IFBAs consist of neutron absorbing material applied as a thin ZrB_2 coating on the outside of the UO_2 fuel pellet. As a result, the neutron absorbing material is a non-removable or integral part of the fuel assembly once it is manufactured.

Two analytical techniques are used to establish the criticality criteria for the storage of IFBA fuel in the fuel storage rack. The first method uses reactivity equivalencing to establish the poison material loading required to meet the criticality limits. The poison material considered in this analysis is a zirconium diboride (ZrB_2) coating manufactured by Westinghouse. The second method uses the fuel assembly infinite multiplication factor to establish a reference reactivity. The reference reactivity point is compared to the fuel assembly peak reactivity to determine its acceptability for storage in the fuel racks.

4.2.1 IFBA Requirement Determination

A series of reactivity calculations are performed to generate a set of IFBA rod number versus enrichment ordered pairs which all yield the equivalent K_{eff} when the fuel is stored in the Region 1 spent fuel racks. The following assumptions were used for the IFBA rod assemblies in the PHOENIX models:

1. The fuel assembly parameters relevant to the criticality analysis are based on the Westinghouse 14x14 OFA. design (see Table 1 on page 27 for fuel parameters).
2. The fuel assembly is modeled at its most reactive point in life.
3. The fuel pellets are modeled assuming nominal values for theoretical density and dishing fraction.
4. No credit is taken for any natural enrichment or reduced enrichment axial blankets.
5. No credit is taken for any U^{234} or U^{236} in the fuel.

6. No credit is taken for any spacer grids or spacer sleeves.
7. The IFBA absorber material is a zirconium diboride (ZrB_2) coating on the fuel pellet. Each IFBA rod has a nominal poison material loading of 1.67 milligrams B^{10} per inch, which is the minimum standard loading offered by Westinghouse for 14x14 OFA fuel assemblies.
8. The IFBA B^{10} loading is reduced by 5 percent to conservatively account for manufacturing tolerances and then by an additional 10% to conservatively model a minimum poison length of 92 inches.
9. The moderator is pure water (no boron) at a temperature of 68°F with a density of 1.0 gm/cm^3.
10. The array is infinite in lateral (x and y) and axial (vertical) extent. This precludes any neutron leakage from the array.

Figure 8 on page 44 shows the constant K_{eff} contour generated for the Region 1 spent fuel racks. Note the endpoint at 0 IFBA rods where the nominal enrichment is 4.0 w/o and at 64(1X) IFBA rods where the nominal enrichment is 5.0 w/o. The interpretation of the endpoint data is as follows: the reactivity of the fuel rack array when filled with fuel assemblies enriched to a nominal 5.0 w/o U^{235} with each containing 64(1.0X) IFBA rods is equivalent to the reactivity of the rack when filled with fuel assemblies enriched to a nominal 4.0 w/o and containing no IFBAs. The data in Figure 8 on page 44 is also provided on Table 7 on page 34 for the 1.0X , 1.5X and 2.0X IFBA rods.

It is important to recognize that the curve in Figure 8 on page 44 is based on reactivity equivalence calculations for the specific enrichment and IFBA combinations in actual rack geometry (and not just on simple comparisons of individual fuel assembly infinite multiplication factors). In this way, the environment of the storage rack and its influence on assembly reactivity is implicitly considered.

The IFBA requirements of Figure 8 on page 44 were developed based on the standard IFBA patterns used by Westinghouse. However, since the worth of individual IFBA rods can change depending on position within the assembly (due to local variations in thermal flux), studies were performed to evaluate this effect and a conservative reactivity margin was included in the development of the IFBA requirement to account for this effect. This assures that the IFBA requirement remains valid at intermediate enrichments where standard IFBA patterns may not be available. In addition, to conservatively account for calculational uncertainties, the IFBA requirements of Figure 8 on page 44 also include a conservatism of approximately 10% on the total number of IFBA rods at the 5.0 w/o end (i.e., about 6 extra IFBA rods for a 5.0 w/o fuel assembly).

Additional IFBA credit calculations were performed to examine the reactivity effects of higher IFBA linear B^{10} loadings (1.5X and 2.0X). These calculations confirm that assembly reactivity remains constant provided the net B^{10} material per assembly is preserved. Therefore, with higher IFBA B^{10} loadings, the required number of IFBA rods per assembly can be reduced by the ratio of the higher loading to the nominal 1.0X loading. For example, using 2.0X IFBA in 5.0 w/o fuel assemblies allows a reduction in the IFBA rod requirement from 64 IFBA rods per assembly to 32 IFBA rods per assembly (64 divided by the ratio 2.0X/1.0X).

4.2.2 Infinite Multiplication Factor

The infinite multiplication factor, K_∞, is used as a reference criticality reactivity point, and offers an alternative method for determining the acceptability of fuel assembly storage in the Region 1 spent fuel racks. The reference K_∞ is determined for a nominal fresh 4.0 w/o fuel assembly.

The fuel assembly K_∞ calculations are performed using the Westinghouse licensed core design code PHOENIX-P[11]. The following assumptions were used to develop the infinite multiplication factor model:

1. The Westinghouse 14x14 OFA fuel assembly was analyzed (see Table 1 on page 27 for fuel parameters). The fuel assembly is modeled at its most reactive point in life and no credit is taken for any discrete burnable absorbers in the assembly.
2. All fuel rods contain uranium dioxide at a nominal enrichment of 4.0 w/o U^{235} over the entire length of each rod.
3. The fuel array model is based on a unit assembly configuration (infinite in the lateral and axial extent) in Ginna reactor geometry (no rack).
4. The moderator is pure water (no boron) at a temperature of 68° F with a density of 1.0 gm/ cm^3.

Calculation of the infinite multiplication factor for the Westinghouse 14x14 OFA fuel assembly in the Ginna core geometry resulted in a reference K_∞ of 1.458. This includes a 1% ΔK reactivity bias to conservatively account for calculational uncertainties. This bias is consistent with the standard conservatism included in the Ginna core design refueling shutdown margin calculations.

For IFBA credit, all 14x14 fuel assemblies placed in the Region 1 spent fuel racks must comply with the enrichment-IFBA requirements of Figure 8 on page 44 or have a reference K_∞ less than or equal to 1.458. By meeting either of these conditions, the maximum rack reactivity will then be less than 0.95, as shown in Section 4.1.

4.3 Sensitivity Analysis and Soluble Boron Worth

To show the dependence of K_{eff} on fuel and storage cells parameters as requested by the NRC[1], the variation of the K_{eff} with respect to the following parameters was developed using the PHOENIX computer code:

1. Fuel enrichment, with a 0.50 w/o U^{235} delta about the nominal case enrichment.
2. Center-to-center spacing of storage cells, with a 0.40 inch delta about the nominal case center-to-center spacing.
3. Wall thickness of storage cells, with a 0.04 inch delta about the nominal case wall thickness.

Results of the sensitivity analysis are shown in Figure 9 on page 45.

PHOENIX calculations were also performed to evaluate the reactivity benefits of soluble boron for the Region 1 spent fuel storage configuration. Results of these calculations are provided in Figure 10 on page 46. As the curve shows, the presence of soluble boron in the Ginna spent fuel pool provides substantial reactivity margin.

5.0 Criticality Analysis of Region 2 Spent Fuel Racks

This section describes the analytical techniques and models employed to perform the criticality analysis and reactivity equivalencing evaluations for the Ginna Region 2 spent fuel storage racks.

Section 5.1 describes the reactivity calculations performed for Region 2 with Westinghouse 14x14 OFA assemblies at nominal enrichments up to 1.95 w/o U^{235}. Section 5.2 describes the analysis which allows for storage of Westinghouse 14x14 OFA and Exxon 14x14 assemblies with nominal enrichments above 1.95 w/o and up to 5.0 w/o U^{235} and Westinghouse 14x14 STD assemblies with nominal enrichments above 1.85 and up to 5.0 w/o U^{235} with minimum burnup requirements. Section 5.3 presents the results of calculations performed to show the reactivity sensitivity of variations in enrichment, center-to-center spacing, and Boraflex loading.

5.1 Reactivity Calculations

To show that storage of burned and fresh Westingouse 14x14 OFA fuel assemblies in the Region 2 spent fuel racks satisfies the 0.95 K_{eff} criticality acceptance criteria, KENO is used to establish a nominal reference reactivity and PHOENIX is used to assess the effects of material and construction tolerance variations. The nominal temperature range of 50°F to 180°F is considered in the analysis. A final 95/95 K_{eff} is developed by statistically combining the individual tolerance impacts with the calculational and methodology uncertainties and summing this term with the nominal KENO reference reactivity.

The following assumptions are used to develop the nominal case KENO model for storage of fuel assemblies in the Ginna Region 2 spent fuel rack:

1. The fuel assembly parameters relevant to the criticality analysis are based on the Westinghouse 14x14 OFA design (see Table 1 on page 27 for fuel parameters).
2. All fuel assemblies contain uranium dioxide at a nominal enrichment of 1.95 w/o over the entire length of each rod.
3. The fuel pellets are modeled assuming nominal values for theoretical density and dishing fraction.
4. No credit is taken for any natural or reduced enrichment axial blankets.
5. No credit is taken for any U^{234} or U^{236} in the fuel, nor is any credit taken for the buildup of fission product poison material.
6. No credit is taken for any spacer grids or spacer sleeves.
7. No credit is taken for any burnable absorber in the fuel rods.
8. The moderator is pure water (no boron) at a temperature of 68°F. A limiting value of 1.0 gm/cm^3 is used for the density of water to conservatively bound the range of normal (50°F to 180°F) spent fuel pool water temperatures.
9. The array is infinite in lateral (x and y) extent and infinite in axial (vertical) extent.
10. All available storage cells are loaded with fuel assemblies as depicted in Figure 5 on page 41.

11. Nominal Boraflex poison plate dimensions for width, thickness and length are assumed.

To conservatively evaluate the effects of Boraflex shrinkage and gap development, the methodology described in Section 2.3 is employed. Five shrinkage/gap scenarios are examined to cover the spectrum of shrinkage-to-gap ratios from 100% gaps to 0% shrinkage through 0% gap and 100% shrinkage. Assignment of which panels have gaps or shrinkage, and the axial location of the gap is based on random selection.

With the above assumptions, the KENO calculation for the nominal case results in a K_{eff} of 0.9231 with a 95 percent probability/95 percent confidence level uncertainty of ± 0.0022 ΔK. This K_{eff} is the nominal reactivity assuming no Boraflex gaps or shrinkage.

The KENO calculation for the worst case of Boraflex gaps and shrinkage results in a K_{eff} of 0.9260 with a 95 percent probability/95 percent confidence level uncertainty of ± 0.0021 ΔK. This K_{eff} will be used as the reference reactivity for the Region 2 storage configuration.

Calculational and methodology biases must be considered in the final K_{eff} summation prior to comparing against the 0.95 K_{eff} limit. The following biases are included:

Methodology: As discussed in Section 2 of this report, benchmarking of the Westinghouse KENO Va methodology resulted in a method bias of 0.0077 ΔK.

B^{10} Self Shielding: To correct for the modeling assumption that individual B^{10} atoms are homogeneously distributed within the absorber material (versus clustered about each B_4C particle), a bias of 0.0014 ΔK is applied.

Water Temperature: To account for the effect of the normal range of spent fuel pool water temperatures (50°F to 180°F) on water cross section properties, a reactivity bias of 0.0021 ΔK is applied. The reactivity effect of spent fuel pool water temperature on water density was considered in the above assumption.

To evaluate the reactivity effects of possible variations in material characteristics and mechanical/ construction dimensions, PHOENIX perturbation calculations are performed. For the Ginna Region 2 spent fuel rack configuration, UO_2 material tolerances are considered along with construction tolerances related to the cell I.D., cell pitch, stainless steel thickness, and Boraflex poison. Uncertainties associated with calculation and methodology accuracy are also considered in the statistical summation of uncertainty components.

The following tolerance and uncertainty components are considered in the total uncertainty statistical summation:

U^{235} Enrichment: The standard DOE enrichment tolerance of ± 0.05 w/o U^{235} about the nominal 1.95 w/o U^{235} reference enrichment was evaluated with PHOENIX and resulted in a reactivity increase of 0.0079 ΔK.

UO_2 Density: A $\pm 2.0\%$ variation about the nominal 95% reference theoretical density was evaluated with PHOENIX and resulted in a reactivity increase of 0.0037 ΔK.

Fuel Pellet Dishing: A variation in fuel pellet dishing fraction from 0.0% to 2.0% (about the nominal 1.1926% reference value) was evaluated with PHOENIX and resulted in a reactivity

increase of 0.0020 ΔK.

Storage Cell I.D., Storage Cell Pitch, and Stainless Steel Thickness: The +0.06 inch tolerance about the nominal 8.25 inch reference cell I.D., the +0.06 inch tolerance about the nominal 8.43 inch reference storage cell pitch, and the ±0.004 inch tolerance about the nominal 0.09 inch reference stainless steel thickness for all rack structures was evaluated with PHOENIX and resulted in a reactivity increase of 0.0004 ΔK.

Boraflex Absorber Width: The ±0.0625 inch tolerance about the nominal 6.625 inch Boraflex panel width was evaluated with PHOENIX and resulted in a reactivity increase of 0.0004 ΔK.

Boraflex Absorber Thickness: The ±0.007 inch tolerance about the nominal 0.075 inch Boraflex panel thickness was evaluated with PHOENIX and resulted in a reactivity increase of 0.0004 ΔK.

Assembly Position: The KENO reference reactivity calculation assumes fuel assemblies are symmetrically positioned within the storage cells since experience has shown that centered fuel assemblies yield equal or more conservative results in rack K_{eff} than non-centered (asymmetric) positioning. Therefore, no reactivity uncertainty needs to be applied for this tolerance since the most reactive configuration is considered in the calculation of the reference K_{eff}.

Calculation Uncertainty: The KENO calculation for the nominal reference reactivity resulted in a K_{eff} with a 95 percent probability/95 percent confidence level uncertainty of ±0.0021 ΔK.

Methodology Uncertainty: As discussed in Section 2 of this report, comparison against benchmark experiments showed that the 95 percent probability/95 percent confidence uncertainty in reactivity, due to method, is not greater than 0.0030 ΔK.

The maximum K_{eff} for the Ginna Region 2 spent fuel storage configuration is developed by adding the calculational and methodology biases and the statistical sum of independent uncertainties to the nominal KENO reference reactivity. The summation is shown in Table 8 on page 35 and results in a maximum K_{eff} of 0.9469.

Since K_{eff} is less than 0.95 including uncertainties at a 95/95 probability/confidence level, the acceptance criteria for criticality is met for storage of Westinghouse 14x14 OFA fuel assemblies with nominal enrichments up to 1.95 w/o U^{235} in the Ginna Region 2 spent fuel racks. Storage of Westinghouse 14x14 STD and Exxon 14x14 is discussed in the next section.

5.2 Burnup Credit Reactivity Equivalencing

Storage of burned fuel assemblies in the Ginna Region 2 spent fuel racks is achievable by means of the concept of reactivity equivalencing. The concept of reactivity equivalencing is predicated upon the reactivity decrease associated with fuel depletion or the addition of IFBA fuel rods. For burnup credit, a series of reactivity calculations are performed to generate a set of enrichment-fuel assembly discharge burnup ordered pairs which all yield an equivalent K_{eff} when stored in the spent fuel storage racks.

Figure 11 on page 47 shows the constant K_{eff} contour generated for the Ginna alternating rows storage configuration. This curve represents combinations of fuel enrichment and discharge burnup which yield the same rack multiplication factor (K_{eff}) as the rack loaded with

Westinghouse 14x14 OFA fresh fuel (zero burnup) at 1.95 w/o U^{235}.

Note in Figure 11 on page 47, the endpoints are 0 MWD/MTU where the Westinghouse 14x14 OFA enrichment is 1.95 w/o, and 36200 MWD/MTU where the Westinghouse 14x14 OFA enrichment is 5.0 w/o. The interpretation of the endpoint data is as follows: the reactivity of the spent fuel rack containing Westinghouse 14x14 OFA 5.00 w/o fuel at 36200 MWD/MTU is equivalent to the reactivity of the rack containing Westinghouse 14x14 OFA 1.95 w/o fresh fuel. The burnup credit curve shown in Figure 11 on page 47 includes a reactivity uncertainty of 0.0121 ΔK, consistent with the minimum burnup requirement of 36200 MWD/MTU for Westinghouse 14x14 OFA at 5.0 w/o.

Since the Westinghouse 14x14 STD is more reactive than the Westinghouse 14x14 OFA fuel at the low enrichment limit for Region 2 spent fuel rack, there is a separate burnup credit curve for the Westinghouse 14x14 STD fuel. Also the Exxon 14x14 is less reactive than the Westinghouse 14x14 OFA, it is conservative to use the Westinghouse 14x14 OFA burnup credit curve for the Exxon 14x14 fuel.

It is important to recognize that the curve in Figure 11 on page 47 is based on calculations of constant rack reactivity. In this way, the environment of the storage rack and its influence on assembly reactivity is implicitly considered. For convenience, the data from Figure 11 on page 47 is also provided in Table 9 on page 36. Use of linear interpolation between the tabulated values is acceptable since the curve shown in Figure 11 on page 47 is linear.

The effect of axial burnup distribution on assembly reactivity has been considered in the development of the Ginna Region 2 burnup credit limit. Previous evaluations have been performed to quantify axial burnup reactivity effects and to confirm that the reactivity equivalencing methodology described in Section 2.2 results in calculations of conservative burnup credit limits[16]. The evaluations show that axial burnup effects can cause assembly reactivity to increase, but the burnup-enrichment combinations required to cause this are well beyond those required by the Ginna Region 2 burnup credit limit. Therefore, additional accounting of axial burnup distribution effects in the Ginna Region 2 burnup credit limit is not necessary.

5.3 Sensitivity Analysis and Soluble Boron Worth

To show the dependence of K_{eff} on fuel and storage cells parameters as requested by the NRC[1], the variation of the K_{eff} with respect to the following parameters was developed using the PHOENIX computer code:

1. Fuel enrichment, with a 0.50 w/o U^{235} delta about the nominal case enrichment.
2. Center-to-center spacing of storage cells, with a 0.3 inch delta about the nominal case center-to-center spacing.
3. Poison loading, with a 0.01 gm-B^{10}/cm^2 delta about the nominal case poison loading.

Results of the sensitivity analysis are shown in Figure 12 on page 48.

PHOENIX calculations were also performed to evaluate the reactivity benefits of soluble boron for the Region 2 spent fuel storage configuration. Results of these calculations are provided in Figure 13 on page 49. As the curve shows, the presence of soluble boron in the Ginna Region 2 spent fuel pool provides substantial reactivity margin.

6.0 Criticality Analysis of Consolidated Rod Storage Canisters in Spent Fuel Racks

This section describes the analytical techniques and models employed to perform the criticality analysis to show that fully or partially loaded consolidated rod storage canisters (CRSC) can be stored in the Ginna Region 1 and Region 2 spent fuel storage racks.

The analysis is based on maintaining a $K_{eff} \leq 0.95$ for storage of the existing CRSC's and future CRSC's for Westinghouse 14x14 STD, Westinghouse 14x14 OFA and Exxon 14x14. The Westinghouse 14x14 STD is the most reactive fuel type in Region 2 spent fuel racks.

Section 6.1 describes the design description of the CRSC in spent fuel racks. Section 6.2 describes the analysis which determines the acceptable range of the number of consolidated rods and confirm the acceptability of the storage of the existing CRSC's.

6.1 Design Description

The CRSC design is depicted schematically in Figure 6 on page 42.

6.2 Reactivity Calculations

The following assumptions are used to develop the nominal case KENO model for storing CRSC in the Ginna spent fuel rack:

1. The fuel assembly parameters relevant to the criticality analysis are based on the Westinghouse 14x14 STD design (see Table 1 on page 27 for fuel parameters).
2. All fuel rods contain uranium dioxide at a nominal enrichment of 1.85 w/o over the entire length of each rod.
4. The fuel pellets are modeled assuming 95% nominal theoretical density and 1.187% nominal dishing fraction.
5. No credit is taken for any natural or reduced enrichment axial blankets.
6. No credit is taken for any U^{234} or U^{236} in the fuel, nor is any credit taken for the buildup of fission product poison material.
7. No credit is taken for any spacer grids or spacer sleeves.
8. No credit is taken for any burnable absorber in the fuel rods.
9. The moderator is pure water (no boron) at a temperature of 68°F. A limiting value of 1.0 gm/cm^3 is used for the density of water to conservatively bound the range of normal (50°F to 180°F) spent fuel pool water temperatures.
10. The array is infinite in lateral (x and y) extent and infinite in axial (vertical) extent.
11. Nominal Boraflex poison plate dimensions for width, thickness and length are assumed.

12. All available storage cells are loaded with fuel assemblies as depicted in Figure 5 on page 41
13. Either fully or partially loaded CRSC can be stored in the fuel racks.
14. The rods are randomly dispersed in the canister.
15. The same uncertainties and biases as used in the 95/95 K_{eff} rack up of the Region 2 spent fuel rack analysis are to be applied to the results of the nominal KENO model for CRSC.

With the above assumptions, the KENO results conservatively show an acceptable range of the number of consolidated rods of no greater than 144 or no less than 256 rods. The storage of consolidated rods between 144 and 256 rods is not acceptable. The plot of the KENO 95/95 K_{eff} versus the number of consolidated rods is shown in Figure 14 on page 50. For the existing CRSC with the number of rods between 144 and 256, KENO calculations with the actual consolidated rod configuration and/or burnup credit show that the 95/95 K_{eff} is less than 0.95

Storage of Westinghouse 14x14 STD fuel at a nominal enrichment of 1.85 w/o U^{235}, and Westinghouse 14x14 OFA or Exxon 14x14 fuel at a nominal enrichment of 1.95 w/o U^{235} is acceptable in the Region 2 storage racks. Storage of Westinghouse 14x14 STD at an enrichment higher than 1.85 w/o U^{235}, and Westinghouse 14x14 OFA or Exxon 14x14 fuel is allowed provided that the minimum burnup requirements in Table 9 on page 36 of Section 5.2 is met. Storage of CRSC in Region 1 spent fuel rack is allowed since Region 2 is the enrichment limiting region.

7.0 Discussion of Postulated Accidents

7.1 Fresh Fuel Storage Racks

Under normal conditions, the fresh fuel racks are maintained in a dry environment. The introduction of water into the fresh fuel rack area is the worst case accident scenario. The water flooding cases analyzed in this report are bounding accident situations which result in the most conservative fuel rack K_{eff}.

Other accidents can be postulated which would cause some reactivity increase (i.e., dropping a fuel assembly between the rack and wall, or dropping an assembly on top of the rack). For these other accident conditions, the double contingency principle is applied. This states that one is not required to assume two unlikely, independent, concurrent events to ensure protection against a criticality accident. Thus, for these other accident conditions, the absence of a moderator in the fresh fuel storage racks can be assumed as a realistic initial condition since assuming its presence would be a second unlikely event.

Experience has shown that the maximum reactivity increase associated with postulated accidents (dropping a fuel assembly between the rack and wall, or dropping an assembly on top of the rack) is less than 10 percent ΔK.

Therefore, since the normal, dry fresh fuel rack reactivity is less than 0.55, and the maximum reactivity increase for the postulated accidents is less than 10 percent ΔK, the maximum rack K_{eff} under these other postulated accidents conditions will be less than 0.95.

7.2 Spent Fuel Storage Racks

Most accident conditions will not result in an increase in K_{eff} of the rack. Examples are:

Fuel assembly drop on top of rack	The rack structure pertinent for criticality is not excessively deformed and the dropped assembly which comes to rest horizontally on top of the rack has sufficient water separating it from the active fuel height of stored assemblies to preclude neutronic interaction.
Fuel assembly drop between rack modules	Design of the spent fuel racks is such that it precludes the insertion of a fuel assembly between rack modules.

However, two accidents can be postulated which would increase reactivity beyond the analyzed condition. One such postulated accident would be a fuel assembly misload into a position for which the restrictions on location, enrichment, or burnup are not satisfied. To very conservatively estimate the reactivity impacts of such an occurrence in the spent fuel racks, the impact of loading a Westinghouse 14x14 OFA fresh assembly at 4.0 w/o U^{235} in the middle of a 3x3 array of Region 2 spent fuel rack cells with Westinghouse 14x14 OFA fresh assemblies at 1.95 w/o U^{235} determined. The reactivity increase associated with this misloading is less than 0.036 ΔK. There is no impact of a misload of a Region 2 assembly into Region 1 since Region 2 enrichment limits

are more conservative than Region 1.

A second accident which could result in increased reactivity would be a "cooldown" event during which the pool temperature would drop below 50°F in Region 2 spent fuel pool or "heatup" event during which the pool temperature would rise to 212°F in Region 1 spent fuel pool. Calculations show that if the Region 2 spent fuel pool water temperature was to decrease from 50°F to 32°F, reactivity could increase by about 0.0021 ΔK, and this still results in a 95/95 $K_{eff} \leq 0.95$. If the Region 1 spent fuel pool water temperature was to increase from 180°F to 212°F, reactivity could increase by 0.0019 ΔK.

For occurrences of any of the above postulated accidents, the double contingency principle of ANSI/ANS 8.1-1983 can be applied. This states that one is not required to assume two unlikely, independent, concurrent events to ensure protection against a criticality accident. Thus, for these postulated accident conditions, the presence of soluble boron in the storage pool water can be assumed as a realistic initial condition since not assuming its presence would be a second unlikely event.

The worth of soluble boron in the Ginna Region 2 spent fuel pool has been calculated with PHOENIX and is shown in Figure 13 on page 49. As the curves show, the presence of soluble boron in the pool water reduces rack reactivity significantly and is more than sufficient to offset the positive reactivity impacts of any of the postulated accidents. To bound the 0.036 ΔK reactivity increase from the most limiting accident in the spent fuel racks, it is estimated that 300 ppm of soluble boron is required.

Therefore should a postulated accident occur which causes a reactivity increase in the Ginna spent fuel racks, K_{eff} will be maintained less than or equal to 0.95 due to the presence of at least 300 ppm of soluble boron in the spent fuel pool water.

7.3 Consolidated Rod Storage Canisters

Accidents can be postulated which would increase reactivity through the loss of containment of the consolidated fuel rods. This loss of containment could occur as a result of spillage from a damaged or mishandled canister. This accident condition is bounded by the uncontrolled release of two assemblies worth (358) of fuel rods at an optimum pitch in the space above the fuel racks. At no time are more rods than this being placed in a CRSC. The maximum 95/95 K_{eff} that can results from the uncontrolled release of 358 fuel rods in cold unborated water is 0.94979 which is lower than the 0.95 limit.

Accidents can also be postulated which may damage fuel assemblies and result in the release of fuel rods from CRSC. Calculations have shown that any fuel rack geometry change resulting in either a decrease in the average fuel rod pitch or an axially misaligned fuel assembly in the fuel racks will result in a decrease in the fuel rack K_{eff}. Any increase in an assembly fuel rod pitch caused by a dropped CRSC will be bounded by the loss of containment of fuel rods in CRSC discussed above.

8.0 Summary of Criticality Results

The acceptance criteria for criticality requires the effective neutron multiplication factor, K_{eff}, in the fresh fuel storage rack to be less than or equal to 0.95, including uncertainties, under flooded conditions and less than or equal to 0.98, including uncertainties, under optimum moderation conditions.

For the storage of fuel assemblies in the spent fuel storage racks, the acceptance criteria for criticality requires the effective neutron multiplication factor, K_{eff}, to be less than or equal to 0.95, including uncertainties, under all conditions.

This report shows that the acceptance criteria for criticality is met for the Ginna Fresh Fuel Storage Racks for the storage of Westinghouse 14x14 OFA fuel assemblies and for the Ginna Spent Fuel Storage Racks for the storage of 14x14 fuel assemblies with the following configurations and enrichment limits:

Fresh Fuel Racks	Storage of fresh fuel assemblies with nominal enrichments up to 5.0 w/o U^{235} utilizing all available storage cells.
Spent Fuel Racks Region 1	Storage of fuel assemblies with nominal enrichments up to 4.0 w/o U^{235} utilizing two out of four checkerboard arrangement. Fresh fuel assemblies with higher initial enrichments up to 5.0 w/o U^{235} can also be stored in these racks provided a minimum number of IFBAs are present in each fuel assembly. IFBAs consist of neutron absorbing material applied as a thin ZrB_2 coating on the outside of the UO_2 fuel pellet. As a result, the neutron absorbing material is a non-removable or integral part of the fuel assembly once it is manufactured.
Spent Fuel Racks Region 2	Storage of Westinghouse 14x14 OFA, Westinghouse 14x14 STD and Exxon 14x14 fuel assemblies utilizing all available storage cells. The Westinghouse 14x14 STD fuel assemblies must have an initial enrichment up to 1.85 w/o U^{235} (nominal) or satisfy a minimum burnup requirement. The Westinghouse 14x14 OFA and the Exxon 14x14 fuel assemblies must have an initial enrichment up to 1.95 w/o U^{235} (nominal) or satisfy the minimum burnup requirement. Storage of Region 2 assemblies in Region 1 spent fuel racks is allowed since Region 2 is the enrichment limiting region.

Consolidated Rod Canisters in Spent Fuel Racks	Storage of future consolidated Westinghouse 14x14 STD fuel rods at a nominal enrichment of 1.85 w/o U^{235}, and Westinghouse 14x14 OFA and Exxon 14x14 fuel rods at a nominal enrichment of 1.95 w/o U^{235} in storage canisters in Region 1 and Region 2 are acceptable provided that the number of consolidated rods is not greater than 144 or no less than 256 rods. Enrichments higher than the nominal values are allowed provided that the minimum burnup requirements are satisfied. Storage of existing consolidated rod storage canisters is acceptable in Region 1 and Region 2 spent fuel racks.

The analytical methods employed herein conform with ANSI N18.2-1973, "Nuclear Safety Criteria for the Design of Stationary Pressurized Water Reactor Plants," Section 5.7 Fuel Handling System; ANSI 57.2-1983, "Design Objectives for LWR Spent Fuel Storage Facilities at Nuclear Power Stations," Section 6.4.2; ANSI 57.3-1983, "Design Requirements for New Fuel Storage Facilities at Light Water Reactor Plants," ANSI N16.9-1975, "Validation of Calculational Methods for Nuclear Criticality Safety"; and the NRC Standard Review Plan, Section 9.1.2, "Spent Fuel Storage".

Table 1. Fuel Parameters Employed in the Criticality Analysis

Parameter	Exxon 14x14	W 14x14 STD	W 14x14 OFA
Number of Fuel Rods per Assembly	179	179	179
Rod Zirc-4 Clad O.D. (inch)	0.424	0.422	0.400
Clad Thickness (inch)	0.030	0.0243	0.0243
Fuel Pellet O.D.(inch)	0.3565	0.3669	0.3444
Fuel Pellet Density (% of Theoretical)	95	95	95
Fuel Pellet Dishing Factor (%)	1.187	1.187	1.1926
Rod Pitch (inch)	0.556	0.556	0.556
Number of Zirc-4 Guide Tubes	16	16	16
Guide Tube O.D. (inch)	0.524	0.539	0.528
Guide Tube Thickness (inch)	0.015	0.017	0.019
Number of Instrument Tubes	1	1	1
Instrument Tube O.D. (inch)	0.424	0.422	0.399
Instrument Tube Thickness (inch)	0.039	0.0240	0.0235

Table 2. Benchmark Critical Experiments

Critical Number	General Description	Enrichment U235 (w/o)	Reflector	Separating Material	Soluble Boron (ppm)	Measured K_{eff}	KENO Reactivity (K_{eff} +/- One Sigma)
1	UO_2 Rod Lattice	2.46	water	water	0	1.0002	0.99347 +/- 0.00234
2	UO_2 Rod Lattice	2.46	water	water	1037	1.0001	0.99361 +/- 0.00193
3	UO_2 Rod Lattice	2.46	water	water	764	1.0000	0.99459 +/- 0.00194
4	UO_2 Rod Lattice	2.46	water	B_4C pins	0	0.9999	0.98766 +/- 0.00217
5	UO_2 Rod Lattice	2.46	water	B_4C pins	0	1.0000	0.98838 +/- 0.00221
6	UO_2 Rod Lattice	2.46	water	B_4C pins	0	1.0097	1.00132 +/- 0.00221
7	UO_2 Rod Lattice	2.46	water	B_4C pins	0	0.9998	0.99570 +/- 0.00225
8	UO_2 Rod Lattice	2.46	water	B_4C pins	0	1.0083	0.99905 +/- 0.00210
9	UO_2 Rod Lattice	2.46	water	water	0	1.0030	0.99660 +/- 0.00299
10	UO_2 Rod Lattice	2.46	water	water	143	1.0001	0.99707 +/- 0.00199
11	UO_2 Rod Lattice	2.46	water	stainless steel	514	1.0000	0.99862 +/- 0.00203
12	UO_2 Rod Lattice	2.46	water	stainless steel	217	1.0000	0.99411 +/- 0.00207
13	UO_2 Rod Lattice	2.46	water	borated aluminum	15	1.0000	0.99229 +/- 0.00218
14	UO_2 Rod Lattice	2.46	water	borated aluminum	92	1.0001	0.98847 +/- 0.00208
15	UO_2 Rod Lattice	2.46	water	borated aluminum	395	0.9998	0.98424 +/- 0.00205
16	UO_2 Rod Lattice	2.46	water	borated aluminum	121	1.0001	0.98468 +/- 0.00209
17	UO_2 Rod Lattice	2.46	water	borated aluminum	487	1.0000	0.99521 +/- 0.00195
18	UO_2 Rod Lattice	2.46	water	borated aluminum	197	1.0002	0.99203 +/- 0.00211
19	UO_2 Rod Lattice	2.46	water	borated aluminum	634	1.0002	0.98924 +/- 0.00201
20	UO_2 Rod Lattice	2.46	water	borated aluminum	320	1.0003	0.99461 +/- 0.00197
21	UO_2 Rod Lattice	2.46	water	borated aluminum	72	0.9997	0.98700 +/- 0.00220
22	UO_2 Rod Lattice	2.35	water	borated aluminum	0	1.0000	0.99347 +/- 0.00128
23	UO_2 Rod Lattice	2.35	water	stainless steel	0	1.0000	0.99566 +/- 0.00116
24	UO_2 Rod Lattice	2.35	water	water	0	1.0000	0.99785 +/- 0.00239
25	UO_2 Rod Lattice	2.35	water	stainless steel	0	1.0000	0.98964 +/- 0.00240
26	UO_2Rod Lattice	2.35	water	borated aluminum	0	1.0000	0.98841 +/- 0.00234
27	UO_2 Rod Lattice	2.35	water	B_4C	0	1.0000	0.99015 +/- 0.00231
28	UO_2 Rod Lattice	4.31	water	stainless steel	0	1.0000	0.99063 +/- 0.00247
29	UO_2 Rod Lattice	4.31	water	water	0	1.0000	0.98986 +/- 0.00228
30	UO_2 Rod Lattice	4.31	water	stainless steel	0	1.0000	1.00011 +/- 0.00248
31	UO_2 Rod Lattice	4.31	water	borated aluminum	0	1.0000	1.00070 +/- 0.00254
32	UO_2 Rod Lattice	4.31	water	borated aluminum	0	1.0000	1.00088 +/- 0.00253
33	U-metal Cylinders	93.2	bare	air	0	1.0000	0.98997 +/- 0.00257
34	U-metal Cylinders	93.2	bare	air	0	1.0000	0.99815 +/- 0.00242
35	U-metal Cylinders	93.2	bare	air	0	1.0000	0.99250 +/- 0.00230
36	U-metal Cylinders	93.2	bare	air	0	1.0000	0.99288 +/- 0.00247
37	U-metal Cylinders	93.2	bare	air	0	1.0000	0.99869 +/- 0.00235
38	U-metal Cylinders	93.2	bare	air	0	1.0000	0.99796 +/- 0.00236
39	U-metal Cylinders	93.2	bare	plexiglass	0	1.0000	0.99799 +/- 0.00261
40	U-metal Cylinders	93.2	paraffin	plexiglass	0	1.0000	1.00061 +/- 0.00265
41	U-metal Cylinders	93.2	bare	plexiglass	0	1.0000	0.99961 +/- 0.00243
42	U-metal Cylinders	93.2	paraffin	plexiglass	0	1.0000	1.01054 +/- 0.00272
43	U-metal Cylinders	93.2	paraffin	plexiglass	0	1.0000	1.00471 +/- 0.00246
44	U-metal Cylinders	93.2	paraffin	plexiglass	0	1.0000	1.00375 +/- 0.00274

Table 3. Benchmark Critical Experiments PHOENIX Comparison

Description of Experiments	Number of Experiments	PHOENIX K_{eff} Using Experiment Buckling
UO_2.		
Al clad	14	0.9947
SS clad	19	0.9944
Borated H_2O	7	0.9940
Subtotal	40	0.9944
U-Metal		
Al clad	41	1.0012
TOTAL	81	0.9978

Table 4. Data for U Metal and UO_2 Critical Experiments (Part 1 of 2)

Case Number	Cell Type	A/O U-235	H2O/U Ratio	Fuel Density (g/cc)	Pellet Diameter (cm)	Material Clad	Clad OD (cm)	Clad Thickness (cm)	Lattice Pitch (cm)	Boron PPM
1	Hexa	1.328	3.02	7.53	1.5265	Aluminum	1.6916	.07110	2.2050	0.0
2	Hexa	1.328	3.95	7.53	1.5265	Aluminum	1.6916	.07110	2.3590	0.0
3	Hexa	1.328	4.95	7.53	1.5265	Aluminum	1.6916	.07110	2.5120	0.0
4	Hexa	1.328	3.92	7.52	.9855	Aluminum	1.1506	.07110	1.5580	0.0
5	Hexa	1.328	4.89	7.52	.9855	Aluminum	1.1506	.07110	1.6520	0.0
6	Hexa	1.328	2.88	10.53	.9728	Aluminum	1.1506	.07110	1.5580	0.0
7	Hexa	1.328	3.58	10.53	.9728	Aluminum	1.1506	.07110	1.6520	0.0
8	Hexa	1.328	4.83	10.53	.9728	Aluminum	1.1506	.07110	1.8060	0.0
9	Square	2.734	2.18	10.18	.7620	SS-304	.8594	.04085	1.0287	0.0
10	Square	2.734	2.92	10.18	.7620	SS-304	.B594	.04085	1.1049	0.0
11	Square	2.734	3.86	10.18	.7620	SS-304	.8594	.04085	1.1938	0.0
12	Square	2.734	7.02	10.18	.7620	SS-304	.8594	.04085	1.4554	0.0
13	Square	2.734	8.49	10.18	.7620	SS-304	.8594	.04085	1.5621	0.0
14	Square	2.734	10.38	10.18	.7620	SS-304	.8594	.04085	1.6891	0.0
15	Square	2.734	2.50	10.18	.7620	SS-304	.B594	.04085	1.0617	0.0
16	Square	2.734	4.51	10.18	.7620	SS-304	.8594	.04085	1.2522	0.0
17	Square	3.745	2.50	10.27	.7544	SS-304	.8600	.04060	1.0617	0.0
18	Square	3.745	4.51	10.37	.7544	SS-304	.8600	.04060	1.2522	0.0
19	Square	3.745	4.51	10.37	.7544	SS-304	.8600	.04060	1.2522	0.0
20	Square	3.745	4.51	10.37	.7544	SS-304	.8600	.04060	1.2522	456.0
21	Square	3.745	4.51	10.37	.7544	SS-304	.8600	.04060	1.2522	709.0
22	Square	3.745	4.51	10.37	.7544	SS-304	.8600	.04060	1.2522	1260.0
23	Square	3.745	4.51	10.37	.7544	SS-304	.8600	.04060	1.2522	1334.0
24	Square	3.745	4.51	10.37	.7544	SS-304	.8600	.04060	1.2522	1477.0
25	Square	4.069	2.55	9.46	1.1278	SS-304	1.2090	.04060	1.5113	0.0
26	Square	4.069	2.55	9.46	1.1278	SS-304	1.2090	.04060	1.5113	3392.0
27	Square	4.069	2.14	9.46	1.1278	SS-304	1.2090	.04060	1.4500	0.0
28	Square	2.490	2.84	10.24	1.0297	Aluminum	1.2060	.08130	1.5113	0.0
29	Square	3.037	2.64	9.28	1.1268	SS-304	1.1701	.07163	1.5550	0.0
30	Square	3.037	8.16	9.28	1.1268	SS-304	1.2701	.07163	2.1980	0.0
31	Square	4.069	2.59	9.45	1.1268	SS-304	1.2701	.07163	1.5550	0.0
32	Square	4.069	3.53	9.45	1.1268	SS-304	1.2701	.07163	1.6840	0.0
33	Square	4.069	8.02	9.45	1.1268	SS-304	1.2701	.07163	2.1980	0.0
34	Square	4.069	9.90	9.45	1.1268	SS-304	1.2701	.07163	2.3810	0.0
35	Square	2.490	2.84	10.24	1.0297	Aluminum	1.2060	.08130	1.5113	1677.0
36	Hexa	2.096	2.06	10.38	1.5240	Aluminum	1.6916	.07112	2.1737	0.0
37	Hexa	2.096	3.09	10.38	1.5240	Aluminum	1.6916	.07112	2.4052	0.0
38	Hexa	2.096	4.12	10.38	1.5240	Aluminum	1.6916	.07112	2.6162	0.0
39	Hexa	2.096	6.14	10.38	1.5240	Aluminum	1.6916	.07112	2.9891	0.0
40	Hexa	2.096	8.20	10.38	1.5240	Aluminum	1.6916	.07112	3.3255	0.0
41	Hexa	1.307	1.01	18.90	1.5240	Aluminum	1.6916	.07112	2.1742	0.0
42	Hexa	1.307	1.51	18.90	1.5240	Aluminum	1.6916	.07112	2.4054	0.0

Table 4. Data for U Metal and UO_2 Critical Experiments (Part 2 of 2)

Case Number	Cell Type	A/O U_{235}	H2O/U Ratio	Fuel Density (g/cc)	Pellet Diameter (cm)	Material Clad	Clad OD (cm)	Clad Thickness (cm)	Lattice Pitch (cm)	Boron PPM
43	Hexa	1.307	2.02	18.90	1.5240	Aluminum	1.6916	.07112	2.6162	0.0
44	Hexa	1.307	3.01	18.90	1.5240	Aluminum	1.6916	.07112	2.9896	0.0
45	Hexa	1.307	4.02	18.90	1.5240	Aluminum	1.6916	.07112	3.3249	0.0
46	Hexa	1.160	1.01	18.90	1.5240	Aluminum	1.6916	.07112	2.1742	0.0
47	Hexa	1.160	1.51	18.90	1.5240	Aluminum	1.6916	.07112	2.4054	0.0
48	Hexa	1.160	2.02	18.90	1.5240	Aluminum	1.6916	.07112	2.6162	0.0
49	Hexa	1.160	3.01	18.90	1.5240	Aluminum	1.6916	.07112	2.9896	0.0
50	Hexa	1.160	4.02	18.90	1.5240	Aluminum	1.6916	.07112	3.3249	0.0
51	Hexa	1.040	1.01	18.90	1.5240	Aluminum	1.6916	.07112	2.1742	0.0
52	Hexa	1.040	1.51	18.90	1.5240	Aluminum	1.6916	.07112	2.4054	0.0
53	Hexa	1.040	2.02	18.90	1.5240	Aluminum	1.6916	.07112	2.6162	0.0
54	Hexa	1.040	3.01	18.90	1.5240	Aluminum	1.6916	.07112	2.9896	0.0
55	Hexa	1.040	4.02	18.90	1.5240	Aluminum	1.6916	.07112	3.3249	0.0
56	Hexa	1.307	1.00	18.90	.9830	Aluminum	1.1506	.07112	1.4412	0.0
57	Hexa	1.307	1.52	18.90	.9830	Aluminum	1.1506	.07112	1.5926	0.0
58	Hexa	1.307	2.02	18.90	.9830	Aluminum	1.1506	.07112	1.7247	0.0
59	Hexa	1.307	3.02	18.90	.9830	Aluminum	1.1506	.07112	1.9609	0.0
60	Hexa	1.307	4.02	18.90	.9830	Aluminum	1.1506	.07112	2.1742	0.0
61	Hexa	1.160	1.52	18.90	.9830	Aluminum	1.1506	.07112	1.5926	0.0
62	Hexa	1.160	2.02	18.90	.9830	Aluminum	1.1506	.07112	1.7247	0.0
63	Hexa	1.160	3.02	18.90	.9830	Aluminum	1.1506	.07112	1.9609	0.0
64	Hexa	1.160	4.02	18.90	.9830	Aluminum	1.1506	.07112	2.1742	0.0
65	Hexa	1.160	1.00	18.90	.9830	Aluminum	1.1506	.07112	1.4412	0.0
66	Hexa	1.160	1.52	18.90	.9830	Aluminum	1.1506	.07112	1.5926	0.0
67	Hexa	1.160	2.02	18.90	.9830	Aluminum	1.1506	.07112	1.7247	0.0
68	Hexa	1.160	3.02	18.90	.9830	Aluminum	1.1506	.07112	1.9609	0.0
69	Hexa	1.160	4.02	18.90	.9830	Aluminum	1.1506	.07112	2.1742	0.0
70	Hexa	1.040	1.33	18.90	19.050	Aluminum	2.0574	.07620	2.8687	0.0
71	Hexa	1.040	1.58	18.90	19.050	Aluminum	2.0574	.07620	3.0086	0.0
72	Hexa	1.040	1.83	18.90	19.050	Aluminum	2.0574	.07620	3.1425	0.0
73	Hexa	1.040	2.33	18.90	19.050	Aluminum	2.0574	.07620	3.3942	0.0
74	Hexa	1.040	2.83	18.90	19.050	Aluminum	2.0574	.07620	3.6284	0.0
75	Hexa	1.040	3.83	18.90	19.050	Aluminum	2.0574	.07620	4.0566	0.0
76	Hexa	1.310	2.02	18.88	1.5240	Aluminum	1.6916	.07112	2.6160	0.0
77	Hexa	1.310	3.01	18.88	1.5240	Aluminum	1.6916	.07112	2.9900	0.0
78	Hexa	1.159	2.02	18.88	1.5240	Aluminum	1.6916	.07112	2.6160	0.0
79	Hexa	1.159	3.01	18.88	1.5240	Aluminum	1.6916	.07112	2.9900	0.0
80	Hexa	1.312	2.03	18.88	.9830	Aluminum	1.1506	.07112	1.7250	0.0
81	Hexa	1.312	3.02	18.88	.9830	Aluminum	1.1506	.07112	1.9610	0.0

Table 5. Comparison of PHOENIX Isotopics Predictions to Yankee Core 5 Measurements

Quantity (Atom Ratio)	% Difference
U^{235}/U	-0.67
U^{236}/U	-0.28
U^{238}/U	-0.03
Pu^{239}/U	+3.27
Pu^{240}/U	+3.63
Pu^{241}/U	-7.01
Pu^{242}/U	-0.20
Pu^{239}/U^{238}	+3.24
Mass(Pu/U)	+1.41
FISS-Pu/TOT-Pu	-0.02

Table 6. Ginna Region 1 Spent Fuel Rack K_{eff} Summary

	ΔK	K_{eff}
Nominal KENO Reference Reactivity:		**0.9271**
Calculational & Methodology Biases:		
Methodology (Benchmark) Bias	+0.0077	
Pool Temperature Bias (50°F - 180°F)	+0.0073	
TOTAL Bias	+0.0150	
Best-Estimate Nominal K_{eff}:		**0.9421**
Tolerances & Uncertainties:		
UO_2 Enrichment Tolerance	+0.0024	
UO_2 Density Tolerance	+0.0027	
Fuel Pellet Dishing Variation	+0.0015	
Storage Cell Wall Thickness Tolerance	+0.0017	
Calculational Uncertainty (95/95)	+0.0041	
Methodology Bias Uncertainty (95/95)	+0.0030	
TOTAL Uncertainty (statistical)	+0.0066	
Final K_{eff} Including Uncertainties & Tolerances:		**0.9487**

Table 7. Ginna Region 1 Spent Fuel Rack IFBA Requirement

Nominal Enrichment (w/o)	1.0X (1.67 mg./in) IFBA Rods In Assembly	1.5X (2.51 mg./in) IFBA Rods In Assembly	2.0X (3.34 mg./in) IFBA Rods In Assembly
4.00	0	0	0
4.50	32	24	16
5.00	64	48	32

Table 8. Ginna Region 2 Spent Fuel Rack K_{eff} Summary

	ΔK	K_{eff}
Nominal KENO Reference Reactivity:		**0.9260**
Calculational & Methodology Biases:		
Methodology (Benchmark) Bias	+0.0077	
Pool Temperature Bias (50°F - 180°F)	+0.0021	
Boraflex B^{10} Self Shielding Bias	+0.0014	
TOTAL Bias	+0.0112	
Best-Estimate Nominal K_{eff}:		**0.9372**
Tolerances & Uncertainties:		
UO_2 Enrichment Tolerance	+0.0079	
UO_2 Density Tolerance	+0.0037	
Fuel Pellet Dishing Variation	+0.0020	
Stainless Steel Wall Thickness Tolerance	+0.0004	
Boraflex Width Tolerance	+0.0004	
Boraflex Thickness Tolerance	+0.0004	
Calculational Uncertainty (95/95)	+0.0021	
Methodology Bias Uncertainty (95/95)	+0.0030	
TOTAL Uncertainty (statistical)	+0.0097	
Final K_{eff} Including Uncertainties & Tolerances:		**0.9469**

Table 9. Ginna Region 2 Spent Fuel Rack Minimum Burnup Requirements

Enrichment (w/o)	W OFA & Exxon Burnup (MWD/MTU)	W STD Burnup (MWD/MTU)
1.85	0	0
1.90	0	1400
2.00	700	2100
2.50	7600	8900
3.00	14500	15700
3.50	20100	21400
4.00	25700	27100
4.50	31000	32400
5.00	36200	37700

NOTE: The use of linear interpolation between the minimum burnups reported above is acceptable.

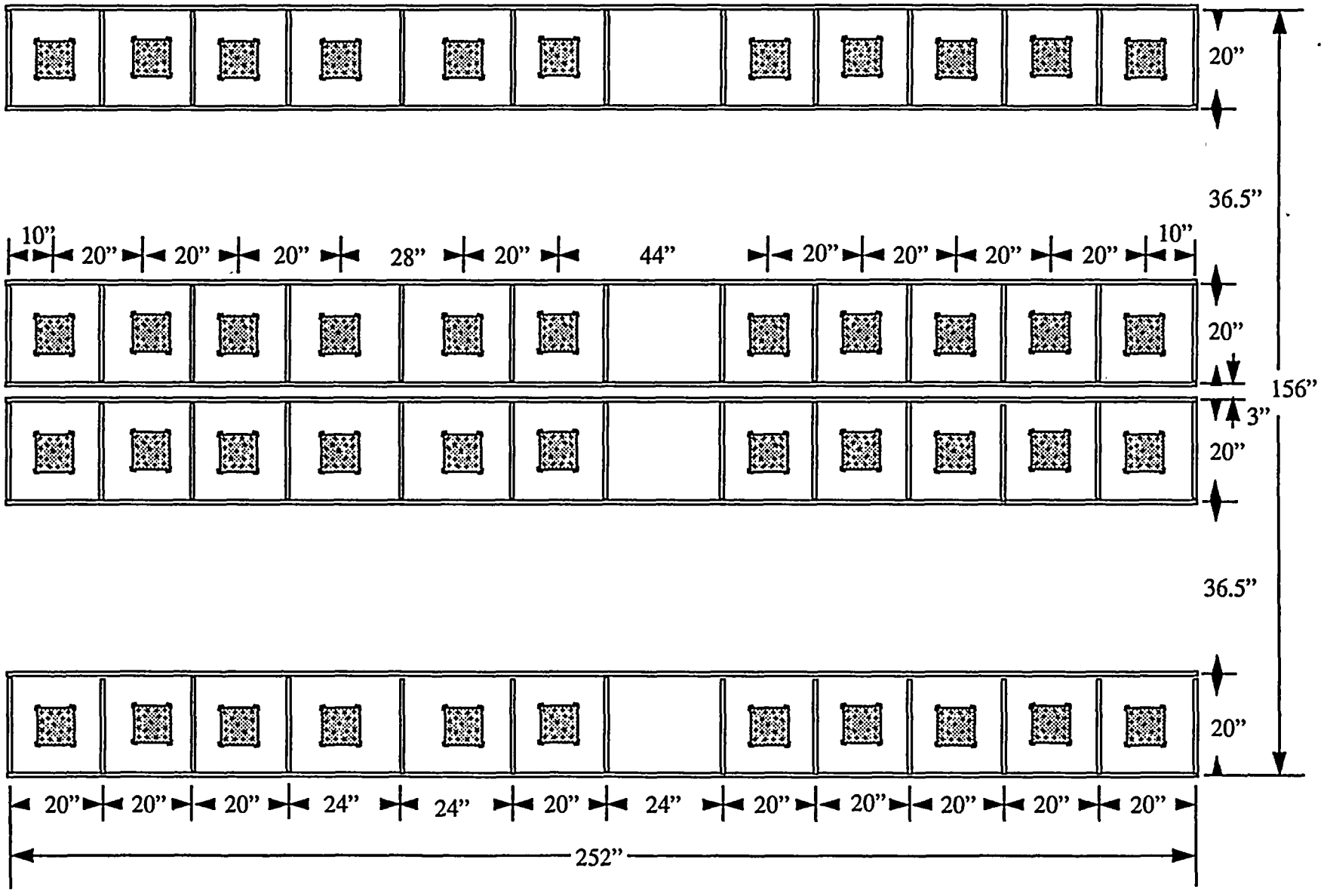

Figure 1. GinnaFresh Fuel Rack Array Layout

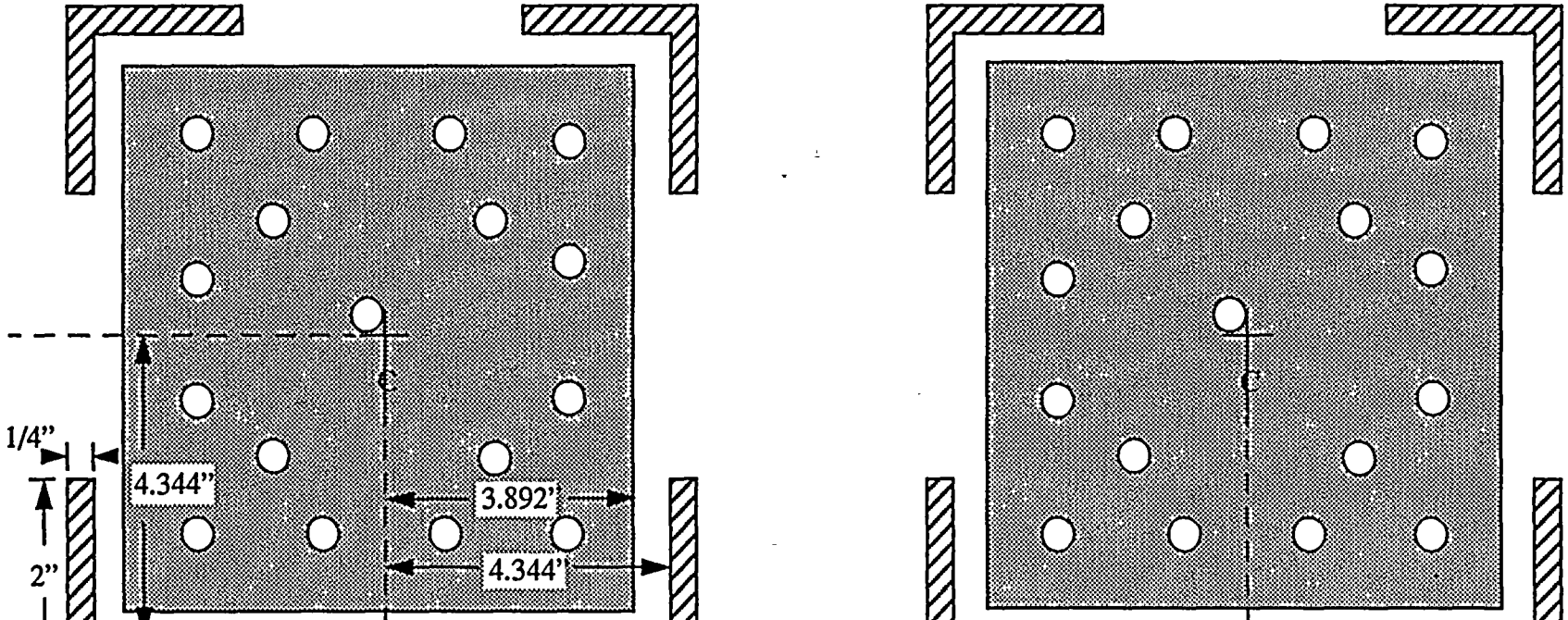

Figure 2. Ginna Fresh Fuel Rack Cell Layout

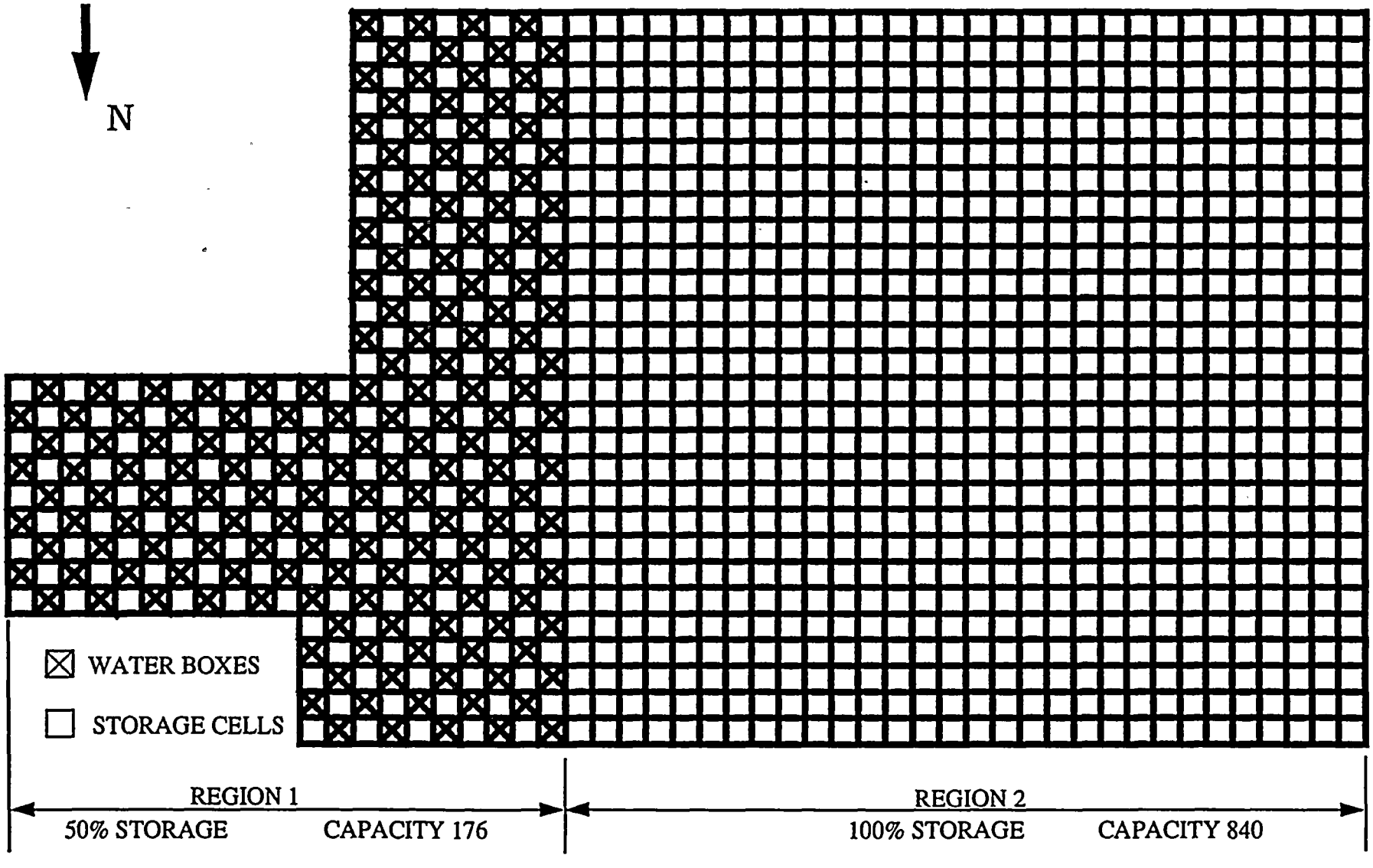

Figure 3. Ginna Spent Fuel Pool Layout

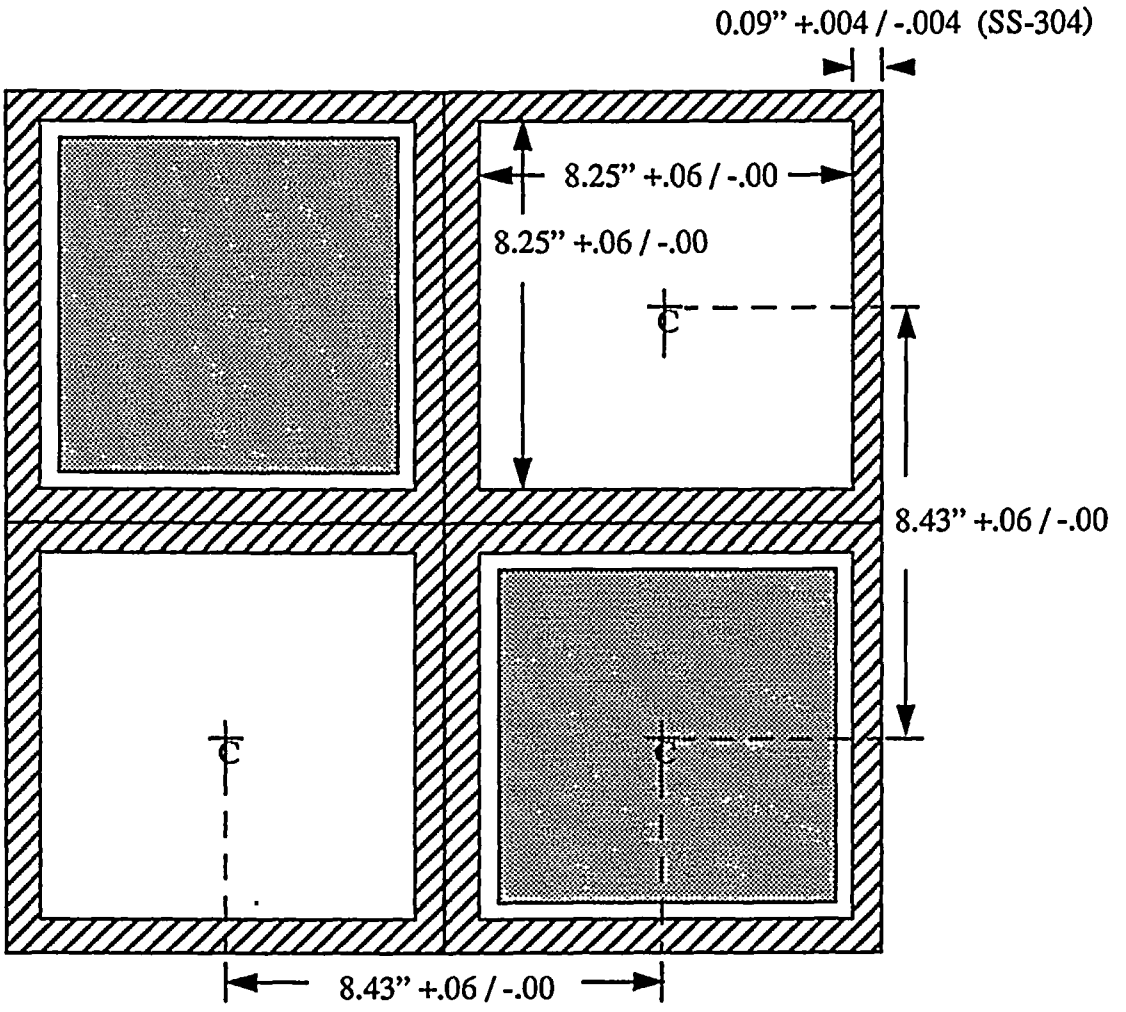

Figure 4. Ginna Region 1 Spent Fuel Storage Cells

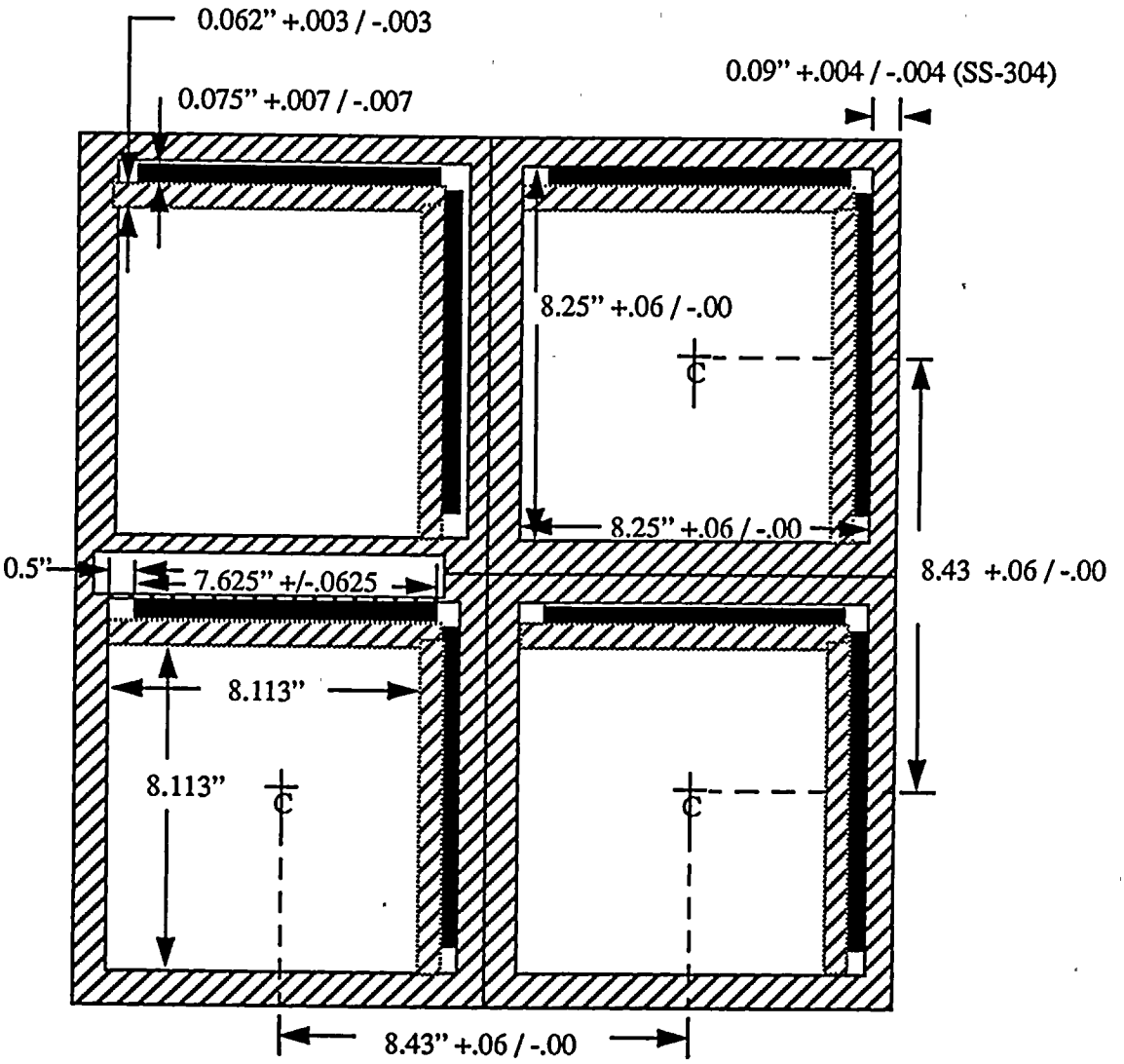

Figure 5. Ginna Region 2 Spent Fuel Storage Cells

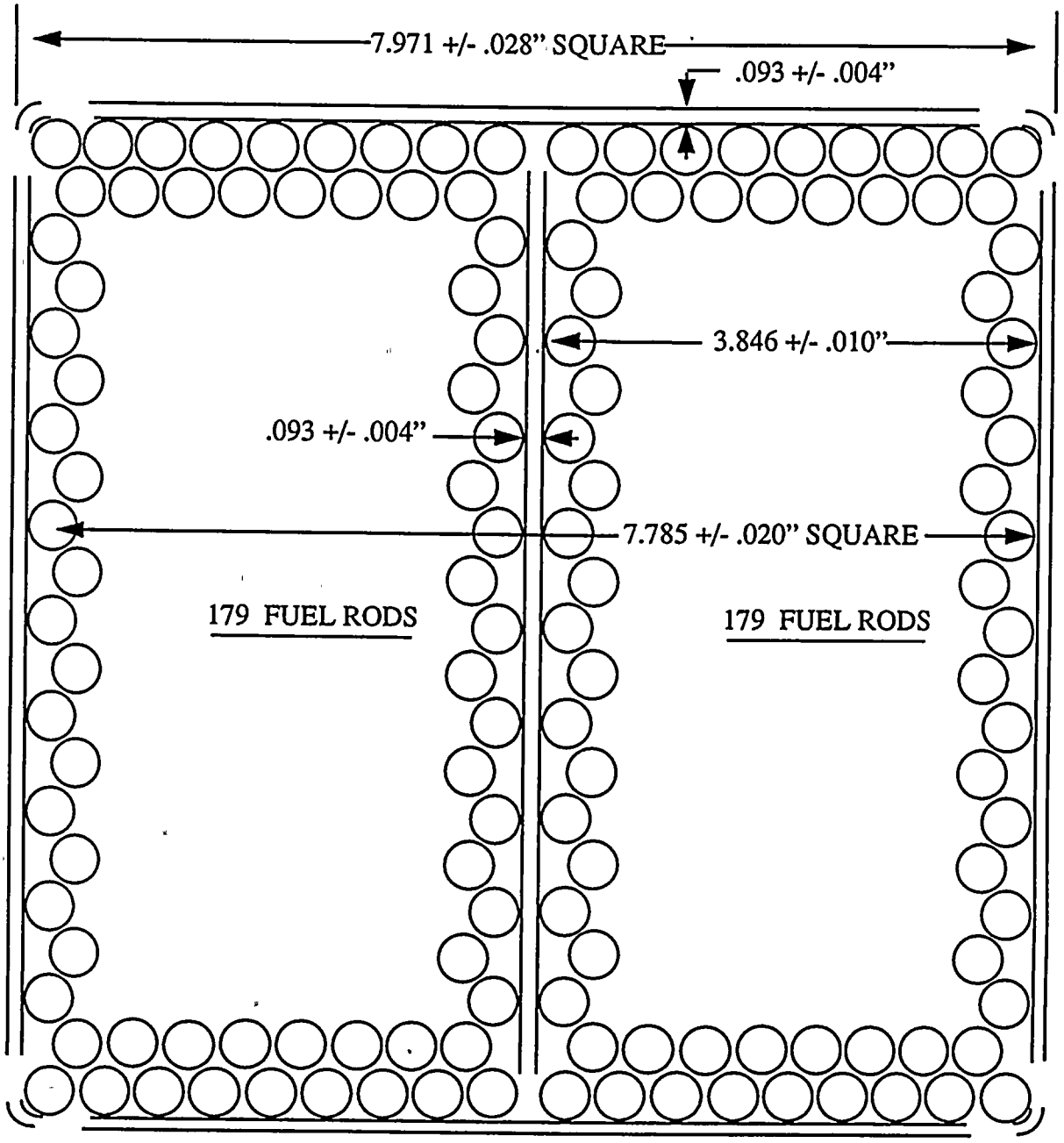

Figure 6. Ginna Schematic for Consolidated Rod Storage Canister

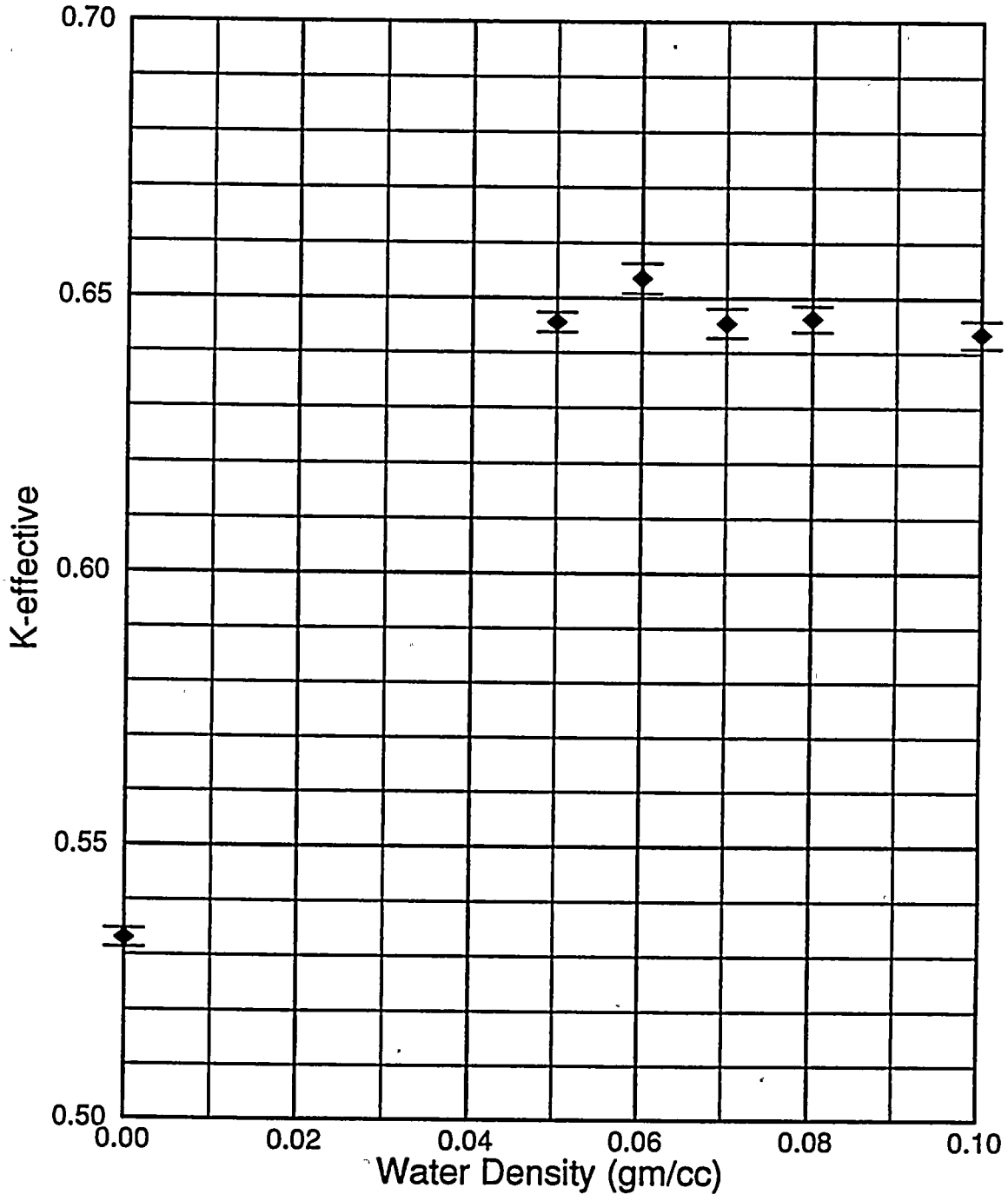

Note: Error Bars Represent a 95/95 Tolerance About The KENO K_{eff}

Figure 7. Ginna Fresh Fuel Rack Optimum Moderation Reactivity Sensitivity

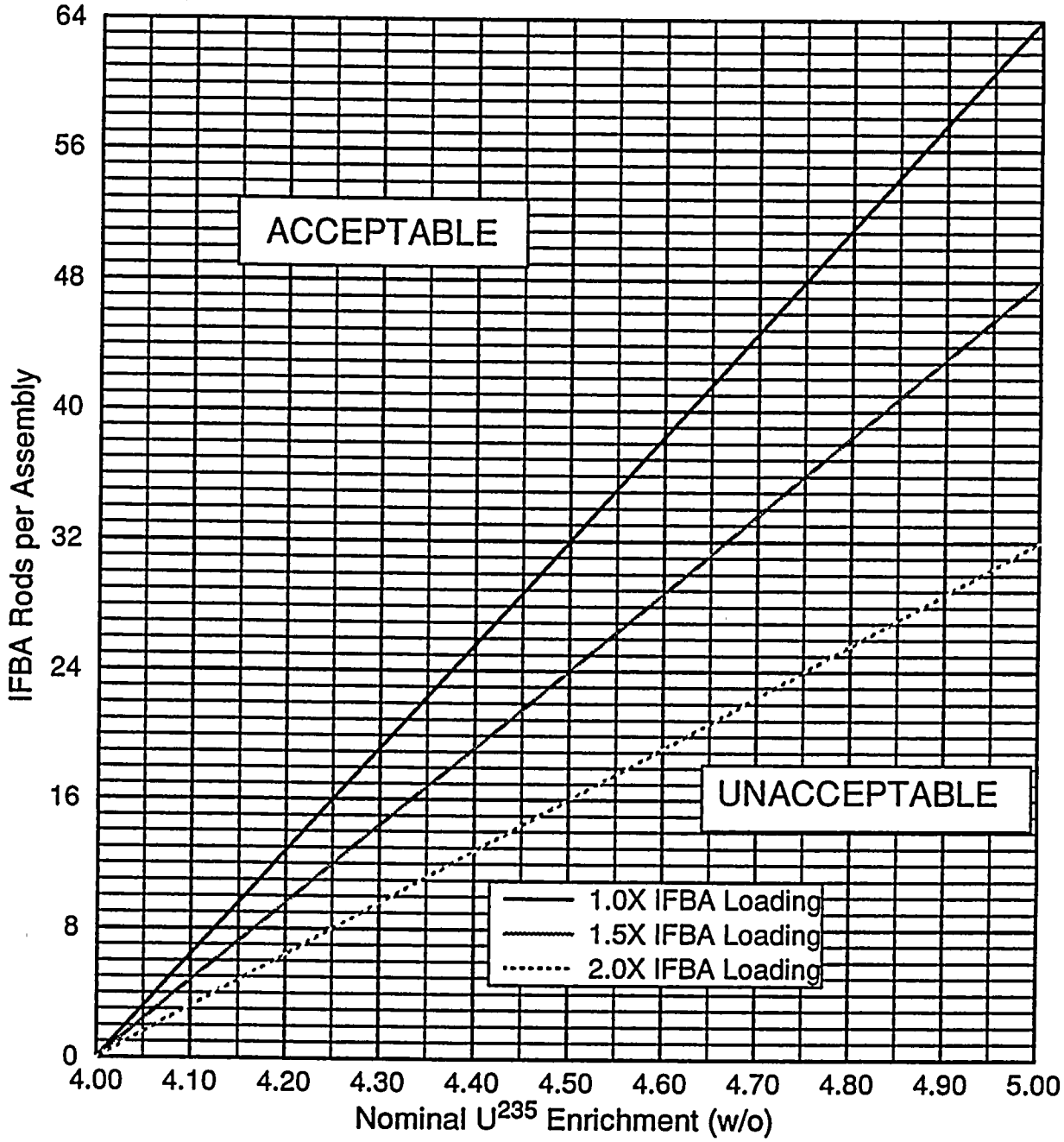

Figure 8. Ginna Region 1 Spent Fuel Rack IFBA Requirement

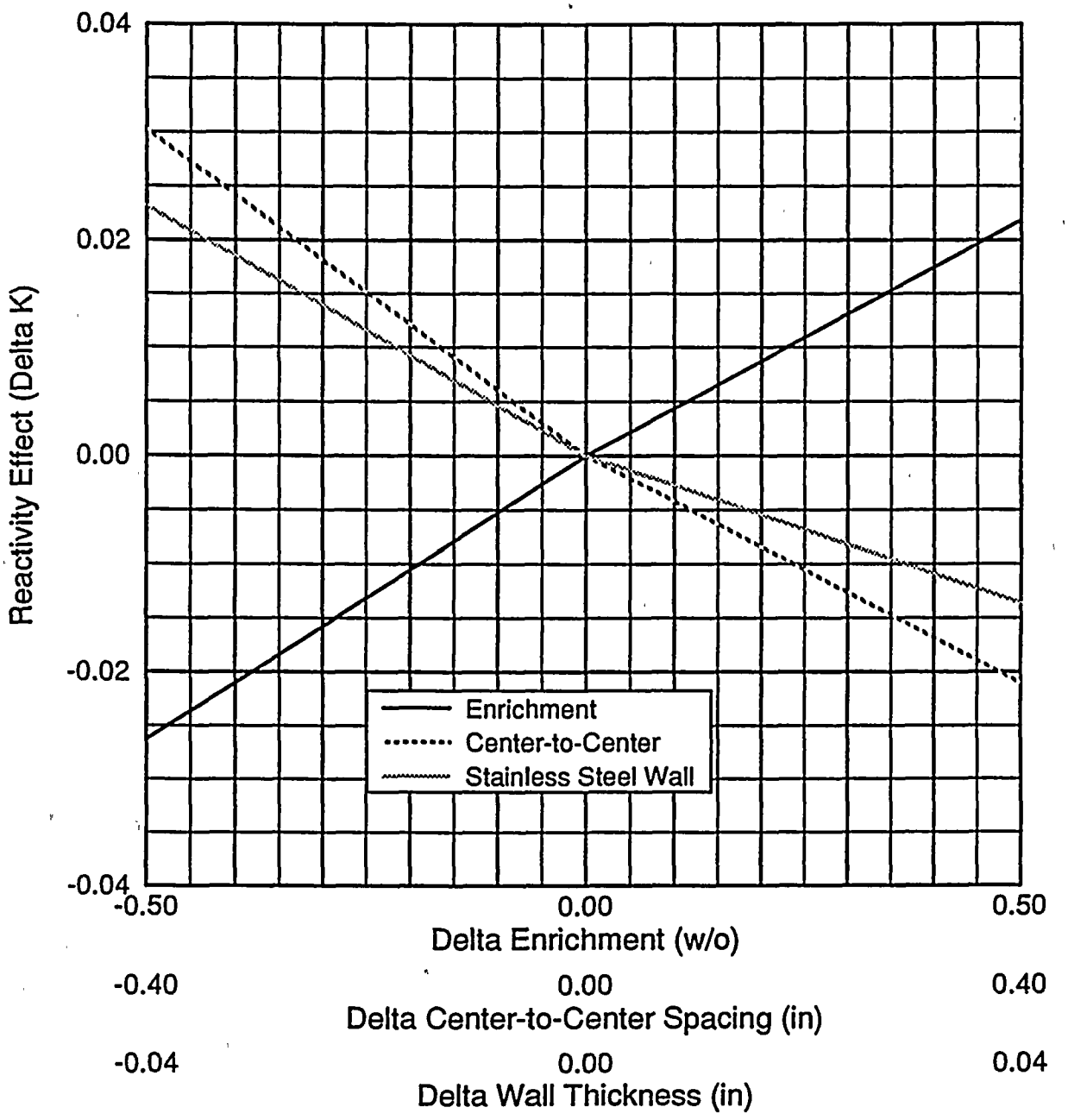

Figure 9. Ginna Region 1 Spent Fuel Reactivity Sensitivity

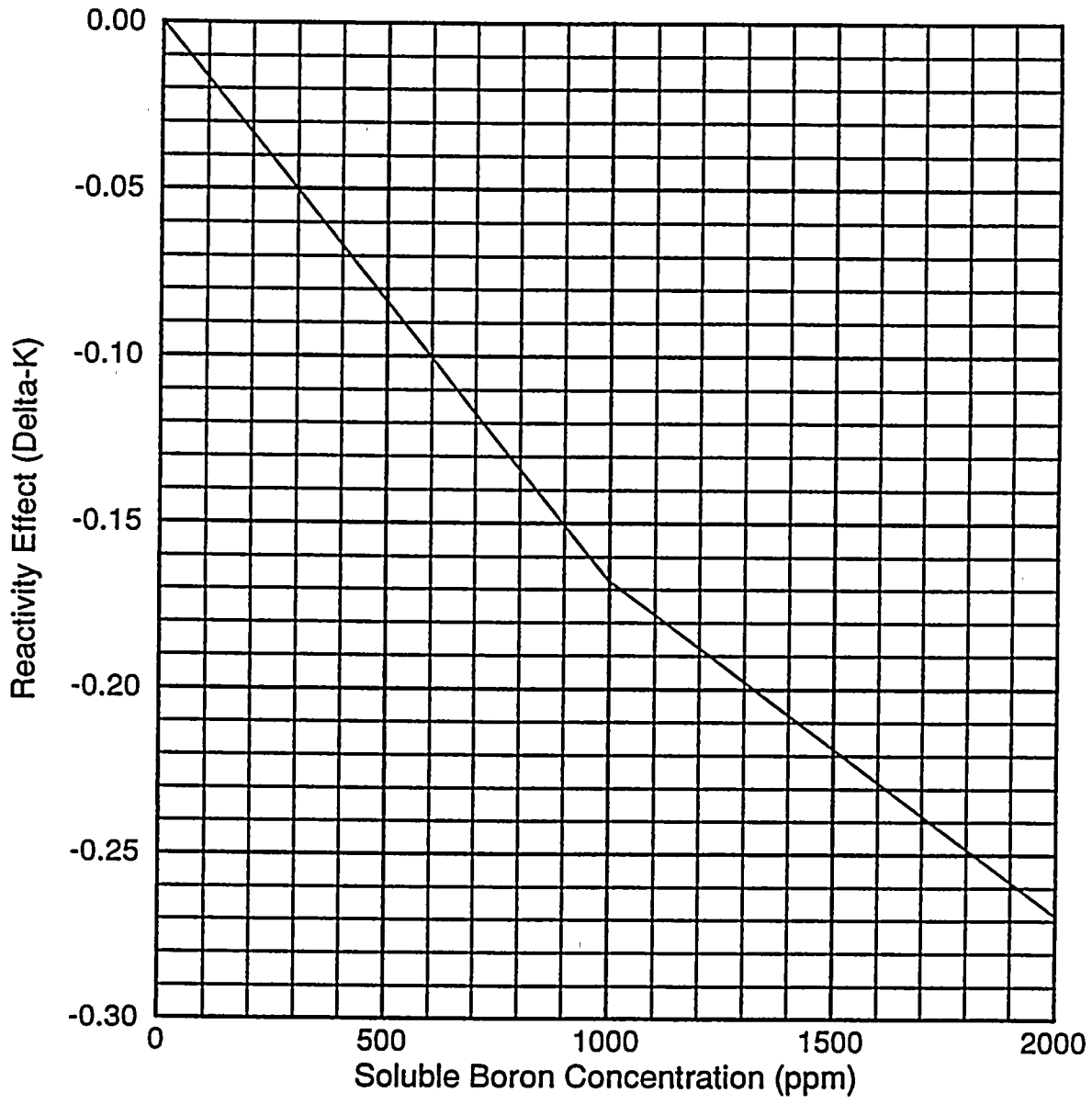

Figure 10. Ginna Region 1 Spent Fuel Rack Soluble Boron Worth

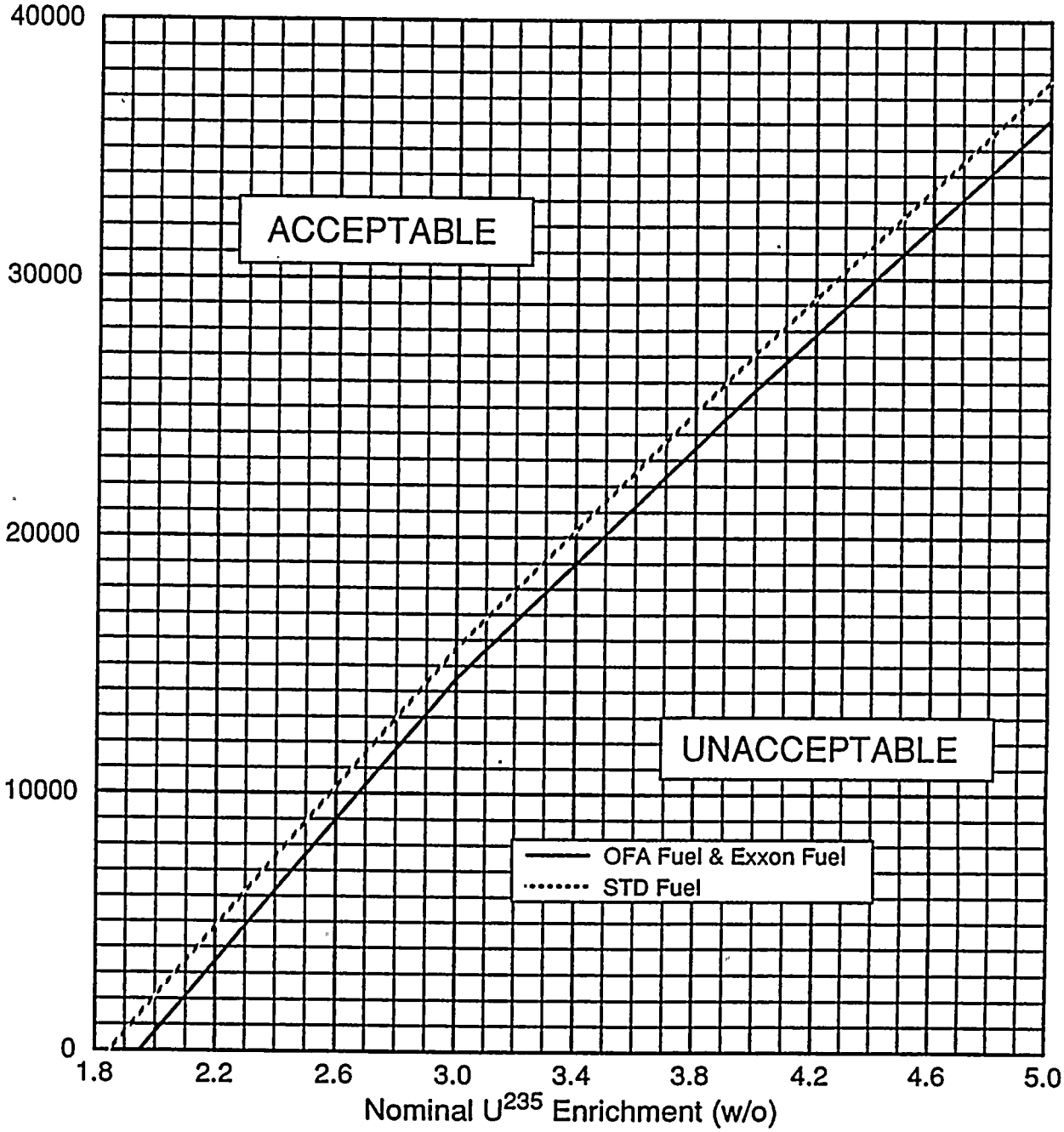

Figure 11. Ginna Region 2 Spent Fuel Rack Burnup Credit

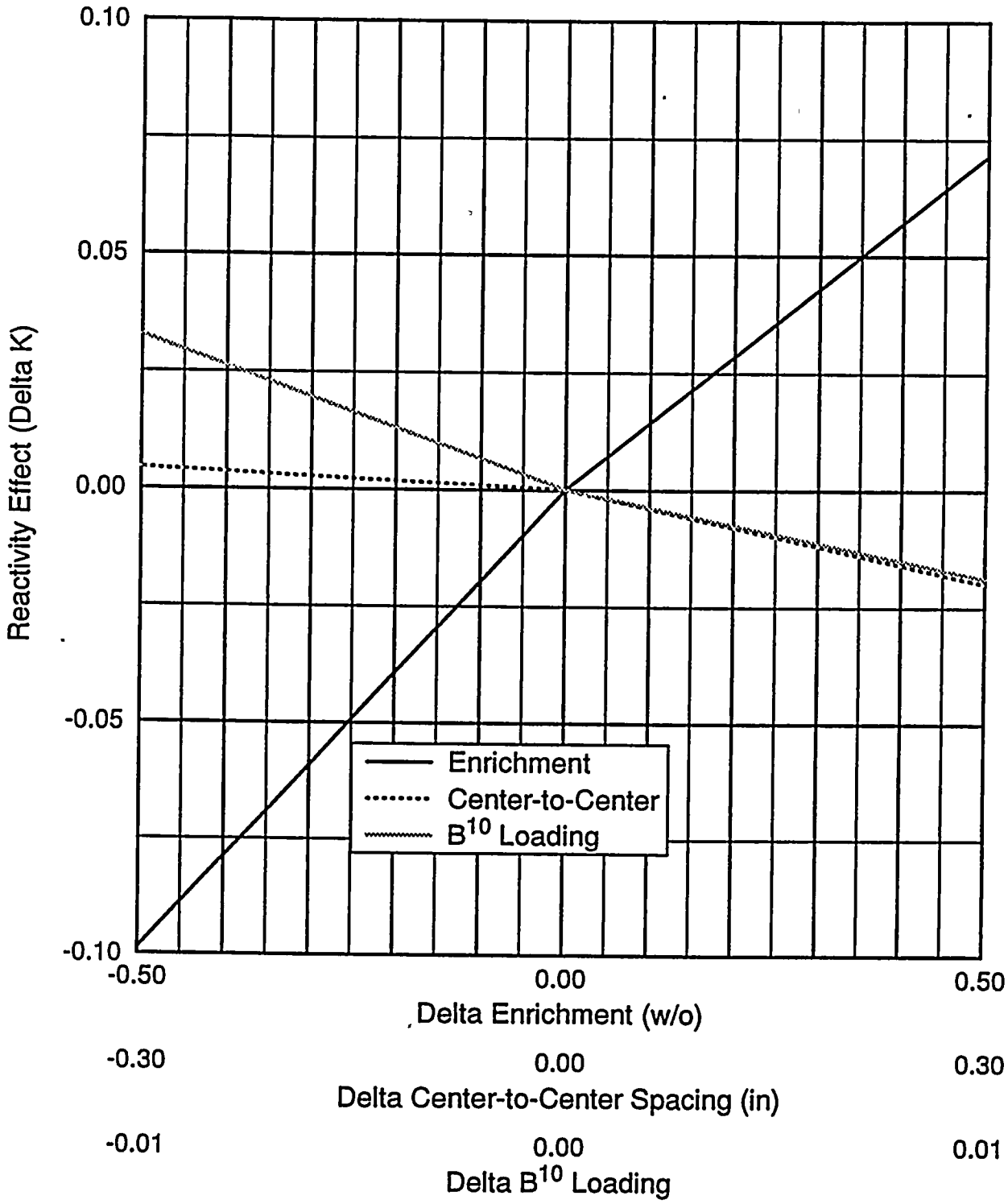

Figure 12. Ginna Region 2 Spent Fuel Rack Reactivity Sensitivity

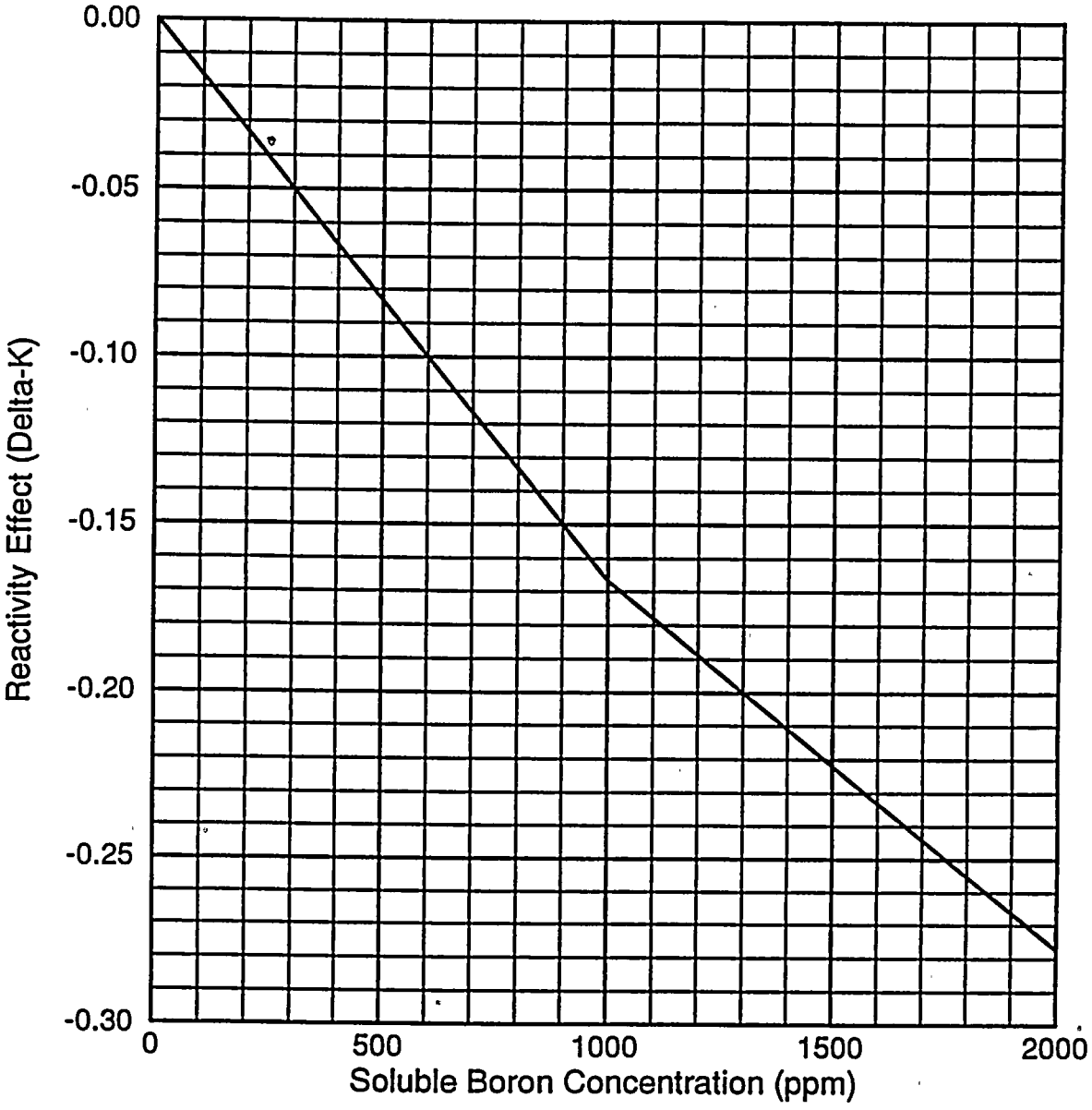

Figure 13. Ginna Region 2 Spent Fuel Rack Soluble Boron Worth

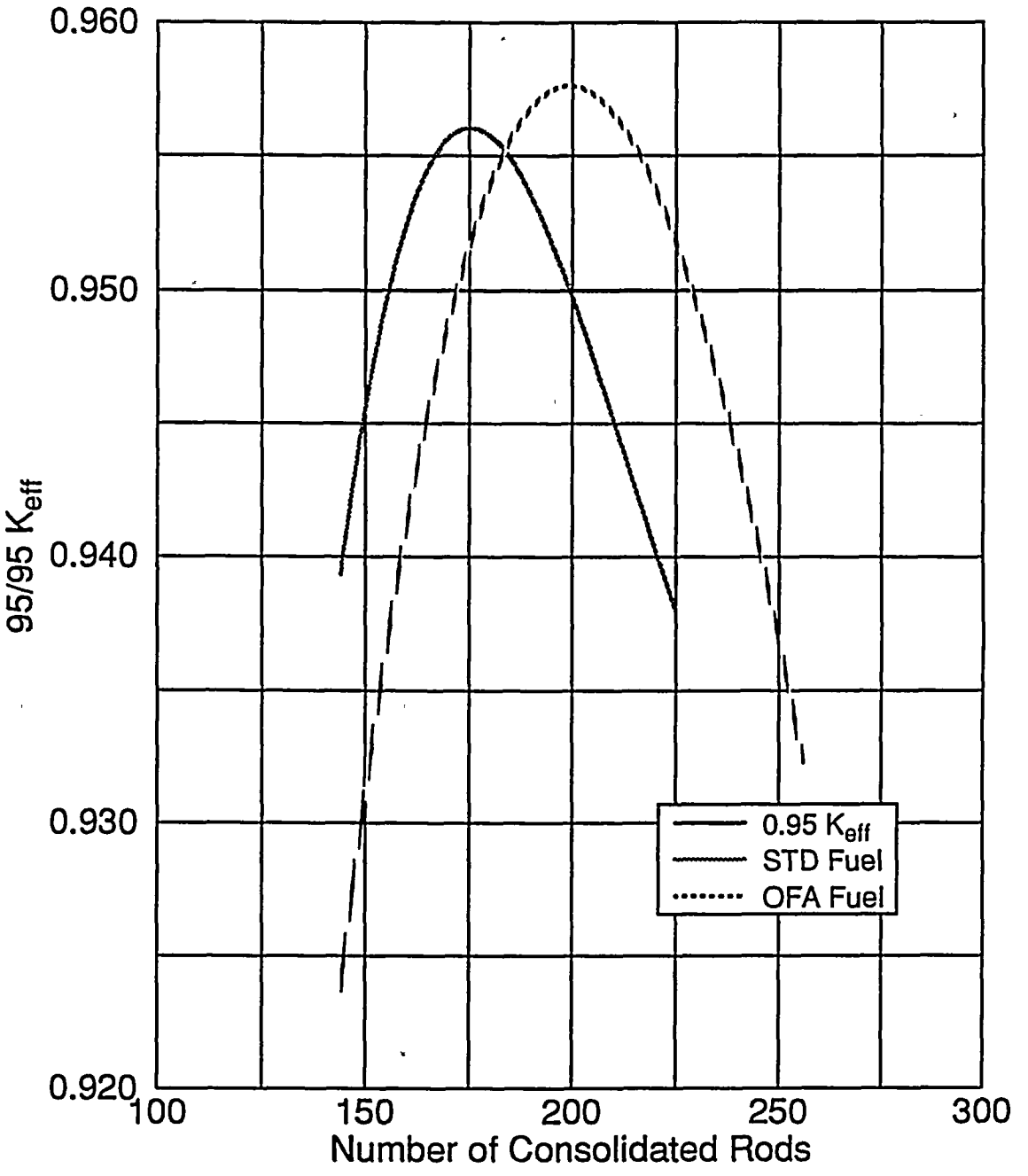

Figure 14. Ginna Reactivity of Consolidated Rods

Bibliography

1. Nuclear Regulatory Commission, Letter to All Power Reactor Licensees from B. K. Grimes, *OT Position for Review and Acceptance of Spent Fuel Storage and Handling Applications*, April 14, 1978.

2. W. E. Ford III, *CSRL-V: Processed ENDF/B-V 227-Neutron-Group and Pointwise Cross-Section Libraries for Criticality Safety, Reactor and Shielding Studies*, ORNL/CSD/TM-160, June 1982.

3. N. M. Greene, *AMPX: A Modular Code System for Generating Coupled Multigroup Neutron-Gamma Libraries from ENDF/B*, ORNL/TM-3706, March 1976.

4. L. M. Petrie and N. F. Landers, *KENO Va--An Improved Monte Carlo Criticality Program With Supergrouping*, NUREG/CR-0200, December 1984.

5. M. N. Baldwin, *Critical Experiments Supporting Close Proximity Water Storage of Power Reactor Fuel*, BAW-1484-7, July 1979.

6. S. R. Bierman and E. D. Clayton, *Criticality Separation Between Subcritical Clusters of 2.35 wt%235U Enriched UO2 Rods in Water with Fixed Neutron Poisons*, PNL-2438, October 1977.

7. S. R. Bierman and E. D. Clayton, *Criticality Separation Between Subcritical Clusters of 4.29 wt%235U Enriched UO2 Rods in Water with Fixed Neutron Poisons*, PNL-2615, August 1979.

8. S. R. Bierman and E. D. Clayton, *Criticality Experiments with Subcritical Clusters of 2.35 wt% and 4.31 wt% 235U Enriched UO2 Rods in Water at a Water-to-Fuel Volume Ratio of 1.6*, PNL-3314, July 1980.

9. J. T. Thomas, *Critical Three-Dimensional Arrays of U(93.2) Metal Cylinders*, Nuclear Science and Engineering, Volume 52, pages 350-359, 1973.

10. D. E. Mueller, W. A. Boyd, and M. W. Fecteau (Westinghouse NFD), *Qualification of KENO Calculations with ENDF/B-V Cross Sections*, American Nuclear Society Transactions, Volume 56, pages 321-323, June 1988.

11. Nguyen, T. Q. et. al., *Qualification of the PHOENIX-P/ANC Nuclear Design System for Pressurized Water Reactor Cores*, WCAP-11596-P-A, June 1988 (Westinghouse Proprietary).

12. England, T. R., *CINDER - A One-Point Depletion and Fission Product Program*, WAPD-TM-334, August 1962.

13. Melehan, J. B., *Yankee Core Evaluation Program Final Report*, WCAP-3017-6094, January 1971.

14. W. A. Boyd and D. E. Mueller (Westinghouse NFD), *Effects of Poison Panel Shrinkage and*

Gaps on Fuel Storage Rack Reactivity, American Nuclear Society Transactions, Volume 56, pages 323-324, June 1988.

15. Davidson, S.L., et al, *VANTAGE 5 Fuel Assembly Reference Core Report, Addendum 1,* WCAP-10444-P-A, March 1986.

16. W. A. Boyd and M. W. Fecteau (Westinghouse NFD), *Effect of Axial Burnup on Fuel Storage Rack Burnup Credit Reactivity,* American Nuclear Society Transactions, Volume 62, Pages 328-329, November 1990.

Attachment B

WCAP-14040, Revision 1

WESTINGHOUSE CLASS 3 (Non-Proprietary)

WCAP-14040

METHODOLOGY USED TO DEVELOP COLD OVERPRESSURE MITIGATING SYSTEM SETPOINTS AND RCS HEATUP AND COOLDOWN LIMIT CURVES

WOG Program
MUHP-3024
Revision 1

J. D. Andrachek
S. M. DiTommaso
M. J. Malone
M. C. Rood

December 1994

WESTINGHOUSE ELECTRIC CORPORATION
Nuclear Technology Division
P.O. Box 355
Pittsburgh, Pennsylvania 15230-0355

TABLE OF CONTENTS

LIST OF FIGURES

1.0 INTRODUCTION

1.1 BACKGROUND

The concept of a PRESSURE AND TEMPERATURE LIMITS REPORT (PTLR) was introduced into the Technical Specifications during the development of NUREG 1431[1], Standard Technical Specifications for Westinghouse PWRs and is consistent with the philosophy of NRC Generic Letter 88-16[2]. The PTLR is similar to the Core Operating Limits Report (COLR), which is currently licensed for several plants and also contained in NUREG 1431. The COLR contains core related limit values which may change from cycle to cycle as they are related to a cycle specific core design. In the same way, a PTLR contains reactor vessel material related limits which may change every fluence cycle as they are related to reactor vessel material and strength. Implementation of the PTLR will allow licensees to relocate their RCS heatup and cooldown curves and COMS setpoints currently contained in the Technical Specifications to the PTLR. Additionally, the Vessel Fluence and Materials tables contained in the Technical Specifications or Bases can be relocated to licensee controlled documents. This process will allow changes to these tables, figures and values to be made without making a License Amendment Request (LAR). These figures are typically revised due to changes in the nil ductility reference temperature (RT_{NDT}), regulations and surveillance capsule withdrawal.

1.2 PURPOSE OF TOPICAL REPORT

In order to implement the PTLR, the analytical methods used to develop the pressure and temperature limits must be consistent with those previously reviewed and approved by the NRC and must be referenced in the Administrative Controls section of the Technical Specifications. Currently, there is no Westinghouse topical report that contains an NRC approved methodology for developing the RCS heatup and cooldown curves and COMS setpoints that can be referenced to implement the PTLR. The purpose of this report is to provide the current Westinghouse methodology for developing the RCS heatup and cooldown curves and COMS

setpoints. When approved by the NRC, this methodology may be referenced by licensees to implement the PTLR.

This topical report does not provide all of the methodologies which can be used to develop RCS heatup and cooldown curves and COMS setpoints but rather a methodology that can be referenced by licensees when approved by the NRC to license the PTLR concept.

1.3 CONTENT OF TOPICAL REPORT

This report contains the methodology used to develop the RCS heatup and cooldown curves in Section 2.0 and the methodology used to develop the COMS setpoints in Section 3.0. The methodology used to develop the COMS enable temperature is also discussed in Section 3.0.

2.0 PRESSURE-TEMPERATURE LIMIT CURVES

2.1 INTRODUCTION

Heatup and cooldown limit curves are calculated using the most limiting value of RT_{NDT} (reference nil-ductility transition temperature) corresponding to the limiting material in the beltline region of the reactor vessel. The most limiting RT_{NDT} of the material in the core (beltline) region of the reactor vessel is determined by using the unirradiated reactor vessel material fracture toughness properties and estimating the irradiation-induced shift (ΔRT_{NDT}). The unirradiated RT_{NDT} is defined as the higher of either the drop weight nil-ductility transition temperature (NDTT) or the temperature at which the material exhibits at least 50 ft-lb of impact energy and 35-mil lateral expansion (both normal to the major working direction) minus 60°F.

RT_{NDT} increases as the material is exposed to fast-neutron irradiation. Therefore, to find the most limiting RT_{NDT} at any time period in the reactor's life, ΔRT_{NDT} due to the radiation exposure associated with that time period must be added to the original unirradiated RT_{NDT}. The extent of the shift in RT_{NDT} is enhanced by certain chemical elements (such as copper and nickel) present in reactor vessel steels. The Nuclear Regulatory Commission (NRC) has published a method for predicting radiation embrittlement in Regulatory Guide 1.99, Revision 2 (Radiation Embrittlement of Reactor Vessel Materials)[3]. Regulatory Guide 1.99, Revision 2, is used for the calculation of adjusted reference temperature (ART) values (irradiated RT_{NDT} with margins for uncertainties) at 1/4t and 3/4t locations. "t" is the thickness of the vessel at the beltline region measured from the clad/base metal interface (Note, thickness of cladding is neglected as specified in the ASME Code, Section III, paragraph NB-3122.3). Using the adjusted reference temperature values, pressure-temperature limit curves are determined in accordance with the requirements of Appendix G, 10 CFR Part 50[4], as augmented by Appendix G, Section XI of the American Society of Mechanical Engineers Boiler and Pressure Vessel (ASME B&PV) Code[5]. The procedure for establishing the pressure-temperature limits is entirely deterministic. The conservatisms included in the limits are (but not limited to):

- An assumed flaw in the wall of the reactor vessel has a depth equal to 1/4 of the thickness of the vessel wall and a length equal to 1-1/2 times the vessel wall thickness,

- A factor of 2 is applied to the membrane stress intensity factor (K_{IM}),

- The limiting toughness is based upon a reference value (K_{Ia}), which is a lower bound of the dynamic crack initiation or arrest toughnesses, and

- 2-sigma margins are applied in determining the adjusted reference temperature (ART).

This section describes the methodology used by Westinghouse Electric Corporation to develop the allowable pressure-temperature relationships for normal plant heatup and cooldown rates that are included in the Pressure-Temperature Limits Report (PTLR). First, the methodology describing how the neutron fluence is calculated for the reactor vessel beltline materials is provided. Next, sections describing fracture toughness properties, adjusted reference temperature calculation, criteria for allowable pressure-temperature relationships, and pressure-temperature curve generation are provided.

2.2 NEUTRON FLUENCE METHODOLOGY

In performing the fast neutron exposure evaluations for a reactor vessel, two distinct sets of transport calculations are typically carried out. The first set, a computation in the conventional forward mode, is used to obtain the neutron fluence rate and relative neutron energy distributions at all locations between the core and the outside of the reactor vessel. The neutron spectral information is required for the interpretation of neutron dosimetry withdrawn from the surveillance capsules for validation of the plant specific calculations.

The second set of calculations consists of a series of adjoint analyses relating the fast neutron flux, $\phi(E > 1.0$ MeV), at various vessel positions to neutron source

distributions within the reactor core. The source importance functions generated from these adjoint analyses provide the basis for all absolute exposure calculations and comparison with measurement. These importance functions, when combined with fuel cycle specific neutron source distributions, yield absolute predictions of neutron exposure at the locations of interest for each cycle of irradiation. It is important to note that the cycle specific neutron source distributions utilized in these analyses include not only spatial variations of fission rates within the reactor core but also account for the effects of varying neutron yield per fission and fission spectrum introduced by the build-up of plutonium as the burnup of individual fuel assemblies increases. The detailed cycle-by-cycle variation of the neutron flux is generally calculated for the maximum flux position and each weld location on the inside of the reactor vessel. Axial calculations are normally not necessary since the maximum beltline fluence is desired. If axial fluence variation is needed, this can be estimated from the axial core power shape or an R,Z calculation can be carried out.

The forward transport calculation for each reactor model is carried out in R,θ geometry using the DOT two-dimensional discrete ordinates code[6] and the SAILOR cross-section library[7]. The SAILOR library is a 47 energy group ENDF/B-IV based data set produced specifically for light water reactor applications. In these analyses, anisotropic scattering is treated with a P_3 (3rd order Legendre polynomial) expansion of the scattering cross-sections and the angular discretization is modeled with an S_8 order of angular quadrature (48 angular directions). Each model is of a one-eighth core segment containing the surveillance capsules. The source distribution is taken to be an average distribution with all fissions attributed to U-235.

All adjoint calculations are carried out using an S_8 order of angular quadrature and the P_3 cross-section approximation from the SAILOR library. The adjoint calculations are run in R,θ geometry to provide neutron source distribution importance functions for the exposure parameter of interest, in this case $\phi(E > 1.0\ MeV)$.

Having the importance functions and appropriate core source distributions, the response of interest is calculated as:

$$R(r,\theta) = \int_{r'} \int_{\theta'} \int_{E} I(r',\theta',E)\, S(r',\theta',E)\, r'\, dr'\, d\theta'\, dE \qquad (2.2\text{-}1)$$

where:

$R(r,\theta)$ = $\phi(E > 1.0$ MeV) at radius r and azimuthal angle θ,

$I(r',\theta',E)$ = Adjoint source importance function at radius r', azimuthal angle, θ', and neutron source energy E for the flux ($E > 1$ MeV) at location r, θ,

$S(r',\theta',E)$ = Neutron source strength at core location r',θ' for energy E.

Although the adjoint importance functions used in the analysis are based on a response function defined by the threshold neutron flux, $\phi(E > 1.0$ MeV), the results of the response calculations indicate that while the variation in fuel loading patterns significantly affects both the magnitude and spatial distribution of the neutron field, changes in the relative neutron energy spectrum are of second order. Thus, the adjoint calculations can be used, together with the neutron spectrum from the forward calculation, to determine other exposure parameters such as displacements per atom (dpa), and threshold dosimetry reaction rates.

In addition to locations at the inner surface of the reactor vessel, adjoint calculations are also carried out for dosimetry locations. These locations are chosen at the geometric center of each surveillance capsule and at cavity dosimetry locations. The capsule center location is used to determine the calculated average exposure of the surveillance specimens. For the Westinghouse capsule design, axial fluence variation is small and is neglected.

The calculated fluence is validated by comparison with benchmark and plant specific measurements, which may include dosimetry from one or more surveillance capsules and, for some plants, reactor cavity dosimetry. On the average, for

Westinghouse plants, surveillance capsule dosimetry indicates that the fluence calculations are biased low. For conservatism, the fluence values used for vessel analyses of pressure-temperature heatup and cooldown limit curves are adjusted by the average bias indicated by the dosimetry measurements for that plant. The methodology used for calculation of neutron fluences is basically consistent with the proposed Regulatory Guide on Reactor Vessel Fluence (DG-1025).

In general, pressure-temperature limits are generated for a particular EFPY (effective full power years) of plant operation. In some cases the fluence at the EFPY of interest is obtained directly from the dosimetry analysis. However, if the fluence is not available from the dosimetry analysis, the peak vessel inner radius fluence at the EFPY of interest is calculated as follows:

$$f = F \times C \times E \qquad (2.2\text{-}2)$$

Where:

- f = the peak vessel inner radius fluence at the EFPY of interest (n/cm^2 ($E > 1.0$ MeV))
- F = Best estimate peak flux at the pressure vessel inner radius (n/cm^2 - sec ($E > 1.0$ MeV))
- C = seconds per year = 3.16×10^7 sec/yr
- E = EFPY of interest

2.3 FRACTURE TOUGHNESS PROPERTIES

The fracture toughness properties of the ferritic material in the reactor coolant pressure boundary are determined in accordance with the requirements of Appendix G, 10 CFR Part 50[4], as augmented by the additional requirements in subsection NB-2331 of Section III of the ASME B&PV Code[8]. These fracture toughness requirements are also summarized in Branch Technical Position MTEB 5-2 ("Fracture Toughness Requirements")[9] of the NRC Regulatory Standard Review Plan.

These fracture toughness requirements are used to determine the value of the reference nil-ductility transition temperature (RT_{NDT}) for unirradiated material (defined as initial RT_{NDT}, IRT_{NDT}) and to calculate the adjusted reference temperature (ART) as described in Section 2.4. Two types of tests are required to determine a material's value of IRT_{NDT}: Charpy V-notch impact (C_v) tests and drop-weight tests. The procedure is as follows:

1) Determine a temperature T_{NDT} that is at or above the nil-ductility transition temperature by drop weight tests.
2) At a temperature not greater than T_{NDT} + 60°F, each specimen of the C_v test shall exhibit at least 35 mils lateral expansion and not less than 50 ft-lb absorbed energy. When these requirements are met, T_{NDT} is the reference temperature RT_{NDT}.
3) If the requirements of (2) above are not met, conduct additional C_v tests in groups of three specimens to determine the temperature T_{Cv} at which they are met. In this case the reference temperature $RT_{NDT} = T_{Cv}$ - 60°F. Thus, the reference temperature RT_{NDT} is the higher of T_{NDT} and (T_{Cv} - 60°F).
4) If the C_v test has not been performed at T_{NDT} + 60°F, or when the C_v test at T_{NDT} + 60°F does not exhibit a minimum of 50 ft-lb and 35 mils lateral expansion, a temperature representing a minimum of 50 ft-lb and 35 mils lateral expansion may be obtained from a full C_v impact curve developed from the minimum data points of all the C_v tests performed as shown in Figure 2.1.

Plants that do not follow the fracture toughness requirements in Branch Technical Position MTEB 5-2 to determine IRT_{NDT} can use alternative procedures. However, sufficient technical justification must be provided for an exemption from the regulations to be granted by the NRC. For example, a study done by B&W Nuclear Technologies[11] used an alternative method to define the IRT_{NDT} value for WF-70 weld metal. Since use of the MTEB 5-2 procedures resulted in a wide scatter of IRT_{NDT} values for WF-70 weld metal, a Linde 80 low upper-shelf material, an alternative method based solely on drop-weight tests was defined for determining

IRT_{NDT} values of WF-70 weld metal. The use of this methodology was approved by the NRC[12] for Commonwealth Edison Company's Zion Units 1 and 2.

2.4 CALCULATION OF ADJUSTED REFERENCE TEMPERATURE

The adjusted reference temperature (ART) for each material in the beltline region is calculated in accordance with Regulatory Guide 1.99, Revision 2[3]. The most limiting ART values (i.e., highest value at 1/4t and 3/4t locations) are used in determining the pressure-temperature limit curves. ART is calculated by the following equation:

$$ART = IRT_{NDT} + \Delta RT_{NDT} + Margin \qquad (2.4\text{-}1)$$

IRT_{NDT} is the reference temperature for the unirradiated material as defined in paragraph NB-2331 of Section III of the ASME Boiler and Pressure Vessel Code[8] and calculated per Section 2.3. If measured values of IRT_{NDT} are not available for the material in question, generic mean values for that class of material can be used if there are sufficient test results to establish a mean and standard deviation for the class.

ΔRT_{NDT} is the mean value of the shift in reference temperature caused by irradiation and is calculated as follows:

$$\Delta RT_{NDT} = CF * f^{(0.28 - 0.10 \log f)} \qquad (2.4\text{-}2)$$

CF (°F) is the chemistry factor and is a function of copper and nickel content. CF is given in Table 1 of Reference 3 for weld metal and in Table 2 in Reference 3 for base metal (Position 1.1 of Regulatory Guide 1.99, Revision 2). In Tables 1 and 2 of Reference 3 "weight-percent copper" and "weight-percent nickel" are the best-estimate values for the material and linear interpolation is permitted. When two or more credible surveillance data sets (as defined in Regulatory Guide 1.99, Revision 2, Paragraph B.4) become available they may be used to calculate the chemistry factor per Position 2.1 of Regulatory Guide 1.99, Revision 2, as follows:

$$CF = \frac{\sum_{i=1}^{n} [A_i \times f_i^{(0.28-0.10\log fi)}]}{\sum_{i=1}^{n} [f_i^{(0.28-0.10\log fi)}]^2} \qquad (2.4\text{-}3)$$

Where "n" is the number of surveillance data points, "A_i" is the measured value of ΔRT_{NDT} and "f_i" is the fluence for each surveillance data point.

If Position 2.1 of Regulatory Guide 1.99, Revision 2, results in a higher value of ART than Position 1.1 of Regulatory Guide 1.99, Revision 2, the ART calculated per Position 2.1 must be used. However, if Position 2.1 of Regulatory Guide 1.99, Revision 2, results in a lower value of ART than Position 1.1 of Regulatory Guide 1.99, Revision 2, either value of ART may be used.

To calculate ΔRT_{NDT} at any depth (e.g., at 1/4t or 3/4t), the following formula is used to attenuate the fast neutron fluence (E>1 MeV) at the specified depth.

$$f = f_{surface} * e^{(-0.24x)} \qquad (2.4\text{-}4)$$

where $f_{surface}$(n/cm^2, E>1 MeV) is the value, calculated per Section 2.2, of the neutron fluence at the base metal surface of the vessel at the location of the postulated defect, and x (in inches) is the depth into the vessel wall measured from the vessel clad/base metal interface. The resultant fluence is then put into equation (2.4-2) to calculate ΔRT_{NDT} at the specified depth.

When two or more credible surveillance capsules have been removed, the measured increase in reference temperature (ΔRT_{NDT}) must be compared to the predicted increase in RT_{NDT} for each surveillance material. The predicted increase in RT_{NDT} is the mean shift in RT_{NDT} calculated by equation (2.4-2) plus two standard deviations ($2\sigma_\Delta$) specified in Regulatory Guide 1.99, Revision 2. If the measured value exceeds the predicted value ($\Delta RT_{NDT} + 2\sigma_\Delta$), a supplement to the PTLR must be provided to demonstrate how the results affect the approved methodology.

Margin is the temperature value that is included in the ART calculations to obtain conservative, upper-bound values of ART for the calculations required by Appendix G to 10 CFR Part 50[4]. Margin is calculated by the following equation:

$$\text{Margin} = 2\sqrt{(\sigma_I^2 + \sigma_\Delta^2)} \qquad (2.4\text{-}5)$$

σ_I is the standard deviation for IRT_{NDT} and σ_Δ is the standard deviation for ΔRT_{NDT}. If IRT_{NDT} is a measured value, σ_I is estimated from the precision of the test method ($\sigma_I = 0$ for a measured IRT_{NDT} of a single material). If IRT_{NDT} is not a measured value and generic mean values for that class of material are used, σ_I is the standard deviation obtained from the set of data used to establish the mean. Per Regulatory Guide 1.99, σ_Δ is 28°F for welds and 17°F for base metal. When surveillance data is used to calculate ΔRT_{NDT}, σ_Δ values may be reduced by one-half. In all cases, σ_Δ need not exceed half of the mean value of ΔRT_{NDT}.

2.5 CRITERIA FOR ALLOWABLE PRESSURE-TEMPERATURE RELATIONSHIPS

The ASME Code requirements[5] for calculating the allowable pressure-temperature limit curves for various heatup and cooldown rates specify that the total stress intensity factor, K_I, for the combined thermal and pressure stresses at any time during heatup or cooldown cannot be greater than the reference stress intensity factor, K_{Ia}, for the metal temperature at that time. K_{Ia} is obtained from the reference fracture toughness curve, defined in Appendix G, to Section XI of the ASME Code[5]. (Note that in Appendix G, to Section III of the ASME Code, the reference fracture toughness is denoted as K_{IR}, whereas in Appendix G of Section XI, the reference fracture toughness is denoted as K_{Ia}. However, the K_{IR} and K_{Ia} curves are identical and are defined with the identical functional form.) The K_{Ia} curve is given by the following equation:

$$K_{Ia} = 26.78 + 1.223 * \exp [0.0145 (T\text{-}RT_{NDT} + 160)] \qquad (2.5\text{-}1)$$

where,

K_{Ia} = reference stress intensity factor as a function of the metal temperature T and the metal reference nil-ductility transition temperature RT_{NDT}, (ksi $\sqrt{in}$). The value of RTNDT is the adjusted reference temperature (ART) of Section 2.4.

The governing equation for generating pressure-temperature limit curves is defined in Appendix G of the ASME Code[5] as follows:

$$C * K_{IM} + K_{IT} < K_{Ia} \qquad (2.5\text{-}2)$$

where,

K_{IM} = stress intensity factor caused by membrane (pressure) stress,

K_{IT} = stress intensity factor caused by the thermal gradients through the vessel wall,

C = 2.0 for Level A and Level B service limits (for heatup and cooldown),

C = 1.5 for hydrostatic and leak test conditions when the reactor core is not critical

(Note: K_{IT} is set to zero for hydrostatic and leak test calculations since these tests are performed at isothermal conditions).

At specific times during the heatup or cooldown transient, K_{Ia} is determined by the metal temperature at the tip of the postulated flaw (the postulated flaw has a depth of one-fourth of the section thickness and a length of 1.5 times the section

thickness per ASME Code, Section XI, paragraph G-2120), the appropriate value for RT_{NDT} at the same location, and the reference fracture toughness equation (2.5-1). The thermal stresses resulting from the temperature gradients through the vessel wall and the corresponding (thermal) stress intensity factor, K_{IT}, for the reference flaw are calculated as described in Section 2.6. From Equation (2.5-2), the limiting pressure stress intensity factors are obtained and, from these, the allowable pressures are calculated as described in Section 2.6.

For the calculation of the allowable pressure versus coolant temperature during cooldown, the reference 1/4t (t=reactor vessel wall thickness) flaw of Appendix G, Section XI to the ASME Code is assumed to exist at the inside of the vessel wall. During cooldown, the controlling location of the flaw is always at the inside of the vessel wall because the thermal gradients that increase with increasing cooldown rates produce tensile stresses at the inside surface that would tend to open (propagate) the existing flaw. Allowable pressure-temperature curves are generated for steady-state (zero rate) and each finite cooldown rate specified. From these curves, composite limit curves are constructed as the minimum of the steady-state or finite rate curve for each cooldown rate specified.

The use of the composite curve in the cooldown analysis is necessary because control of the cooldown procedure is based on the measurement of reactor coolant temperature, whereas the limiting pressure is actually dependent on the material temperature at the tip of the assumed flaw. During cooldown, the 1/4t vessel location is at a higher temperature than the fluid adjacent to the vessel inner diameter. This condition, of course, is not true for the steady-state situation. It follows that, at any given reactor coolant temperature, the temperature difference across the wall developed during cooldown results in a higher value of K_{Ia} at the 1/4t location for finite cooldown rates than for steady-state operation. Furthermore, if conditions exist so that the increase in K_{Ia} exceeds K_{IT}, the calculated allowable pressure during cooldown will be greater than the steady-state value.

The above procedures are needed because there is no direct control on temperature at the 1/4t location and, therefore, allowable pressures could be lower if the rate

of cooling is decreased at various intervals along a cooldown ramp. The use of the composite curve eliminates this problem and ensures conservative operation of the system for the entire cooldown period.

Three separate calculations are required to determine the limit curves for finite heatup rates. As is done in the cooldown analysis, allowable pressure-temperature relationships are developed for steady-state conditions as well as finite heatup rate conditions assuming the presence of a 1/4t flaw at the inside of the wall. The heatup results in compressive stresses at the inside surface that alleviate the tensile stresses produced by internal pressure. The metal temperature at the crack tip lags the coolant temperature; therefore, the K_{Ia} for the inside 1/4t flaw during heatup is lower than the K_{Ia} for the same flaw during steady-state conditions at the same coolant temperature. However, conditions may exist so that the effects of compressive thermal stresses and lower K_{Ia}'s do not offset each other and the pressure-temperature curve based on finite heatup rates could become limiting. Therefore, both cases have to be analyzed in order to ensure that at any coolant temperature, the lower value of the allowable pressure calculated for steady-state and finite heatup rates is obtained for the inside 1/4t flaw.

The third portion of the heatup analysis concerns the calculation of the pressure-temperature limitations for the case of a 1/4t outside surface flaw. Unlike the situation at the vessel inside surface, the thermal gradients established at the outside surface during heatup produce stresses which are tensile in nature and therefore tend to reinforce any pressure stresses present. These thermal stresses are dependent on both the rate of heatup and coolant temperature during the heatup ramp. Since the thermal stresses at the outside are tensile and increase with increasing heatup rates, each heatup rate is analyzed on an individual basis.

Following the generation of the three pressure-temperature curves, the final limit curves are produced by constructing a composite curve based on a point-by-point comparison of the steady-state data and finite heatup rate data for both inside and outside surface flaws. At any given temperature, the allowable pressure is taken to be the lesser of the three values taken from the curves under consideration. The use of the composite curve is necessary to set conservative heatup limitations

because it is not possible to predict which condition is most limiting because of local differences in irradiation (RTNDT), metal temperature and thermal stresses. With the composite curve, the pressure limit is at all times based on analysis of the most critical situation.

Finally, the 1983 Amendment to 10CFR50[4] has a rule which addresses the metal temperature of the closure head flange and vessel flange regions. This rule states that the metal temperature of the closure flange regions must exceed the material unirradiated RT_{NDT} by at least 120°F for normal operation and 90°F for hydrostatic pressure tests and leak tests when the pressure exceeds 20 percent of the preservice hydrostatic test pressure. In addition, when the core is critical, the pressure-temperature limits for core operation (except for low power physics tests) require that the reactor vessel be at a temperature equal to or higher than the minimum temperature required for the inservice hydrostatic test, and at least 40°F higher than the minimum permissible temperature in the corresponding pressure-temperature curve for heatup and cooldown. These limits are incorporated into the pressure-temperature limit curves wherever applicable.

Figure 2.2 shows an example of a heatup curve using a heatup rate of 60°F/Hr applicable for the first 16 EFPY. Figure 2.3 shows an example of cooldown curves using rates of 0, 20, 40, 60, and 100°F/Hr applicable for the first 16 EFPY. Allowable combinations of temperature and pressure for specific temperature change rates are below and to the right of the limit lines shown in Figures 2.2 and 2.3. Note that the step in these curves are due to the previously described flange requirements [4].

2.6 PRESSURE-TEMPERATURE CURVE GENERATION METHODOLOGY

2.6.1 Thermal and Stress Analyses

The time-dependent temperature solution utilized in both the heatup and cooldown analysis is based on the one-dimensional transient heat conduction equation

$$\rho C \frac{\partial T}{\partial t} = K\left[\frac{\partial^2 T}{\partial r^2} + \frac{1}{r}\frac{\partial T}{\partial r}\right] \qquad (2.6.1\text{-}1)$$

with the following boundary conditions applied at the inner and outer radii of the reactor vessel,

$$\text{at } r = r_i, \qquad -K\frac{\partial T}{\partial r} = h(T - T_c) \qquad (2.6.1\text{-}2)$$

$$\text{at } r = r_o, \qquad \frac{\partial T}{\partial r} = 0 \qquad (2.6.1\text{-}3)$$

where,

- r_i = reactor vessel inner radius
- r_o = reactor vessel outer radius
- ρ = material density
- C = material specific heat
- K = material thermal conductivity
- T = local temperature
- r = radial location
- t = time
- h = heat transfer coefficient between the coolant and the vessel wall
- T_c = coolant temperature

These equations are solved numerically to generate the position and time-dependent temperature distributions, T(r,t), for all heatup and cooldown rates of interest.

With the results of the heat transfer analysis as input, position and time-dependent distributions of hoop thermal stress are calculated using the formula for the thermal stress in a hollow cylinder given by Timoshenko[14].

$$\sigma_\theta(r,t) = \frac{E\alpha}{1-\nu}\frac{1}{r^2}\left[\frac{r^2 + r_i^2}{r_o^2 - r_i^2}\int_{r_i}^{r_o} T(r,t)r\,dr + \int_{r_i}^{r} T(r,t)r\,dr - T(r,t)r^2\right] \qquad (2.6.1\text{-}4)$$

where,

$\sigma_\theta(r,t)$ = hoop stress at location and time t

E = modulus of elasticity

α = coefficient of linear expansion

ν = Poisson's ratio

The quantities E and α are temperature-dependent properties. However, to simplify the analysis, E and α are evaluated at an equivalent wall temperature at a given time:

$$T_{eqv} = \frac{2\int_{r_i}^{r_o} T(r)\,r\,dr}{r_o^2 - r_i^2} \qquad (2.6.1\text{-}5)$$

E and α are calculated as a function of this equivalent temperature and the Eα product in equation (2.6.1-4) is treated as a constant in the computation of hoop thermal stress.

The linear bending (σ_b) and constant membrane (σ_m) stress components of the thermal hoop stress profile are approximated by the linearization technique presented in Appendix A, to Section XI of the ASME Code[15]. These stress components are used for determining the thermal stress intensity factors, K_{IT}, as described in the following subsection.

2.6.2 Steady-State Analyses

Using the calculated beltline metal temperature and the metal reference nil-ductility transition temperature, the reference stress intensity factor (K_{Ia}) is determined in Equation (2.5-1) at the 1/4t location where "t" represents the vessel wall thickness. At the 1/4t location, a 1/4 thickness flaw is assumed to originate at the vessel inside radius.

The allowable pressure $P(T_c)$ is a function of coolant temperature, and the pressure temperature curve is calculated for the steady state case at the assumed 1/4t inside surface flaw. First, the maximum allowable membrane (pressure) stress

intensity factor is determined using the factor of 2.0 from equation (2.5-2) and the following equation:

$$K_{IM(max)} = \frac{K_{Ia}(T - RT_{NDT})_{1/4t}}{2.0} \qquad (2.6.2\text{-}1)$$

where,

$K_{Ia}(T\text{-}RT_{NDT})$ = allowable reference stress intensity factor as a function of $T\text{-}RT_{NDT}$ at 1/4t.

Next, the maximum allowable pressure stress is determined using an iterative process and the following three equations:

$$Q = \phi^2 - 0.212\left(\frac{\sigma_p}{\sigma_y}\right)^2 \qquad (2.6.2\text{-}2)$$

$$\sigma_p = \frac{K_{IM(max)}}{1.1 M_K \sqrt{\frac{\pi a}{Q}}} \qquad (2.6.2\text{-}3)$$

$$K_{IP} = 1.1 M_K \sigma_p \sqrt{\frac{\pi a}{Q}} \qquad (2.6.2\text{-}4)$$

where,

- Q = flaw shape factor modified for plastic zone size[16],
- ϕ = is the elliptical integral of the 2nd kind ($\phi = 1.11376$ for the fixed aspect ratio of 3 of the code reference flaw)[16],
- 0.212 = plastic zone size correction factor[16],
- σ_p = pressure stress,
- σ_y = yield stress,
- 1.1 = correction factor for surface breaking flaws,
- M_K = correction factor for constant membrane stress[16], M_K as function of relative flaw depth (a/t) is shown in Figure 2.4,
- a = crack depth of 1/4t,

K_{IP} = pressure stress intensity factor.

The maximum allowable pressure stress is determined by incrementing σ_p from an initial value of 0.0 psi until a pressure stress is found that computes a K_{IP} value within 1.0001 of the $K_{IM(max)}$ value. After the maximum allowable σ_p is found, the maximum allowable internal pressure is determined by

$$P(T_c) = \sigma_p \left[\frac{r_o^2 - r_i^2}{r_o^2 + r_i^2} \right] \qquad (2.6.2\text{-}5)$$

where,

$P(T_c)$ = calculated allowable pressure as a function of coolant temperature.

2.6.3 Finite Cooldown Rate Analyses

For each cooldown rate the pressure-temperature curve is calculated at the inside 1/4t location. First, the thermal stress intensity factor is calculated for a coolant temperature at a given time using the following equation from the Welding Research Council[16]:

$$K_{IT} = \left[\sigma_m 1.1 M_K + \sigma_b M_B \right] \sqrt{\frac{\pi a}{Q}} \qquad (2.6.3\text{-}1)$$

where,

σ_m = constant membrane stress component from the linearized thermal hoop stress distribution,

σ_b = linear bending stress component from the linearized thermal hoop stress distribution,

M_K = correction factor for membrane stress[16], (see Figure 2.4),

M_B = correction factor for bending stress[16], M_B as a function of relative flaw depth (a/t) is shown in Figure 2.5.

The flaw shape factor Q in equation (2.6.2-6) is calculated from[16]:

$$Q = \phi^2 - 0.212\left(\frac{\sigma_m + \sigma_b}{\sigma_y}\right)^2 \qquad (2.6.3\text{-}2)$$

Once K_{IT} is computed, the maximum allowable membrane (pressure) stress intensity factor is determined using the factor of 2.0 from equation (2.5-2) and the following equation:

$$K_{IM(max)} = \frac{K_{Ia}(T - RT_{NDT})_{1/4t} - K_{IT}(T_c)_{1/4t}}{2.0} \qquad (2.6.3\text{-}3)$$

From $K_{IM(max)}$, the maximum allowable pressure is determined using the iterative process described above and equations (2.6.2-2) through (2.6.2-5).

The steady-state pressure-temperature curve of Section 2.6.2 is compared to the cooldown curves for the 1/4t inside surface flaw at each cooldown rate. At any time, the allowable pressure is the lesser of the two values, and the resulting curve is called the composite cooldown limit curve.

Finally, the 10 CFR Part 50[4] rule for closure flange regions is incorporated into the cooldown composite curve as described in Section 2.5.

2.6.4 Finite Heatup Rate Analyses

Using the calculated beltline metal temperature and the metal reference nil-ductility transition temperature, the reference stress intensity factor (K_{Ia}) is determined in Equation (2.5-1) at both the 1/4t and 3/4t locations where "t" represents the vessel wall thickness. At the 1/4t location, a 1/4 thickness flaw is assumed to originate at the vessel inside radius. At the 3/4t location, a 1/4t flaw is assumed to originate on the outside of the vessel.

For each heatup rate a pressure-temperature curve is calculated at the 1/4t and 3/4t locations. First, the thermal stress intensity factor is calculated at the 1/4t and 3/4t locations for a coolant temperature at a given time using equation (2.6.3-1) from Section 2.6.3.

Once K_{IT} is computed, the maximum allowable membrane (pressure) stress intensity factors at the 1/4t and 3/4t locations are determined using the following equations:

$$\text{At 1/4t,} \quad K_{IM(max)1/4t} = \frac{K_{Ia}(T-RT_{NDT})_{1/4t} - K_{IT}(T_c)_{1/4t}}{2.0} \qquad (2.6.4\text{-}1)$$

$$\text{At 3/4t,} \quad K_{IM(max)3/4t} = \frac{K_{Ia}(T-RT_{NDT})_{3/4t} - K_{IT}(T_c)_{3/4t}}{2.0} \qquad (2.6.4\text{-}2)$$

From $K_{IM(max)1/4t}$ and $K_{IM(max)3/4t}$, the maximum allowable pressure at both the 1/4t and 3/4t locations is determined using the iterative process described in Section 2.6.2 and equations (2.6.2-2) through (2.6.2-5).

As was done with the cooldown case, the steady state pressure-temperature curve of Section 2.6.2 is compared with the 1/4t and 3/4t location heatup curves for each heatup rate, with the lowest of the three being used to generate the composite heatup limit curve. The composite curve is then adjusted for the 10 CFR Part 50[4] rule for closure flange requirements.

2.6.5 Hydrostatic and Leak Test Curve Analyses

The minimum inservice hydrostatic leak test curve is determined by calculating the minimum allowable temperature at two pressure values (pressure values of 2000 psig and 2485 psig, approximately 110% of operating pressure, are generally used). The curve is generated by drawing a line between the two pressure-temperature data points. The governing equation for generating the hydrostatic leak test pressure-temperature limit curve is defined in Appendix G, Section XI, of the ASME Code[5] as follows:

$$1.5 * K_{IM} < K_{Ia} \qquad (2.6.5\text{-}1)$$

where, K_{IM} is the stress intensity factor caused by the membrane (pressure) stress and K_{Ia} is the reference stress intensity factor as defined in equation (2.5-1). Note

that the thermal stress intensity factor is neglected (i.e. KIT=0) since the hydrostatic leak test is performed at isothermal conditions.

The pressure stress is determined by,

$$\sigma_p = \left[\frac{r_o^2 + r_i^2}{r_o^2 - r_i^2}\right] P \qquad (2.6.5\text{-}2)$$

where,

P = the input pressure (generally 2000 and 2485 psig)

Next, the pressure stress intensity factor is calculated for a 1/4t flaw by,

$$K_{IM} = \left[1.1\, M_K \sqrt{\frac{\pi a}{Q}}\right] \sigma_p \qquad (2.6.5\text{-}3)$$

The K_{IM} result is multiplied by the 1.5 factor of equation (2.5-2) and divided by 1000,

$$K_{HYD} = \frac{1.5\, K_{IM}}{1000} \qquad (2.6.5\text{-}4)$$

Finally, the minimum allowable temperature is determined by setting K_{HYD} to K_{Ia} in equation (2.5-1) and solving for temperature T:

$$T = \frac{\ln\left[\frac{(K_{HYD} - 26.78)}{1.223}\right]}{0.0145} + RT_{NDT} - 160.0 \qquad (2.6.5\text{-}5)$$

The 1983 Amendment to 10CFR50[3] has a rule which addresses the test temperature for hydrostatic pressure tests. This rule states that, when there is no fuel in the reactor vessel during hydrostatic pressure tests or leak tests, the minimum allowable test temperature must be 60°F above the adjusted reference

temperature of the beltline region material that is controlling. If fuel is present in the reactor vessel during hydrostatic pressure tests or leak tests, the requirements of this section and Section 2.5 must be met, depending on whether the core is critical during the test.

2.7 Minimum Boltup Temperature

The minimum boltup temperature is equal to the material RT_{NDT} of the stressed region. The RT_{NDT} is calculated in accordance with the methods described in Branch Technical Position MTEB 5-2. The Westinghouse position is that the minimum boltup temperature be no lower than 60° F. Thus, the minimum boltup temperature should be 60° F or the material RT_{NDT}, whichever is higher.

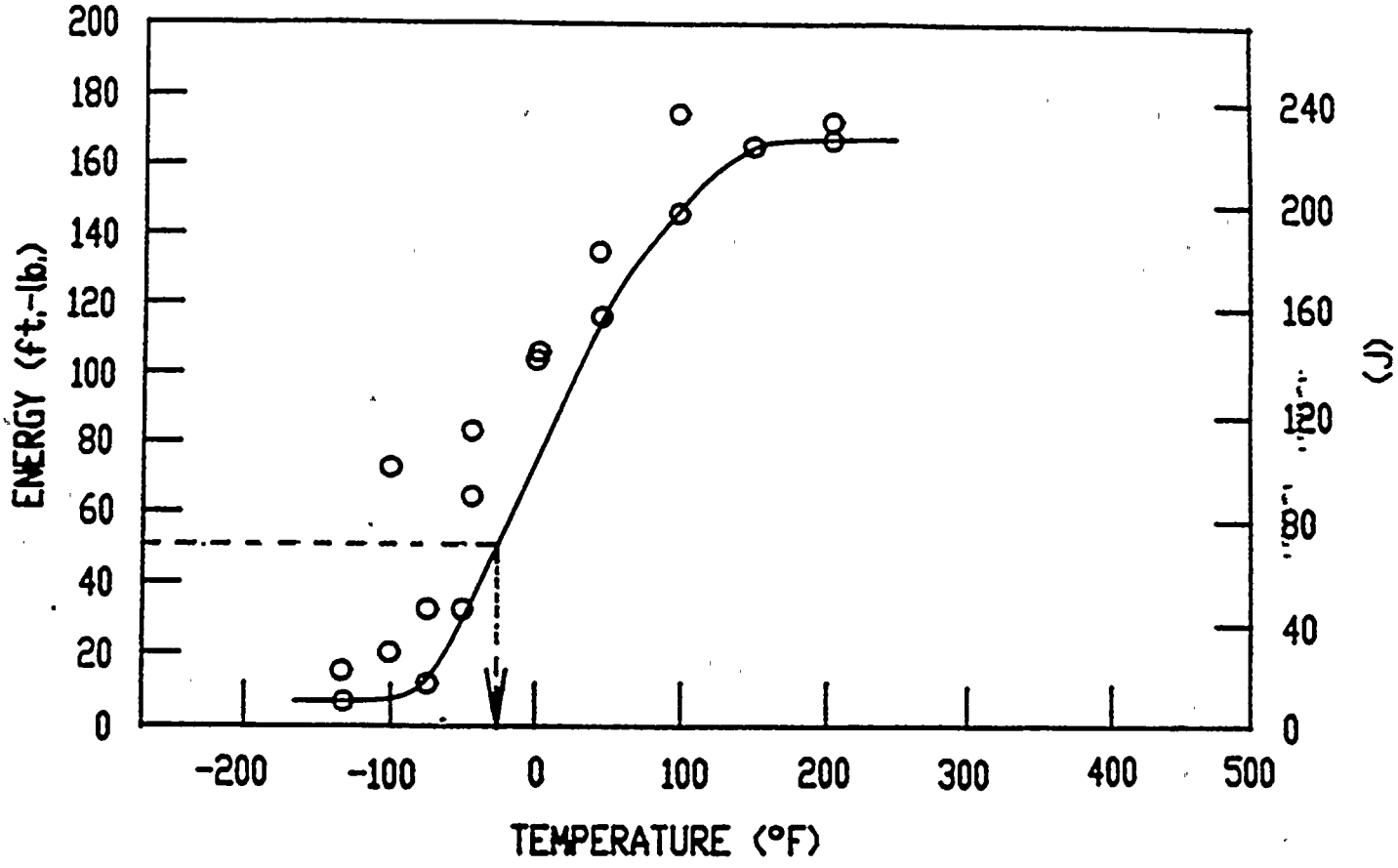

Figure 2.1: Example of a Charpy Impact Energy Curve Used to Determine IRT_{NDT} (Note: 35 mils lateral expansion is required at indicated temperature)

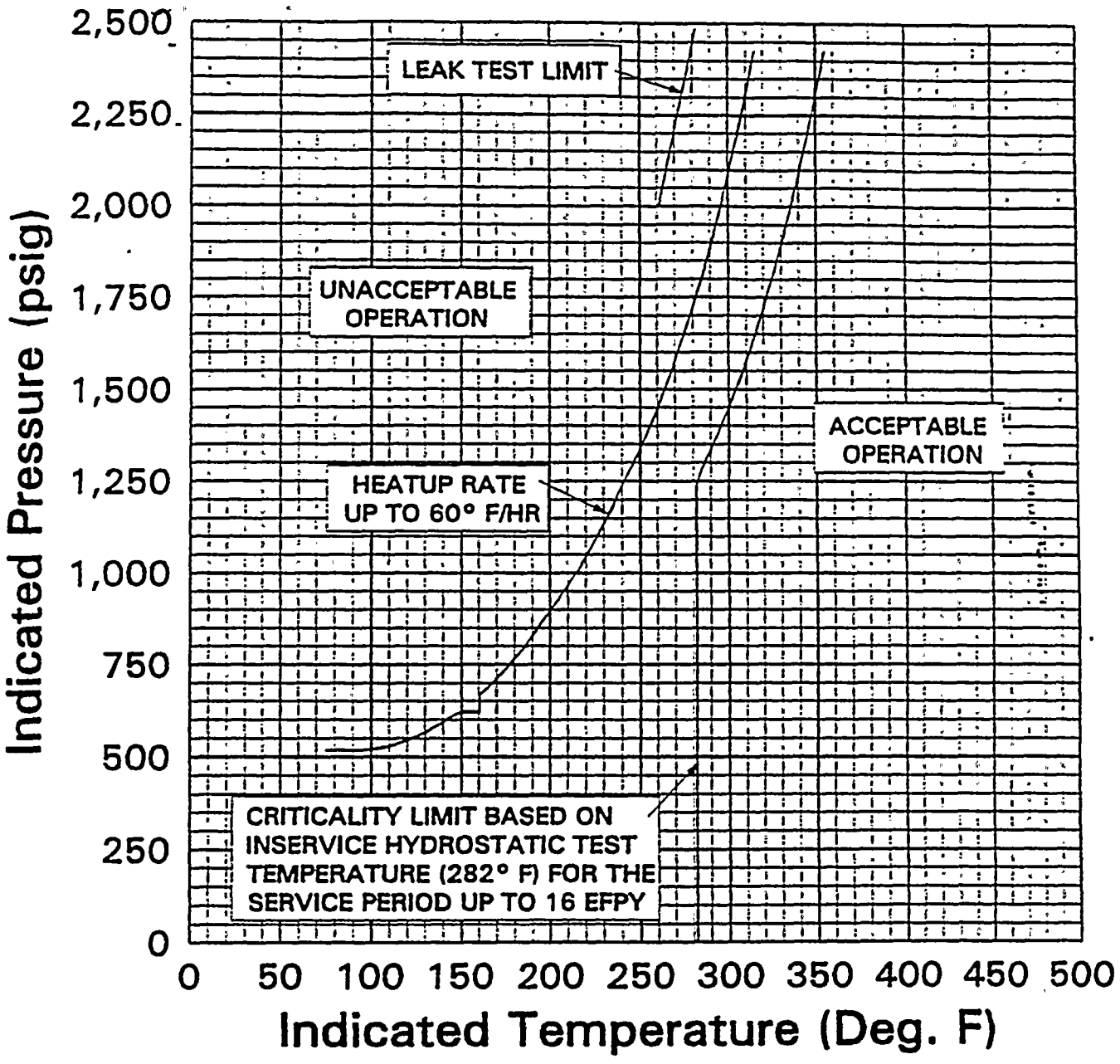

Figure 2.2: Heatup Pressure-Temperature Limit Curve For Heatup Rates up to 60°F/Hr

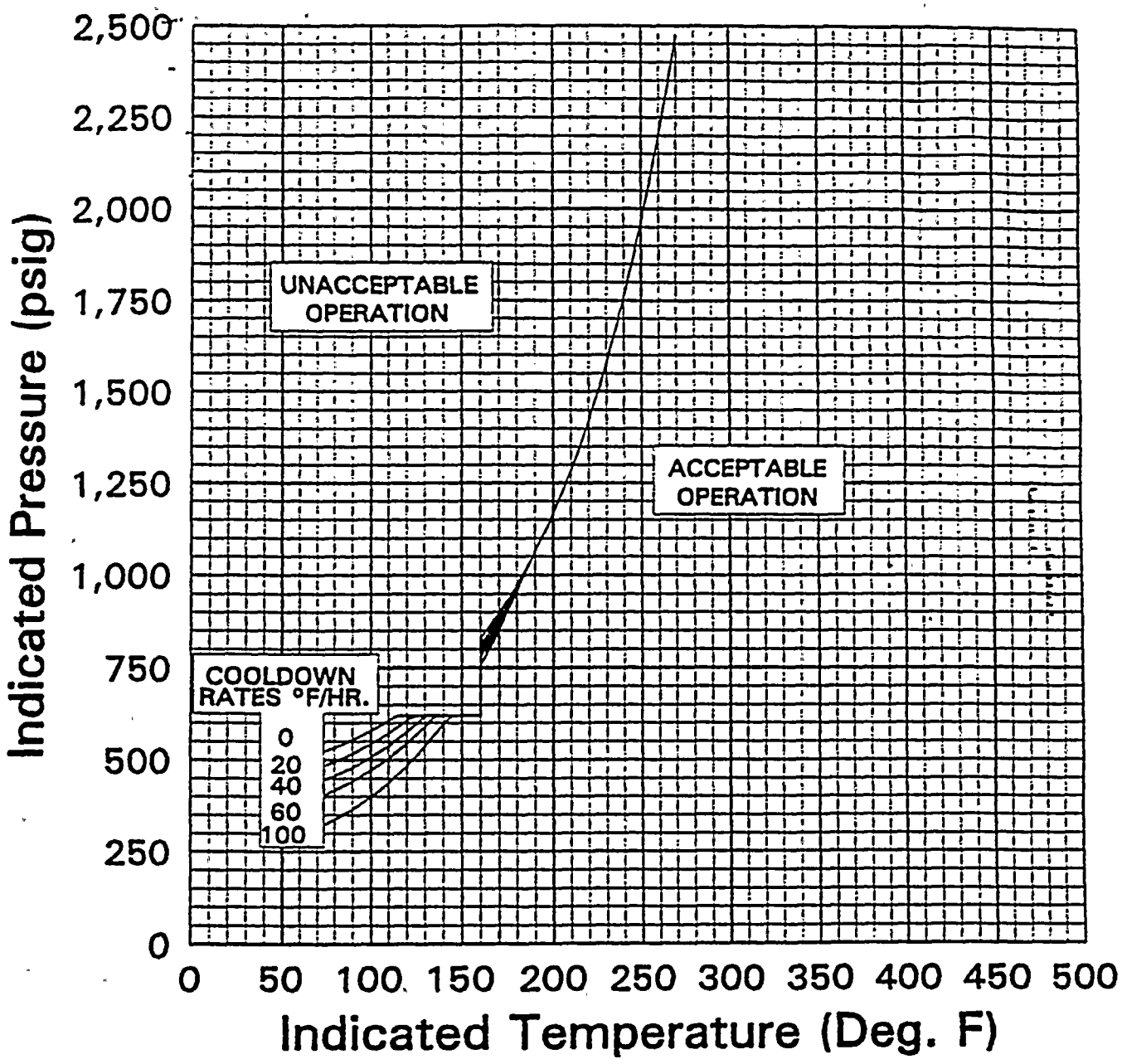

Figure 2.3: Cooldown Pressure-Temperature Limit Curves For Cooldown Rates up to 100°F/Hr

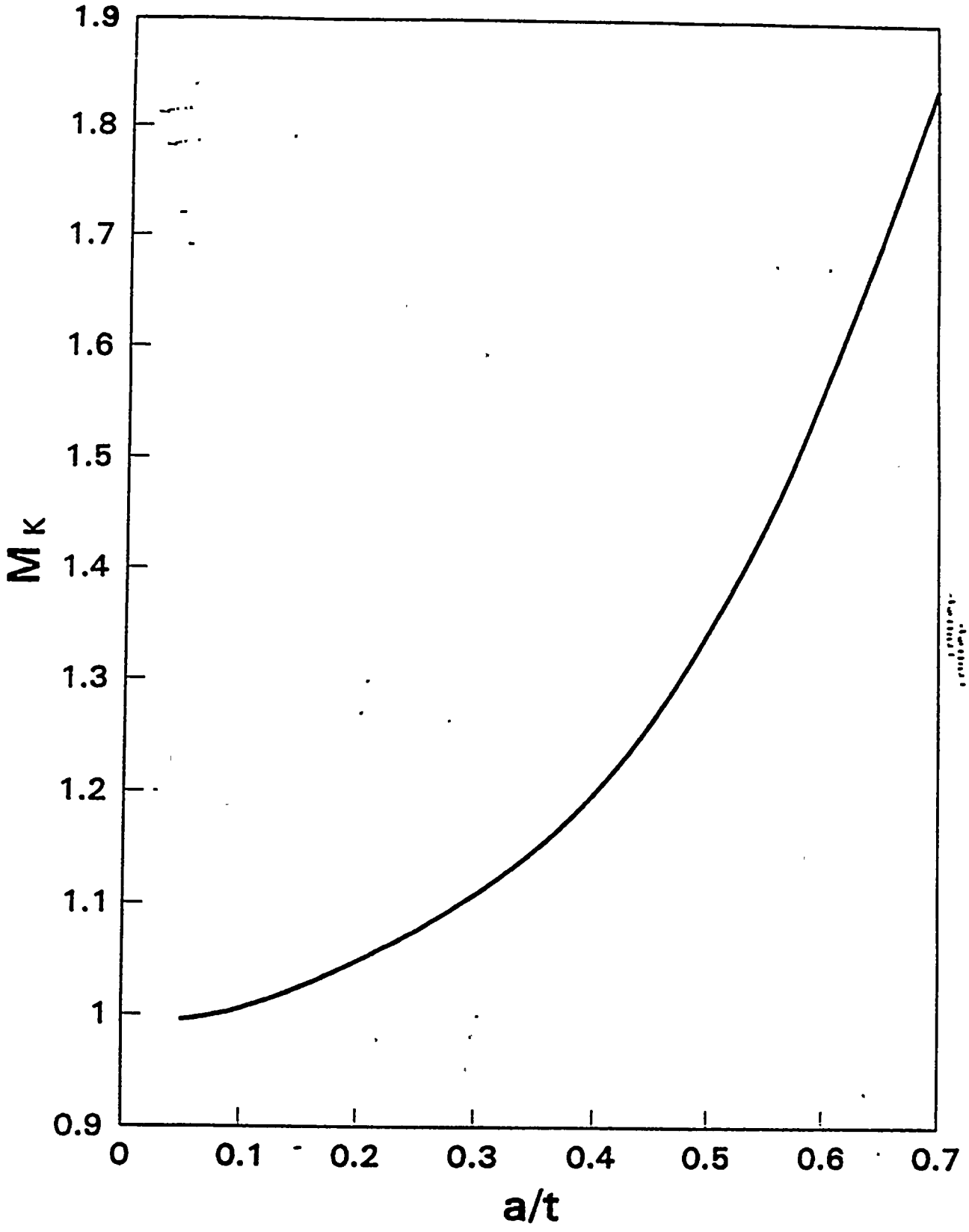

Figure 2.4: Membrane Stress Correction Factor (M_K) vs. a/t Ratio for Flaws Having Length to Depth Ratio of 6

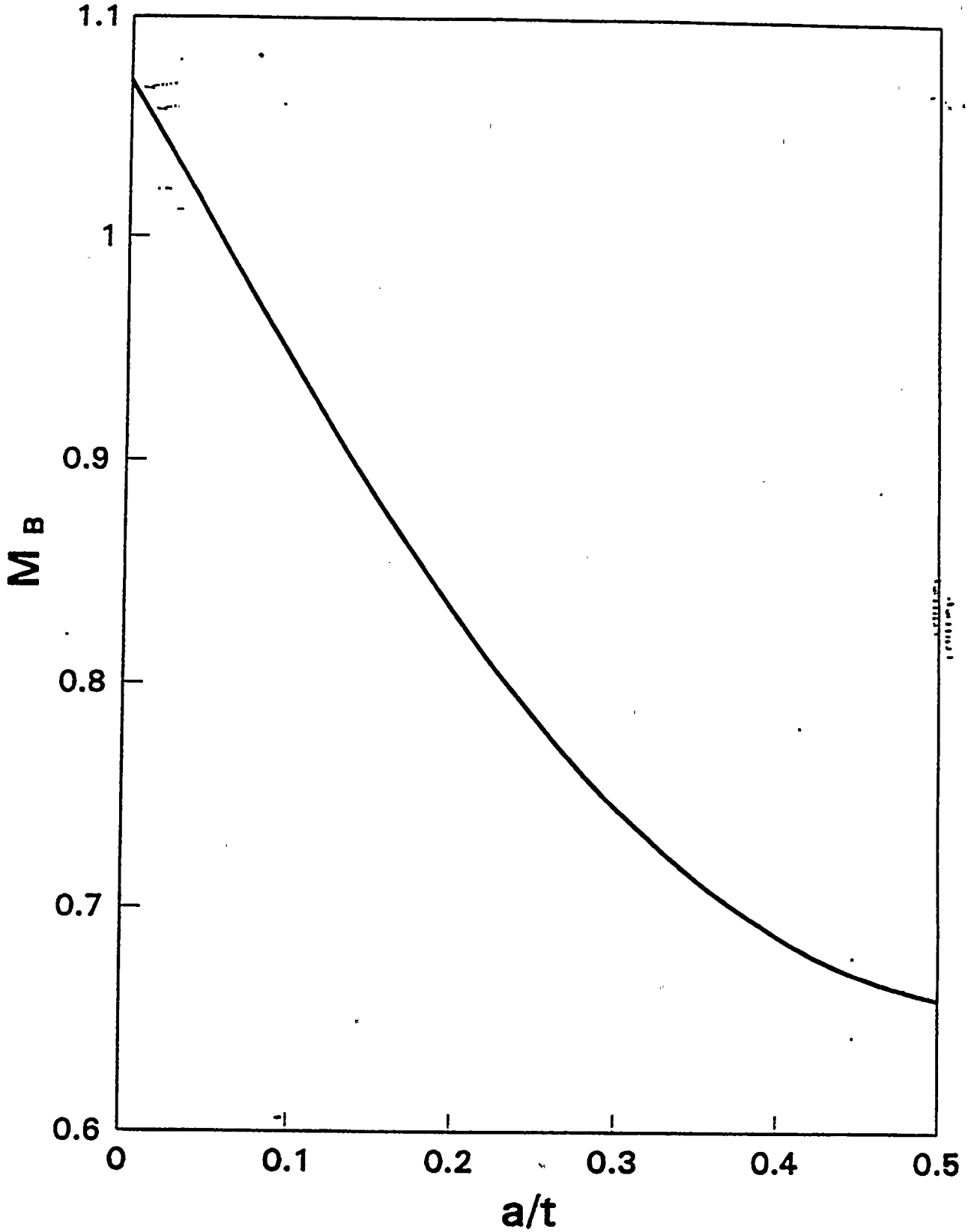

Figure 2.5: Bending Stress Correction Factor (M_B) vs. a/t Ratio for Flaws Having Length to Depth Ratio of 6.

3.0 COLD OVERPRESSURE MITIGATING SYSTEM (COMS)

3.1 INTRODUCTION

The purpose of the COMS is to supplement the normal plant operational administrative controls and the water relief valves in the Residual Heat Removal System (RHRS) when they are unavailable to protect the reactor vessel from being exposed to conditions of fast propagating brittle fracture. This has been achieved by conservatively choosing COMS setpoints which prevent exceeding the pressure/temperature limits established by 10 CFR Part 50 Appendix G[4] requirements. The COMS is desig ned to provide the capability, during relatively low temperature operation (typically less than 350°F), to automatically prevent the RCS pressure from exceeding the applicable limits. Once the system is enabled, no operator action is involved for the COMS to perform its intended pressure mitigation function. Thus, no operator action is modelled in the analyses supporting the setpoint selection, although operator action may be initiated to ultimately terminate the cause of the overpressure event.

The PORVs located near the top of the pressurizer, together with additional actuation logic from the wide-range pressure channels, are utilized to mitigate potential RCS overpressure transients defined below if the RHRS water relief valves are inadvertently isolated from the RCS. The COMS provides the supplemental relief capacity for specific transients which would not be mitigated by the RHRS relief valves. In addition, a limit on the PORV piping is accommodated due to the potential for water hammer effects to be developed in the piping associated with these valves as a result of the cyclic opening and closing characteristics during mitigation of an overpressure transient. Thus, a pressure limit more restrictive than the 10CFR50, Appendix G[4] allowable is imposed above a certain temperature so that the loads on the piping from a COMS event would not affect the piping integrity.

Two specific transients have been defined, with the RCS in a water-solid condition, as the design basis for COMS. Each of these scenarios assumes as an initial condition that the RHRS is isolated from the RCS, and thus the relief capability of

the RHRS relief valves is not available. The first transient consists of a heat injection scenario in which a reactor coolant pump in a single loop is started with the RCS temperature as much as 50°F lower than the steam generator secondary side temperature and the RHRS has been inadvertently isolated. This results in a sudden heat input to a water-solid RCS from the steam generators, creating an increasing pressure transient. The second transient has been defined as a mass injection scenario into a water-solid RCS caused by the simultaneous isolation of the RHRS, isolation of letdown and failure of the normal charging flow controls to the full flow condition. Various combinations of charging and safety injection flows may also be evaluated on a plant-specific basis. The resulting mass injection/letdown mismatch causes an increasing pressure transient.

3.2 COMS Setpoint Determination

Westinghouse has developed the following methodology which is employed to determine PORV setpoints for mitigation of the COMS design basis cold overpressurization transients. This methodology maximizes the available operating margin for setpoint selection while maintaining an appropriate level of protection in support of reactor vessel integrity.

3.2.1 Parameters Considered

The selection of proper COMS setpoints for actuating the PORVs requires the consideration of numerous system parameters including:

a. Volume of reactor coolant involved in transient
b. RCS pressure signal transmission delay
c. Volumetric capacity of the relief valves versus opening position
d. Stroke time of the relief valves (open & close)
e. Initial temperature and pressure of the RCS
f. Mass input rate into RCS
g. Temperature of injected fluid

h. Heat transfer characteristics of the steam generators

i. Initial temperature asymmetry between RCS and steam generator secondary water

j. Mass of steam generator secondary water

k. RCP startup dynamics

l. 10CFR50, Appendix G pressure/temperature characteristics of the reactor vessel

m. Pressurizer PORV piping/structural analysis limitations

n. Dynamic and static pressure difference between reactor vessel midplane and location of wide range pressure transmitter

These parameters are input to a specialized version of the LOFTRAN computer code which calculates the maximum and minimum system pressures.

3.2.2 Pressure Limits Selection

The function of the COMS is to protect the reactor vessel from fast propagating brittle fracture. This has been implemented by choosing COMS setpoints which prevent exceeding the limits prescribed by the applicable pressure/temperature characteristic for the specific reactor vessel material in accordance with rules given in Appendix G to 10CFR50[4]. The COMS design basis takes credit for the fact that overpressure events most likely occur during isothermal conditions in the RCS. Therefore, it is appropriate to utilize the steady-state Appendix G limit. In addition, the COMS also provides for an operational consideration to maintain the integrity of the PORV piping. A typical characteristic 10CFR50 Appendix G curve is shown by Figure 3.1 where the allowable system pressure increases with increasing temperature. This type of curve sets the nominal upper limit on the pressure which should not be exceeded during RCS increasing pressure transients based on reactor vessel material properties. Superimposed on this curve is the PORV piping limit which is conservatively used, for setpoint development, as the maximum allowable pressure above the temperature at which it intersects with the 10CFR50 Appendix G curve.

When a relief valve is actuated to mitigate an increasing pressure transient, the release of a volume of coolant through the valve will cause the pressure increase to be slowed and reversed as described by Figure 3.2. The system pressure then decreases, as the relief valve releases coolant, until a reset pressure is reached where the valve is signalled to close. Note that the pressure continues to decrease below the reset pressure as the valve recloses. The nominal lower limit on the pressure during the transient is typically established based solely on an operational consideration for the reactor coolant pump #1 seal to maintain a nominal differential pressure across the seal faces for proper film-riding performance.

The nominal upper limit (based on the minimum of the steady-state 10CFR50 Appendix G requirement and the PORV piping limitations) and the nominal RCP #1 seal performance criteria create a pressure range from which the setpoints for both PORVs may be selected as shown on Figures 3.3 and 3.4.

3.2.3 Mass Input Consideration

For a particular mass input transient to the RCS, the relief valve will be signalled to open at a specific pressure setpoint. However, as shown on Figure 3.2, there will be a pressure overshoot during the delay time before the valve starts to move and during the time the valve is moving to the full open position. This overshoot is dependent on the dynamics of the system and the input parameters, and results in a maximum system pressure somewhat higher than the set pressure. Similarly there will be a pressure undershoot, while the valve is relieving, both due to the reset pressure being below the setpoint and to the delay in stroking the valve closed. The maximum and minimum pressures reached (P_{MAX} and P_{MIN}) in the transient are a function of the selected setpoint (P_S) as shown on Figure 3.3. The shaded area represents an optimum range from which to select the setpoint based on the particular mass input case. Several mass input cases may be run at various input flow rates to bound the allowable setpoint range.

3.2.4 Heat Input Consideration

The heat input case is done similarly to the mass input case except that the locus of transient pressure values versus selected setpoints may be determined for several values of the initial RCS temperature. This heat input evaluation provides a range of acceptable setpoints dependent on the reactor coolant temperature, whereas the mass input case is limited to the most restrictive low temperature condition only (i.e. the mass injection transient is not sensitive to temperature). The shaded area on Figure 3.4 describes the acceptable band for a heat input transient from which to select the setpoint for a particular initial reactor coolant temperature.

3.2.5 Final Setpoint Selection

By superimposing the results of multiple mass input and heat input cases evaluated, (from a series of figures such as 3.3 and 3.4) a range of allowable PORV setpoints to satisfy both conditions can be determined. Each of the two PORVs may have a different pressure setpoint versus temperature specification such that only one valve will open at a time and mitigate the transient (i.e. staggered setpoints). The second valve operates only if the first fails to open on command. This design supports a single failure assumption as well as minimizing the potential for both PORVs to open simultaneously, a condition which may create excessive pressure undershoot and challenge the RCP #1 seal performance criteria. However, each of the sets of staggered setpoints must result in the system pressure staying below the P_{MAX} pressure limit shown on Figures 3.3 and 3.4 when either valve is utilized to mitigate the transient.

The function generator used to program the pressure versus setpoint curves for each valve has a limited number of programmable break points (typically 9). These are strategically defined in the final selection process, with consideration given to the slope of any line segment, which is limited to approximately 24 psi/°F.

The selection of the setpoints for the PORVs considers the use of nominal upper and lower pressure limits. The upper limits are specified by the minimum of the steady-state cooldown curve as calculated in accordance with Appendix G to 10CFR50[4] or the peak RCS pressure based upon piping/structural analysis loads. The lower pressure extreme is specified by the reactor coolant pump #1 seal minimum differential pressure performance criteria. Since both the upper and lower pressure values are conservatively determined, the uncertainties in the pressure and temperature instrumentation utilized by the COMS are not explicitly accounted for in the selection of the COMS PORV setpoints. Accounting for the effects of instrumentation uncertainty would impose additional unnecessary restrictions on the setpoint development, which is already based on conservative pressure limits (such as a safety factor of 2 on pressure stress, use of a lower bound K_{IR} curve and an assumed ¼T flaw depth with a length equal to 1½ times the vessel wall thickness) as discussed in section 2 of this report, without a commensurate increase in the level of protection afforded to reactor vessel integrity.

3.3 Application of ASME Code Case N-514

ASME Code Case N-514[17] allows low temperature overpressure protection systems (LTOPS, as the code case refers to COMS) to limit the maximum pressure in the reactor vessel to 110% of the pressure determined to satisfy Appendix G, paragraph G-2215, of Section XI of the ASME Code[5]. (Note, that the setpoint selection methodology as discussed in Section 3.2.5 specifically utilizes the steady-state curve.) The application of ASME Code Case N-514 increases the operating margin in the region of the pressure-temperature limit curves where the COMS system is enabled. Code Case N-514 requires LTOPS to be effective at coolant temperatures less than 200°F or at coolant temperatures corresponding to a reactor vessel metal temperature less than RT_{NDT} + 50°F, whichever is greater. RT_{NDT} is the highest adjusted reference temperature for weld or base metal in the beltline region at a distance one-fourth of the vessel section thickness from the vessel inside surface, as determined by Regulatory Guide 1.99, Revision 2. Although expected soon, use of Code Case N-514 has not yet been formally approved by the NRC. In the interim, an exemption to the regulations must be

granted by the NRC before Code Case N-514 can be used in the determination of the COMS setpoints and enable temperature.

3.4 Enable Temperature for COMS

The enable temperature is the temperature below which the COMS system is required to be operable. The definition of the enabling temperature currently approved and supported by the NRC is described in Branch Technical Position RSB 5-2[18]. This position defines the enable temperature for LTOP systems as the water temperature corresponding to a metal temperature of at least RT_{NDT} + 90°F at the beltline location (1/4t or 3/4t) that is controlling in the Appendix G limit calculations. This definition is also supported by Westinghouse and is mostly based on material properties and fracture mechanics, with the understanding that material temperatures of RT_{NDT} + 90°F at the critical location will be well up the transition curve from brittle to ductile properties, and therefore brittle fracture of the vessel is not expected.

The ASME Code Case N-514 supports an enable temperature of RT_{NDT} + 50°F or 200°F, whichever is greater as described in Section 3.3. This definition is also supported by Westinghouse and can be used by requesting an exemption to the regulations or when ASME Code Case N-514 is formally approved by the NRC.

The RCS cold leg temperature limitation for starting an RCP is the same value as the COMS enable temperature to ensure that the basis of the heat injection transient is not violated. The Standard Technical Specifications (STS) prohibit starting an RCP when any RCS cold leg temperatures is less than or equal to the COMS enable temperature unless the secondary side water temperature of each steam generator is less than or equal to 50°F above each of the RCS cold leg temperatures.

FIGURE 3.1

TYPICAL APPENDIX G

P/T CHARACTERISTICS

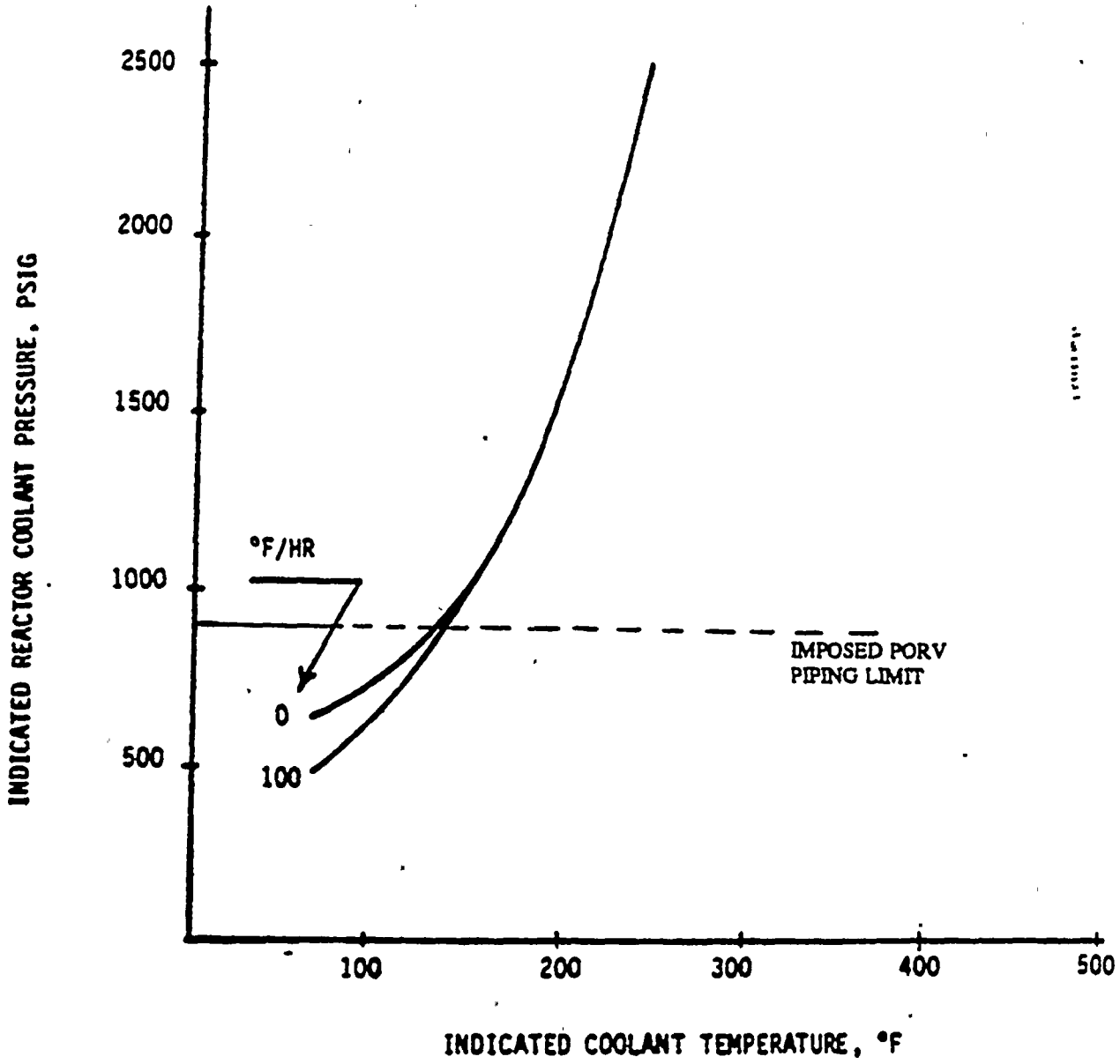

FIGURE 3.2

TYPICAL PRESSURE TRANSIENT

(1 RELIEF VALVE CYCLE)

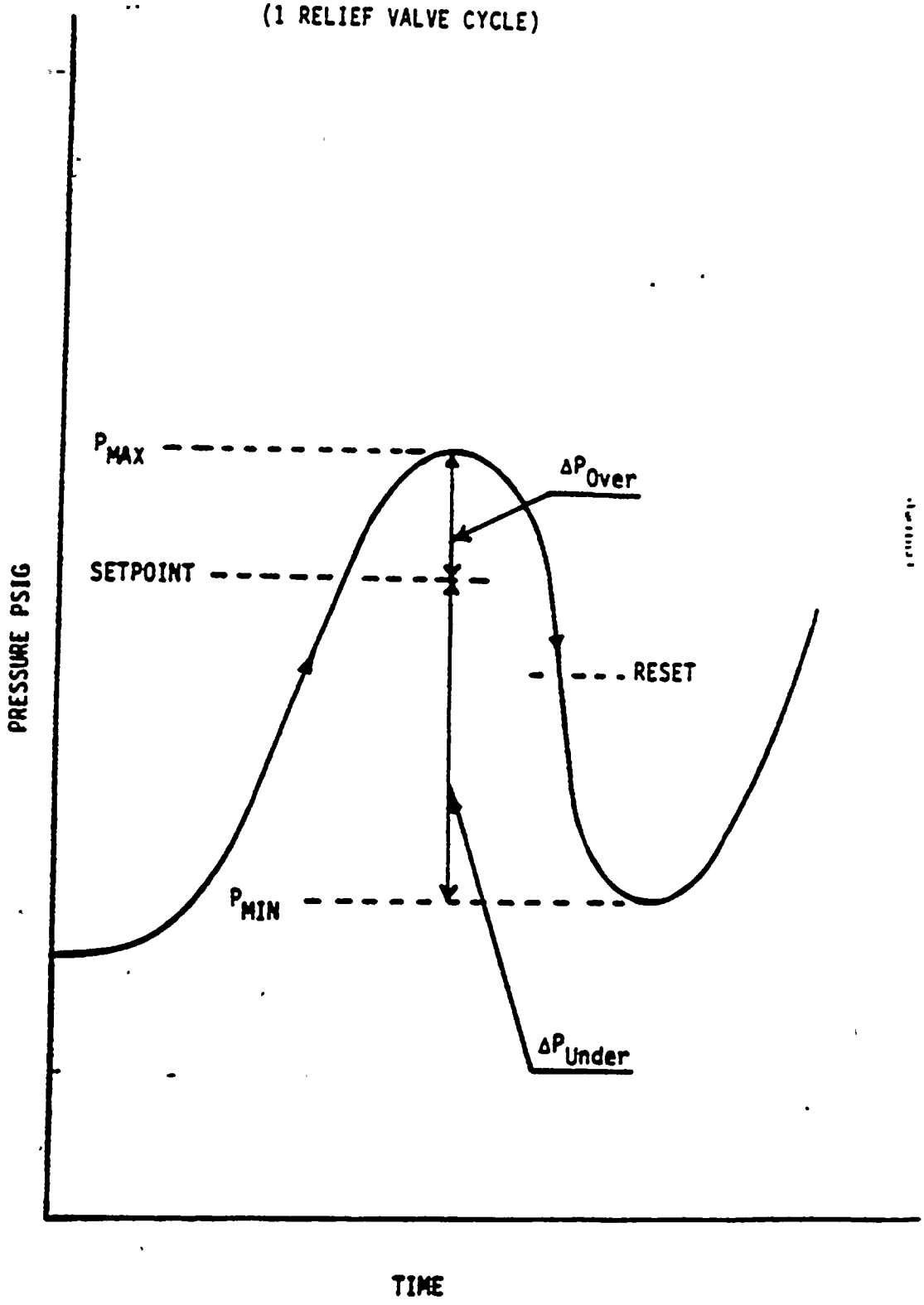

FIGURE 3.3

SETPOINT
DETERMINATION
(MASS INPUT)

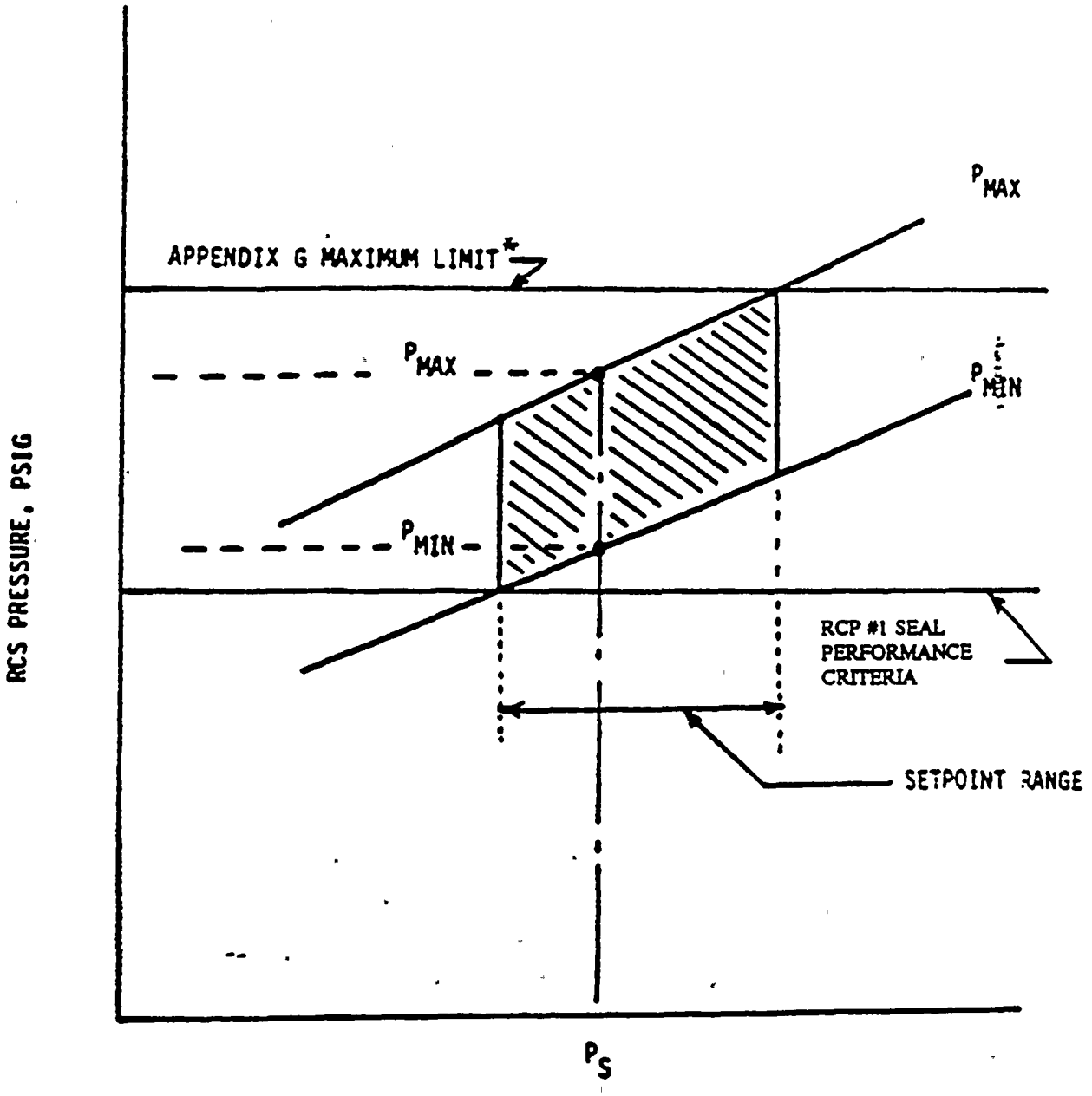

* The maximum pressure limit is the minimum of the Appendix G limit or the PORV discharge piping structural analysis limit.

FIGURE 3.4

SETPOINT
DETERMINATION
(HEAT INPUT)

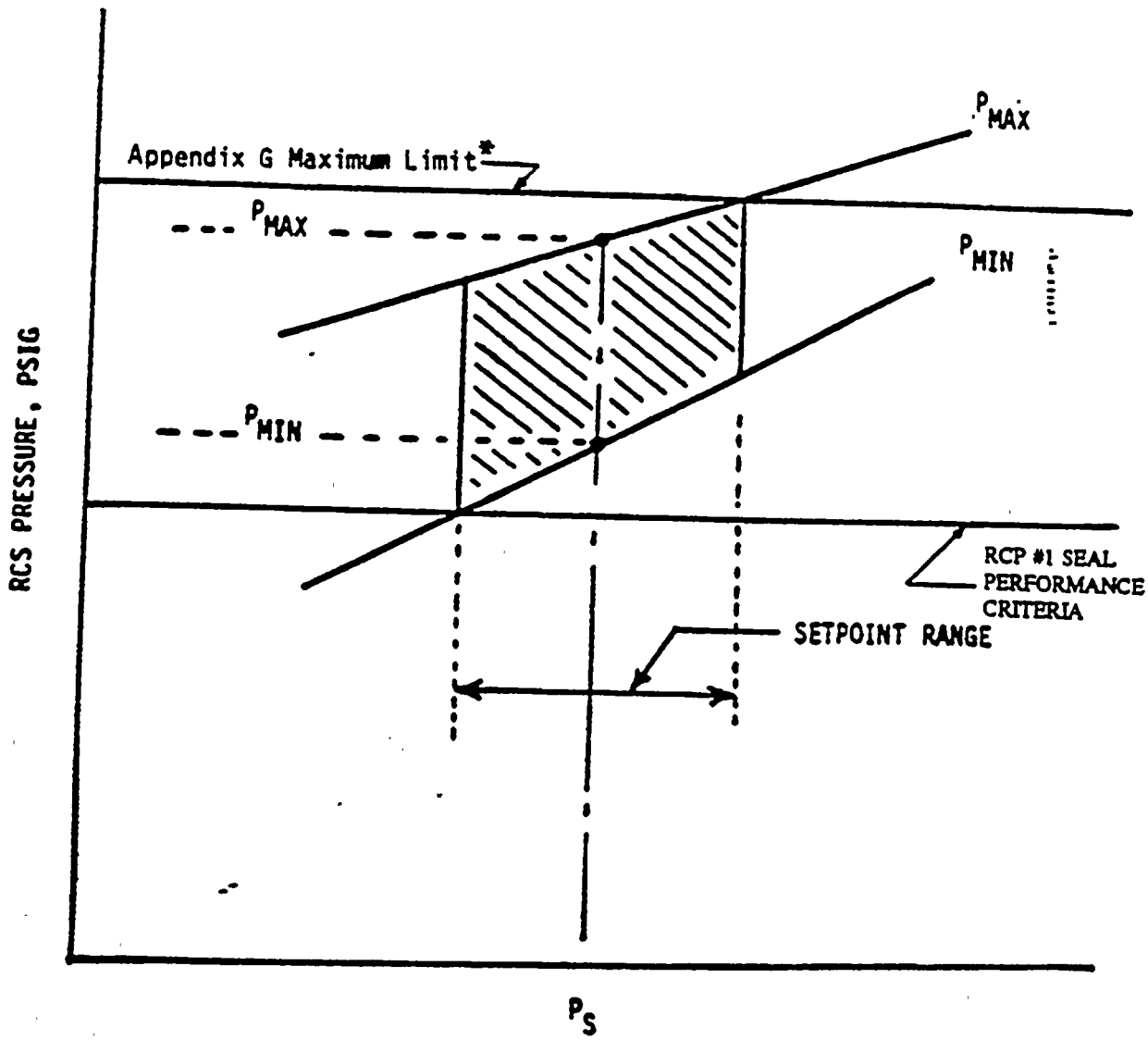

* The maximum pressure limit is the minimum of the Appendix G limit or the PORV discharge piping structural analysis limit.

4.0 REFERENCES

1. NUREG 1431, "Standard Technical Specifications for Westinghouse Pressurized Water Reactors", Revision 0, September, 1992.

2. U.S. Nuclear Regulatory Commission, "Removal of Cycle-Specific Parameter Limits from Technical Specifications", Generic Letter 88-16, October, 1988.

3. U.S. Nuclear Regulatory Commission, Radiation Embrittlement of Reactor Vessel Materials, Regulatory Guide 1.99, Revision 2, May, 1988.

4. Code of Federal Regulations, Title 10, Part 50, "Fracture Toughness Requirements for Light-Water Nuclear Power Reactors", Appendix G, Fracture Toughness Requirements.

5. ASME Boiler and Pressure Vessel Code, Section XI, "Rules for Inservice Inspection of Nuclear Power Plant Components", Appendix G, Fracture Toughness Criteria For Protection Against Failure.

6. R. G. Soltesz, R. K. Disney, J. Jedruch, and S. L. Ziegler, Nuclear Rocket Shielding Methods, Modification, Updating and Input Data Preparation. Vol. 5--Two-Dimensional Discrete Ordinates Transport Technique, WANL-PR(LL)-034, Vol. 5, August 1970.

7. ORNL RSIC Data Library Collection DLC-76 SAILOR Coupled Self-Shielded, 47 Neutron, 20 Gamma-Ray, P3, Cross Section Library for Light Water Reactors.

8. ASME Boiler and Pressure Vessel Code, Section III, "Rules for Construction of Nuclear Power Plant Components", Division 1, Subsection NB: Class 1 Components.

9. Branch Technical Position MTEB 5-2, "Fracture Toughness Requirements", NUREG-0800 Standard Review Plan 5.3.2, Pressure-Temperature Limits, July 1981, Rev. 1.

10. ASTM E-208, Standard Test Method for Conducting Drop-Weight Test to Determine Nil-Ductility Transition Temperature of Ferritic Steels, ASTM Standards, Section 3, American Society for Testing and Materials.

11. B&W Owners Group Report BAW-2202, "Fracture Toughness Characterization of WF-70 Weld Material", B&W Owners Group Materials Committee, September 1993.

12. Letter, Clyde Y. Shiraki, Nuclear Regulatory Commission, to D. L. Farrar, Commonwealth Edison Company, "Exemption from the Requirement to Determine the Unirradiated Reference Temperature in Accordance with the Method Specified in 10 CFR 50.61(b) (2) (i) (TAC NOS. M84546 and M84547)", Docket Nos. 50-295 and 50-304, February 22, 1994.

13. Code of Federal Regulations, Title 10, Part 50, "Fracture Toughness Requirements for Light-Water Nuclear Power Reactors", Appendix H, Reactor Vessel Material Surveillance Program Requirements.

14. Timoshenko, S. P. and Goodier, J. N., Theory of Elasticity, Third Edition, McGraw-Hill Book Co., New York, 1970.

15. ASME Boiler and Pressure Vessel Code, Section XI, "Rules for Inservice Inspection of Nuclear Power Plant Components", Appendix A, Analysis of Flaws, Article A-3000, Method For K_I Determination.

16. WRC Bulletin No. 175, "PVRC Recommendations on Toughness Requirements for Ferritic Materials", Welding Research Council, New York, August 1972.

17. ASME Boiler and Pressure Vessel Code Case N-514, Section XI, Division 1, "Low Temperature Overpressure Protection", Approval date: February 12, 1992.

18. Branch Technical Position RSB 5-2, "Overpressurization Protection of Pressurized Water Reactors While Operating at Low Temperatures", NUREG-0800 Standard Review Plan 5.2.2, Overpressure Protection, November 1988, Rev. 2.

Attachment C

RG&E Specific Methodology for Determining LTOPS Setpoints
(Replaces Section 3.0 of WCAP-14040)
(Both a final copy and redline copy of WCAP-14040 are provided)

3.0 LOW TEMPERATURE OVERPRESSURE PROTECTION SYSTEM (LTOPS)

3.1 INTRODUCTION

The purpose of the LTOPS is to supplement the normal plant operational administrative controls to protect the reactor vessel from being exposed to conditions of fast propagating brittle fracture. The LTOPS also protects the Residual Heat Removal (RHR) System from overpressurization. This has been achieved by conservatively choosing an LTOPS setpoint which prevents the RCS from exceeding the pressure/temperature limits established by 10 CFR Part 50 Appendix G[4] requirements, and the RHR System from exceeding 110% of its design pressure. The LTOPS is designed to provide the capability, during relatively low temperature operation (typically less than 350°F), to automatically prevent the RCS pressure from exceeding the applicable limits. Once the system is enabled, no operator action is involved for the LTOPS to perform its intended pressure mitigation function. Thus, no operator action is modelled in the analyses supporting the setpoint selection, although operator action may be initiated to ultimately terminate the cause of the overpressure event.

The PORVs located near the top of the pressurizer, together with additional actuation logic from the low-range pressure channels, are utilized to mitigate potential RCS overpressure transients. The LTOPS provides the relief capacity for specific transients which would not be mitigated by the RHR System relief valve. In addition, a limit on the PORV piping is accommodated due to the potential for water hammer effects to be developed in the piping associated with these valves as a result of the cyclic opening and closing characteristics during mitigation of an overpressure transient. Thus, a pressure limit more restrictive than the 10CFR50, Appendix G[4] allowable is imposed above a certain temperature so that the loads on the piping from a LTOPS event would not affect the piping integrity.

Two specific transients have been defined, with the RCS in a water-solid condition, as the design basis for LTOPS. Each of these scenarios assumes no RHR System heat removal capability. The RHR System relief valve (203) does not actuate during the transients. The first transient consists of a heat injection scenario in which a

reactor coolant pump in a single loop is started with the RCS temperature as much as 50°F lower than the steam generator secondary side temperature. This results in a sudden heat input to a water-solid RCS from the steam generators, creating an increasing pressure transient. The second transient has been defined as a mass injection scenario into a water-solid RCS caused by the simultaneous isolation of the RHR System, isolation of letdown, and failure of the normal charging flow controls to the full flow condition. Various combinations of charging and safety injection flows may also be evaluated on a plant-specific basis. The resulting mass injection/letdown mismatch causes an increasing pressure transient.

3.2 LTOPS Setpoint Determination

Rochester Gas and Electric and Babcock & Wilcox Nuclear Technology (BWNT) have developed the following methodology which is employed to determine PORV setpoints for mitigation of the LTOPS design basis cold overpressurization transients. This methodology maximizes the available operating margin for setpoint selection while maintaining an appropriate level of protection in support of reactor vessel and RHR System integrity.

3.2.1 Parameters Considered

The selection of proper LTOPS setpoint for actuating the PORVs requires the consideration of numerous system parameters including:

a. Volume of reactor coolant involved in transient
b. RCS pressure signal transmission delay
c. Volumetric capacity of the relief valves versus opening position, including the potential for critical flow
d. Stroke time of the relief valves (open & close)
e. Initial temperature and pressure of the RCS and steam generator
f. Mass input rate into RCS
g. Temperature of injected fluid

h. Heat transfer characteristics of the steam generators

i. Initial temperature asymmetry between RCS and steam generator secondary water

j. Mass of steam generator secondary water

k. RCP startup dynamics

l. 10CFR50, Appendix G[4] pressure/temperature characteristics of the reactor vessel

m. Pressurizer PORV piping/structural analysis limitations

n. Dynamic and static pressure differences throughout the RCS and RHRS

o. RHR System pressure limits

p. Loop assymetry for RCP start cases

q. Dynamic and static pressure differences throughout the RCS and RHRS

These parameters are modelled in the BWNT RELAP5/MOD2-B&W computer code (Ref. 19) which calculates the maximum and minimum system pressures.

3.2.2 Pressure Limits Selection

The function of the LTOPS is to protect the reactor vessel from fast propagating brittle fracture. This has been implemented by choosing a LTOPS setpoint which prevents exceeding the limits prescribed by the applicable pressure/temperature characteristic for the specific reactor vessel material in accordance with rules given in Appendix G to 10CFR50[4]. The LTOPS design basis takes credit for the fact that overpressure events most likely occur during isothermal conditions in the RCS. Therefore, it is appropriate to utilize the steady-state Appendix G limit. In addition, the LTOPS also provides for an operational consideration to maintain the integrity of the PORV piping, and to protect the RHR System from overpressure during the LTOPS design basis transients. A typical characteristic 10CFR50 Appendix G curve is shown by Figure 3.1 where the allowable system pressure increases with increasing temperature. This type of curve sets the nominal upper limit on the pressure which should not be exceeded during RCS increasing pressure transients based on reactor vessel material properties. Superimposed on this curve is the PORV piping limit and RHR System pressure limit which is conservatively

used, for setpoint development, as the maximum allowable pressure above the temperature at which it intersects with the 10CFR50 Appendix G curve.

When a relief valve is actuated to mitigate an increasing pressure transient, the release of a volume of coolant through the valve will cause the pressure increase to be slowed and reversed as described by Figure 3.2. The system pressure then decreases, as the relief valve releases coolant, until a reset pressure is reached where the valve is signalled to close. Note that the pressure continues to decrease below the reset pressure as the valve recloses. The nominal lower limit on the pressure during the transient is typically established based solely on an operational consideration for the reactor coolant pump #1 seal to maintain a nominal differential pressure across the seal faces for proper film-riding performance. In the event that the available range is insufficient to concurrently accomodate the upper and lower pressure limits, the upper pressure limits are given preference.

The nominal upper limit (based on the minimum of the steady-state 10CFR50 Appendix G requirement, the RHR System pressure limit, and the PORV piping limitations) and the nominal RCP #1 seal performance criteria create a pressure range from which the setpoints for both PORVs may be selected as shown on Figures 3.3 and 3.4.

3.2.3 Mass Input Consideration

For a particular mass input transient to the RCS, the relief valve will be signalled to open at a specific pressure setpoint. However, as shown on Figure 3.2, there will be a pressure overshoot during the delay time before the valve starts to move and during the time the valve is moving to the full open position. This overshoot is dependent on the dynamics of the system and the input parameters, and results in a maximum system pressure somewhat higher than the set pressure. Similarly there will be a pressure undershoot, while the valve is relieving, both due to the reset pressure being below the setpoint and to the delay in stroking the valve closed. The maximum and minimum pressures reached (P_{MAX} and P_{MIN}) in the transient are a function of the selected setpoint (P_S) as shown on Figure 3.3. The

shaded area represents an optimum range from which to select the setpoint based on the particular mass input case. Several mass input cases may be run at various input flow rates to bound the allowable setpoint range.

3.2.4 Heat Input Consideration

The heat input case is done similarly to the mass input case except that the locus of transient pressure values versus selected setpoints may be determined for several values of the initial RCS temperature. This heat input evaluation provides a range of acceptable setpoints dependent on the reactor coolant temperature, whereas the mass input case is limited to the most restrictive low temperature condition only (i.e. the mass injection transient is not sensitive to temperature). The shaded area on Figure 3.4 describes the acceptable band for a heat input transient from which to select the setpoint for a particular initial reactor coolant temperature. If the LTOPS is a single setpoint system, the most limiting result is used throughout.

3.2.5 Final Setpoint Selection

By superimposing the results of multiple mass input and heat input cases evaluated, (from a series of figures such as 3.3 and 3.4) a range of allowable PORV setpoints to satisfy both conditions can be determined. For a single setpoint system, the most limitting setpoint is chosen, with the upper pressure limit given precedence if both limits cannot be accomodated.

The selection of the setpoints for the PORVs considers the use of nominal upper and lower pressure limits. The upper limits are specified by the minimum of the steady-state cooldown curve as calculated in accordance with Appendix G to 10CFR50[4] or the peak RCS or RHR System pressure based upon piping/structural analysis loads. The lower pressure extreme is specified by the reactor coolant pump #1 seal minimum differential pressure performance criteria. Since both the upper and lower pressure values are conservatively determined, the uncertainties

in the pressure and temperature instrumentation utilized by the LTOPS are not explicitly accounted for in the selection of the LTOPS PORV setpoints. Accounting for the effects of instrumentation uncertainty would impose additional unnecessary restrictions on the setpoint development, which is already based on conservative pressure limits (such as a safety factor of 2 on pressure stress, use of a lower bound K_{IR} curve and an assumed ¼T flaw depth with a length equal to 1½ times the vessel wall thickness) as discussed in Section 2 of this report, without a commensurate increase in the level of protection afforded to reactor vessel integrity.

3.3 Application of ASME Code Case N-514

ASME Code Case N-514[17] allows low temperature overpressure protection systems (LTOP) to limit the maximum pressure in the reactor vessel to 110% of the pressure determined to satisfy Appendix G, paragraph G-2215, of Section XI of the ASME Code[5]. (Note, that the setpoint selection methodology as discussed in Section 3.2.5 specifically utilizes the steady-state curve.) The application of ASME Code Case N-514 increases the operating margin in the region of the pressure-temperature limit curves where the LTOPS system is enabled. Code Case N-514 requires LTOPS to be effective at coolant temperatures less than 200°F or at coolant temperatures corresponding to a reactor vessel metal temperature less than RT_{NDT} + 50°F, whichever is greater. RT_{NDT} is the highest adjusted reference temperature for weld or base metal in the beltline region at a distance one-fourth of the vessel section thickness from the vessel inside surface, as determined by Regulatory Guide 1.99, Revision 2. Although expected soon, use of Code Case N-514 has not yet been formally approved by the NRC. In the interim, an exemption to the regulations must be granted by the NRC before Code Case N-514 can be used in the determination of the LTOPS setpoint(s) and enable temperature.

3.4 Enable Temperature for LTOPS

The enable temperature is the temperature below which the LTOPS system is required to be operable. The definition of the enabling temperature currently approved and supported by the NRC is described in Branch Technical Position RSB 5-2[18]. This position defines the enable temperature for LTOP systems as the water temperature corresponding to a metal temperature of at least RT_{NDT} + 90°F at the beltline location (1/4t or 3/4t) that is controlling in the Appendix G limit calculations. This definition is mostly based on material properties and fracture mechanics, with the understanding that material temperatures of RT_{NDT} + 90°F at the critical location will be well up the transition curve from brittle to ductile properties, and therefore brittle fracture of the vessel is not expected.

The ASME Code Case N-514 supports an enable temperature of RT_{NDT} + 50°F or 200°F, whichever is greater as described in Section 3.3. This definition is also supported by Westinghouse and can be used by requesting an exemption to the regulations or when ASME Code Case N-514 is formally approved by the NRC.

The RCS cold leg temperature limitation for starting an RCP is the same value as the LTOPS enable temperature to ensure that the basis of the heat injection transient is not violated. The Standard Technical Specifications (STS) prohibit starting an RCP when any RCS cold leg temperatures is less than or equal to the LTOPS enable temperature unless the secondary side water temperature of each steam generator is less than or equal to 50°F above each of the RCS cold leg temperatures.

Figure 3.1

TYPICAL APPENDIX G
P/T CHARACTERISTICS

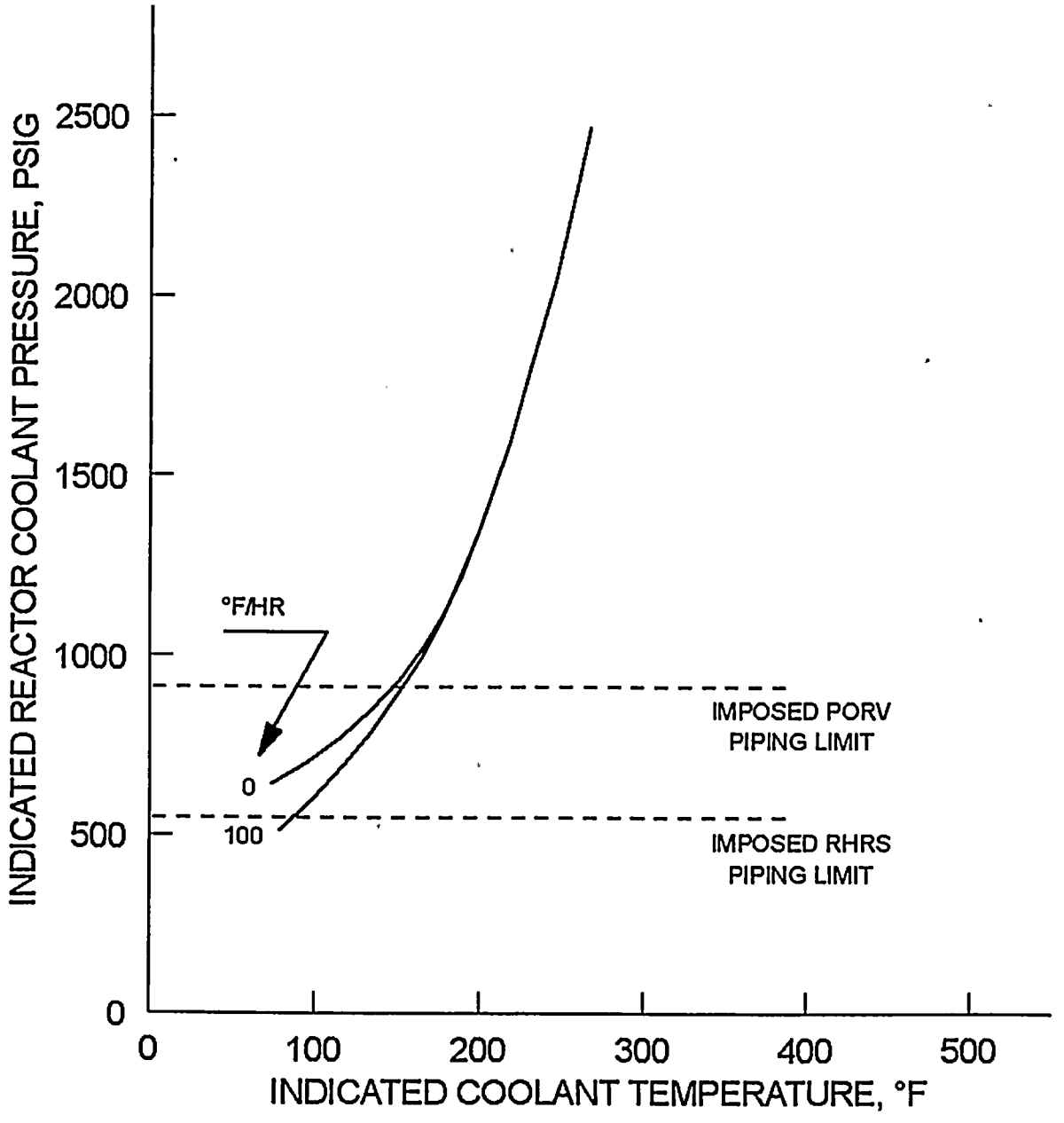

Figure 3.2

TYPICAL PRESSURE TRANSIENT
(1 RELIEF VAVLE CYCLE)

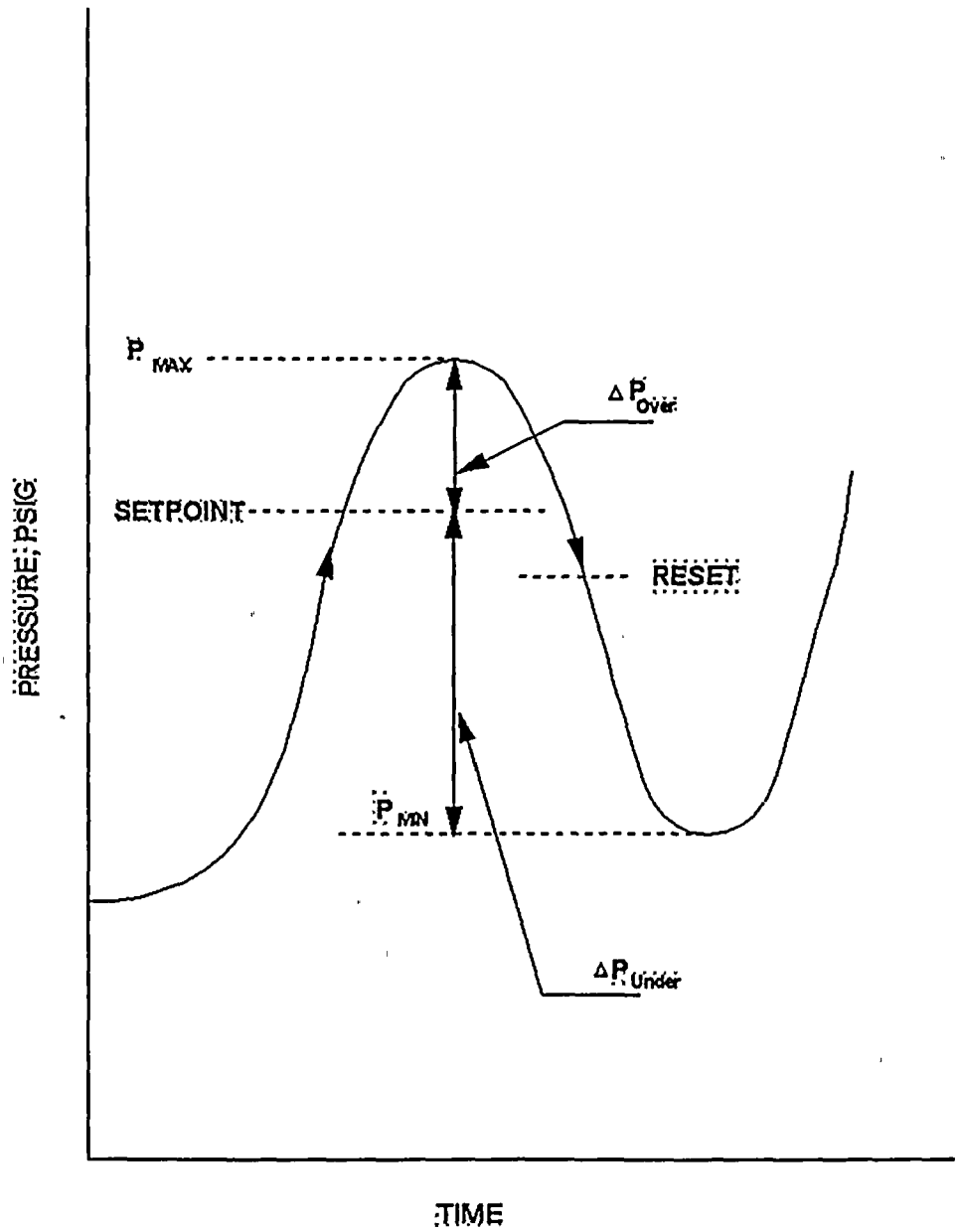

Figure 3.3

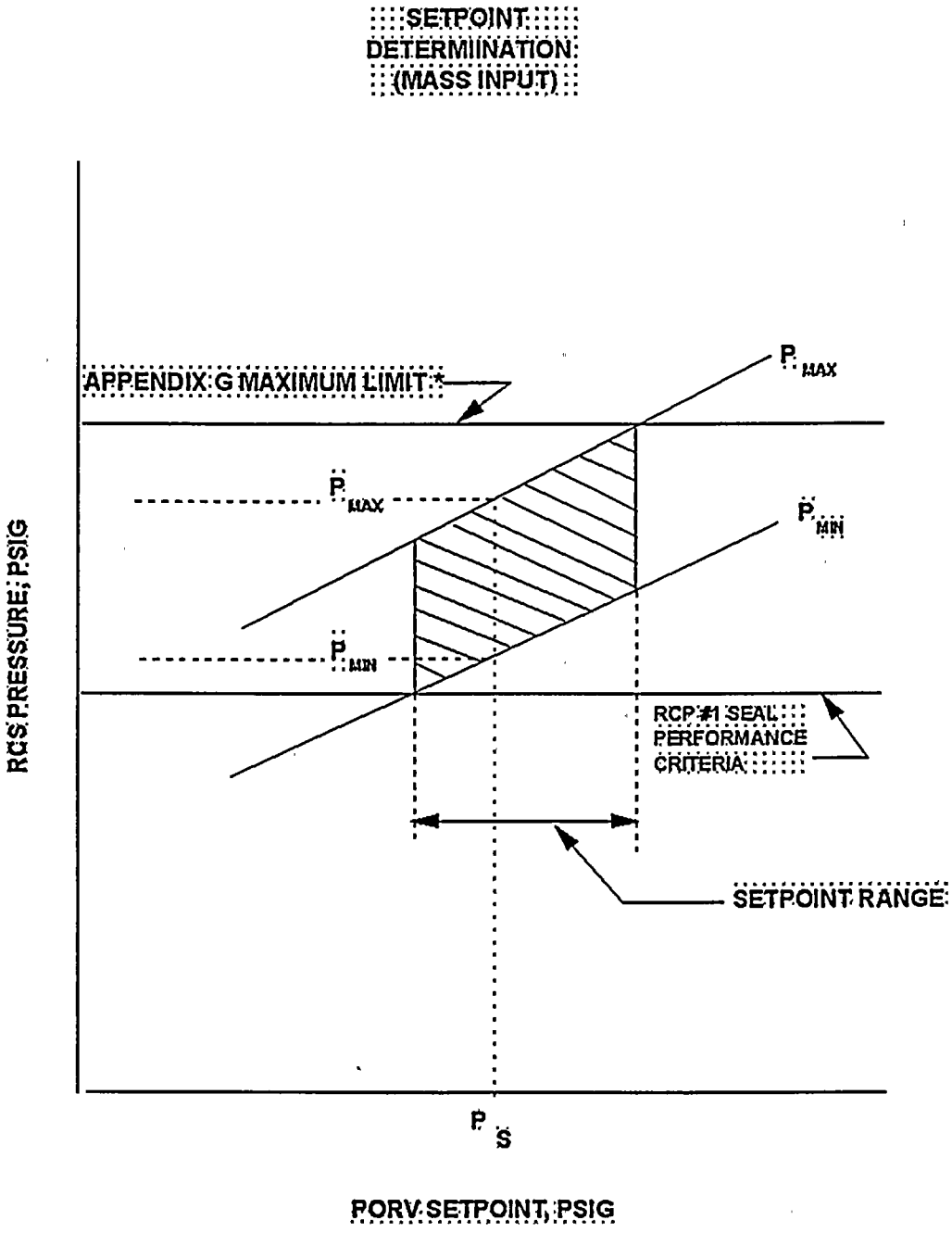

* The maximum pressure limit is the minimum of the Appendix G limit, the PORV discharge piping structural analysis limit, or the RHR system limit.

Figure 3.4

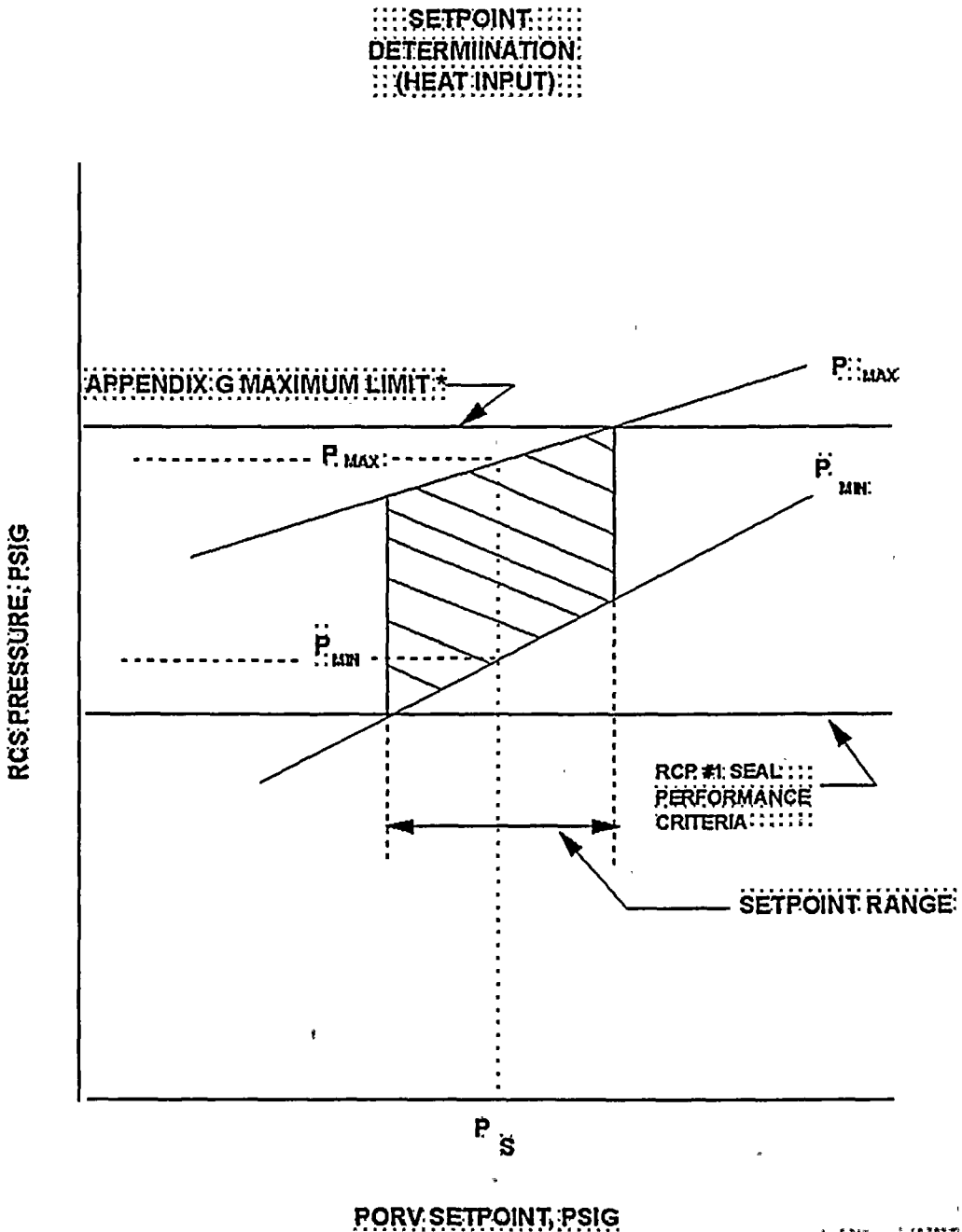

* The maximum pressure limit is the minimum of the Appendix G limit, the PORV discharge piping structural analysis limit, or the RHR system limit

4.0 REFERENCES

1. NUREG 1431, "Standard Technical Specifications for Westinghouse Pressurized Water Reactors", Revision 0, September, 1992.

2. U.S. Nuclear Regulatory Commission, "Removal of Cycle-Specific Parameter Limits from Technical Specifications", Generic Letter 88-16, October, 1988.

3. U.S. Nuclear Regulatory Commission, Radiation Embrittlement of Reactor Vessel Materials, Regulatory Guide 1.99, Revision 2, May, 1988.

4. Code of Federal Regulations, Title 10, Part 50, "Fracture Toughness Requirements for Light-Water Nuclear Power Reactors", Appendix G, Fracture Toughness Requirements.

5. ASME Boiler and Pressure Vessel Code, Section XI, "Rules for Inservice Inspection of Nuclear Power Plant Components", Appendix G, Fracture Toughness Criteria For Protection Against Failure.

6. R. G. Soltesz, R. K. Disney, J. Jedruch, and S. L. Ziegler, Nuclear Rocket Shielding Methods, Modification, Updating and Input Data Preparation. Vol. 5--Two-Dimensional Discrete Ordinates Transport Technique, WANL-PR(LL)-034, Vol. 5, August 1970.

7. ORNL RSIC Data Library Collection DLC-76 SAILOR Coupled Self-Shielded, 47 Neutron, 20 Gamma-Ray, P3, Cross Section Library for Light Water Reactors.

8. ASME Boiler and Pressure Vessel Code, Section III, "Rules for Construction of Nuclear Power Plant Components", Division 1, Subsection NB: Class 1 Components.

9. Branch Technical Position MTEB 5-2, "Fracture Toughness Requirements", NUREG-0800 Standard Review Plan 5.3.2, Pressure-Temperature Limits, July 1981, Rev. 1.

10. ASTM E-208, Standard Test Method for Conducting Drop-Weight Test to Determine Nil-Ductility Transition Temperature of Ferritic Steels, ASTM Standards, Section 3, American Society for Testing and Materials.

11. B&W Owners Group Report BAW-2202, "Fracture Toughness Characterization of WF-70 Weld Material", B&W Owners Group Materials Committee, September 1993.

12. Letter, Clyde Y. Shiraki, Nuclear Regulatory Commission, to D. L. Farrar, Commonwealth Edison Company, "Exemption from the Requirement to Determine the Unirradiated Reference Temperature in Accordance with the Method Specified in 10 CFR 50.61(b) (2) (i) (TAC NOS. M84546 and M84547)", Docket Nos. 50-295 and 50-304, February 22, 1994.

13. Code of Federal Regulations, Title 10, Part 50, "Fracture Toughness Requirements for Light-Water Nuclear Power Reactors", Appendix H, Reactor Vessel Material Surveillance Program Requirements.

14. Timoshenko, S. P. and Goodier, J. N., Theory of Elasticity, Third Edition, McGraw-Hill Book Co., New York, 1970.

15. ASME Boiler and Pressure Vessel Code, Section XI, "Rules for Inservice Inspection of Nuclear Power Plant Components", Appendix A, Analysis of Flaws, Article A-3000, Method For K_I Determination.

16. WRC Bulletin No. 175, "PVRC Recommendations on Toughness Requirements for Ferritic Materials", Welding Research Council, New York, August 1972.

17. ASME Boiler and Pressure Vessel Code Case N-514, Section XI, Division 1, "Low Temperature Overpressure Protection", Approval date: February 12, 1992.

18. Branch Technical Position RSB 5-2, "Overpressurization Protection of Pressurized Water Reactors While Operating at Low Temperatures", NUREG-0800 Standard Review Plan 5.2.2, Overpressure Protection, November 1988, Rev. 2.

19. BWNT, "RELAPS/MOD2, An Advanced Computer Program for Light-Water Reactor LOCA and Non-LOCA Transient Analysis," BAW-10164P-A.

3.0 LOW TEMPERATURE OVERPRESSURE PROTECTION SYSTEM (LTOPS)

3.1 INTRODUCTION

The purpose of the LTOPS is to supplement the normal plant operational administrative controls to protect the reactor vessel from being exposed to conditions of fast propagating brittle fracture. The LTOPS also protects the Residual Heat Removal (RHR) System from overpressurization. This has been achieved by conservatively choosing an LTOPS setpoint which prevents the RCS from exceeding the pressure/temperature limits established by 10 CFR Part 50 Appendix G[4] requirements, and the RHR System from exceeding 110% of its design pressure. The LTOPS is designed to provide the capability, ~~0 C O L D OVERPRESSURE MITIGATING SYSTEM (COMS)~~

~~3.1 INTRODUCTION~~

~~The purpose of the COMS is to supplement the normal plant operational administrative controls and the water relief valves in the Residual Heat Removal System (RHRS) when they are unavailable to protect the reactor vessel from being exposed to conditions of fast propagating brittle fracture. This has been achieved by conservatively choosing COMS setpoints which prevent exceeding the pressure/temperature limits established by 10 CFR Part 50 Appendix G[4] requirements. The COMS is designed to provide the capability,~~ during relatively low temperature operation (typically less than 350°F), to automatically prevent the RCS pressure from exceeding the applicable limits. Once the system is enabled, no operator action is involved for the LTOPS to perform its intended pressure mitigation function. ~~no operator action is involved for the COMS to perform its intended pressure mitigation function.~~ Thus, no operator action is modelled in the analyses supporting the setpoint selection, although operator action may be initiated to ultimately terminate the cause of the overpressure event.

The PORVs located near the top of the pressurizer, together with additional actuation logic from the low-range pressure channels, are utilized to mitigate potential RCS overpressure transients. The LTOPS provides the relief capacity for

specific transients which would not be mitigated by the RHR System relief valve, together with additional actuation logic from the wide-range pressure channels, are utilized to mitigate potential RCS overpressure transients defined below if the RHRS water relief valves are inadvertently isolated from the RCS. The COMS provides the supplemental relief capacity for specific transients which would not be mitigated by the RHRS relief valves. In addition, a limit on the PORV piping is accommodated due to the potential for water hammer effects to be developed in the piping associated with these valves as a result of the cyclic opening and closing characteristics during mitigation of an overpressure transient. Thus, a pressure limit more restrictive than the 10CFR50, Appendix G[3] allowable is imposed above a certain temperature so that the loads on the piping from a LTOPS event would not affect the piping integrity. Appendix G[4] allowable is imposed above a certain temperature so that the loads on the piping from a COMS event would not affect the piping integrity.

Two specific transients have been defined, with the RCS in a water-solid condition, as the design basis for LTOPS. Each of these scenarios assumes no RHR System heat removal capability. The RHR System relief valve (203) does not actuate during the transients. The first transient consists of a heat injection scenario in which a reactor coolant pump in a single loop is started with the RCS temperature as much as 50°F lower than the steam generator secondary side temperature. as the design basis for COMS. Each of these scenarios assumes as an initial condition that the RHRS is isolated from the RCS, and thus the relief capability of the RHRS relief valves is not available. The first transient consists of a heat injection scenario in which a reactor coolant pump in a single loop is started with the RCS temperature as much as 50°F lower than the steam generator secondary side temperature and the RHRS has been inadvertently isolated. This results in a sudden heat input to a water-solid RCS from the steam generators, creating an increasing pressure transient. The second transient has been defined as a mass injection scenario into a water-solid RCS caused by the simultaneous isolation of the RHR System, isolation of letdown, and failure of the normal charging flow controls to the full flow condition. The second transient has been defined as a mass injection scenario into a water-solid RCS caused by the simultaneous isolation of the RHRS, isolation of letdown and failure of the normal charging flow controls to the full flow

~~condition.~~ Various combinations of charging and safety injection flows may also be evaluated on a plant-specific basis. The resulting mass injection/letdown mismatch causes an increasing pressure transient.

3.2 LTOPS Setpoint Determination

Rochester Gas and Electric and Babcock & Wilcox Nuclear Technology (BWNT) have developed the following methodology which is employed to determine PORV setpoints for mitigation of the LTOPS design basis cold overpressurization transients. This methodology maximizes the available operating margin for setpoint selection while maintaining an appropriate level of protection in support of reactor vessel and RHR System integrity. ~~2 COMS Setpoint Determination~~

~~Westinghouse has developed the following methodology which is employed to determine PORV setpoints for mitigation of the COMS design basis cold overpressurization transients. This methodology maximizes the available operating margin for setpoint selection while maintaining an appropriate level of protection in support of reactor vessel integrity.~~

3.2.1 Parameters Considered

The selection of proper LTOPS setpoint for actuating the PORVs requires the consideration of numerous system parameters including: ~~The selection of proper COMS setpoints for actuating the PORVs requires the consideration of numerous system parameters including:~~

a. Volume of reactor coolant involved in transient
b. RCS pressure signal transmission delay
c. Volumetric capacity of the relief valves versus opening position, including the potential for critical flow

~~Volumetric capacity of the relief valves versus opening position~~

d. Stroke time of the relief valves (open & close)

e. Initial temperature and pressure of the RCS and steam generator ~~Initial temperature and pressure of the RCS~~

f. Mass input rate into RCS

g. Temperature of injected fluid

h. Heat transfer characteristics of the steam generators

i. Initial temperature asymmetry between RCS and steam generator secondary water

j. Mass of steam generator secondary water

k. RCP startup dynamics

l. 10CFR50, Appendix G[3] pressure/temperature characteristics of the reactor vessel ~~Appendix G pressure/temperature characteristics of the reactor vessel~~

m. Pressurizer PORV piping/structural analysis limitations

n. Dynamic and static pressure differences throughout the RCS and RHRS

o. RHR System pressure limits

p. Loop assymetry for RCP start cases

q. Dynamic and static pressure differences throughout the RCS and RHRS

These parameters are modelled in the BWNT RELAP5/MOD2-B&W computer code (Ref. 19) which calculates the maximum and minimum system pressures. ~~Dynamic and static pressure difference between reactor vessel midplane and location of wide range pressure transmitter~~

~~These parameters are input to a specialized version of the LOFTRAN computer code which calculates the maximum and minimum system pressures.~~

3.2.2 Pressure Limits Selection

The function of the LTOPS is to protect the reactor vessel from fast propagating brittle fracture. This has been implemented by choosing a LTOPS setpoint which prevents exceeding the limits prescribed by the applicable pressure/temperature

characteristic for the specific reactor vessel material in accordance with rules given in Appendix G to 10CFR50[3]. The LTOPS design basis takes credit for the fact that overpressure events most likely occur during isothermal conditions in the RCS. ~~The function of the COMS is to protect the reactor vessel from fast propagating brittle fracture. This has been implemented by choosing COMS setpoints which prevent exceeding the limits prescribed by the applicable pressure/temperature characteristic for the specific reactor vessel material in accordance with rules given in Appendix G to 10CFR50[4]. The COMS design basis takes credit for the fact that overpressure events most likely occur during isothermal conditions in the RCS.~~ Therefore, it is appropriate to utilize the steady-state Appendix G limit. In addition, the LTOPS also provides for an operational consideration to maintain the integrity of the PORV piping, and to protect the RHR System from overpressure during the LTOPS design basis transients. ~~the COMS also provides for an operational consideration to maintain the integrity of the PORV piping.~~ A typical characteristic 10CFR50 Appendix G curve is shown by Figure 3.1 where the allowable system pressure increases with increasing temperature. This type of curve sets the nominal upper limit on the pressure which should not be exceeded during RCS increasing pressure transients, based on reactor vessel material properties. Superimposed on this curve is the PORV piping limit and RHR System pressure limit which is conservatively used. ~~Superimposed on this curve is the PORV piping limit which is conservatively used,~~ for setpoint development, as the maximum allowable pressure above the temperature at which it intersects with the 10CFR50 Appendix G curve.

~~When a relief valve is actuated to mitigate an increasing pressure transient,~~

~~When a relief valve is actuated to mitigate an increasing pressure transient,~~ When a relief valve is actuated to mitigate an increasing pressure transient, the release of a volume of coolant through the valve will cause the pressure increase to be slowed and reversed as described by Figure 3.2. The system pressure then decreases, as the relief valve releases coolant, until a reset pressure is reached where the valve is signalled to close. Note that the pressure continues to decrease below the reset pressure as the valve recloses. The nominal lower limit on the

pressure during the transient is typically established based solely on an operational consideration for the reactor coolant pump #1 seal to maintain a nominal differential pressure across the seal faces for proper film-riding performance. In the event that the available range is insufficient to concurrently accomodate the upper and lower pressure limits, the upper pressure limits are given preference.

The nominal upper limit (based on the minimum of the steady-state 10CFR50 Appendix G requirement, the RHR System pressure limit, and the PORV piping limitations) and the nominal RCP #1 seal performance criteria create a pressure range from which the setpoints for both PORVs may be selected as shown on Figures 3.

~~The nominal upper limit (based on the minimum of the steady-state 10CFR50 Appendix G requirement and the PORV piping limitations) and the nominal RCP #1 seal performance criteria create a pressure range from which the setpoints for both PORVs may be selected as shown on Figures 3.~~3 and 3.4.

3.2.3 Mass Input Consideration

For a particular mass input transient to the RCS, the relief valve will be signalled to open at a specific pressure setpoint. However, as shown on Figure 3.2, there will be a pressure overshoot during the delay time before the valve starts to move and during the time the valve is moving to the full open position. This overshoot is dependent on the dynamics of the system and the input parameters, and results in a maximum system pressure somewhat higher than the set pressure. Similarly there will be a pressure undershoot, while the valve is relieving, both due to the reset pressure being below the setpoint and to the delay in stroking the valve closed. The maximum and minimum pressures reached (P_{MAX} and P_{MIN}) in the transient are a function of the selected setpoint (P_S) as shown on Figure 3.3. The shaded area represents an optimum range from which to select the setpoint based on the particular mass input case. Several mass input cases may be run at various input flow rates to bound the allowable setpoint range.

3.2.4 Heat Input Consideration

The heat input case is done similarly to the mass input case except that the locus of transient pressure values versus selected setpoints may be determined for several values of the initial RCS temperature. This heat input evaluation provides a range of acceptable setpoints dependent on the reactor coolant temperature, whereas the mass input case is limited to the most restrictive low temperature condition only (i.e. the mass injection transient is not sensitive to temperature). The shaded area on Figure 3.4 describes the acceptable band for a heat input transient from which to select the setpoint for a particular initial reactor coolant temperature. If the LTOPS is a single setpoint system, the most limiting result is used throughout.

3.2.5 Final Setpoint Selection

By superimposing the results of multiple mass input and heat input cases evaluated, (from a series of figures such as 3.3 and 3.4) a range of allowable PORV setpoints to satisfy both conditions can be determined. For a single setpoint system, the most limitting setpoint is chosen, with the upper pressure limit given precedence if both limits cannot be accomodated. ~~Each of the two PORVs may have a different pressure setpoint versus temperature specification such that only one valve will open at a time and mitigate the transient (i.e. staggered setpoints). The second valve operates only if the first fails to open on command. This design supports a single failure assumption as well as minimizing the potential for both PORVs to open simultaneously, a condition which may create excessive pressure undershoot and challenge the RCP #1 seal performance criteria. However, each of the sets of staggered setpoints must result in the system pressure staying below the P_{MAX} pressure limit shown on Figures 3.3 and 3.4 when either valve is utilized to mitigate the transient.~~

~~The function generator used to program the pressure versus setpoint curves for each valve has a limited number of programmable break points (typically 9). These~~

~~are strategically defined in the final selection process, with consideration given to the slope of any line segment, which is limited to approximately 24 psi/°F.~~

The selection of the setpoints for the PORVs considers the use of nominal upper and lower pressure limits. The upper limits are specified by the minimum of the steady-state cooldown curve as calculated in accordance with Appendix G to 10CFR50[4] or the peak RCS or RHR System pressure based upon piping/structural analysis loads. ~~The upper limits are specified by the minimum of the steady-state cooldown curve as calculated in accordance with Appendix G to 10CFR50[4] or the peak RCS pressure based upon piping/structural analysis loads.~~ The lower pressure extreme is specified by the reactor coolant pump #1 seal minimum differential pressure performance criteria. Since both the upper and lower pressure values are conservatively determined, the uncertainties in the pressure and temperature instrumentation utilized by the LTOPS are not explicitly accounted for in the selection of the LTOPS PORV setpoints; ~~the uncertainties in the pressure and temperature instrumentation utilized by the COMS are not explicitly accounted for in the selection of the COMS PORV setpoints.~~ Accounting for the effects of instrumentation uncertainty would impose additional unnecessary restrictions on the setpoint development, which is already based on conservative pressure limits (such as a safety factor of 2 on pressure stress, use of a lower bound K_{Ir} curve and an assumed ¼T flaw depth with a length equal to 1½ times the vessel wall thickness) as discussed in Section 2 of this report; ~~use of a lower bound K_{Ir} curve and an assumed ¼T flaw depth with a length equal to 1½ times the vessel wall thickness) as discussed in section 2 of this report,~~ without a commensurate increase in the level of protection afforded to reactor vessel integrity.

3.3 Application of ASME Code Case N-514

ASME Code Case N-514[17] allows low temperature overpressure protection systems (LTOP) to limit the maximum pressure in the reactor vessel to 110% of the pressure determined to satisfy Appendix G. ~~ASME Code Case N-514[17] allows low temperature overpressure protection systems (LTOPS, as the code case refers to COMS) to limit the maximum pressure in the reactor vessel to 110% of the~~

~~pressure determined to satisfy Appendix G,~~ paragraph G-2215, of Section XI of the ASME Code[5]. (Note, that the setpoint selection methodology as discussed in Section 3.2.5 specifically utilizes the steady-state curve.) The application of ASME Code Case N-514 increases the operating margin in the region of the pressure-temperature limit curves where the LTOPS system is enabled.) ~~The application of ASME Code Case N-514 increases the operating margin in the region of the pressure-temperature limit curves where the COMS system is enabled.~~ Code Case N-514 requires LTOPS to be effective at coolant temperatures less than 200°F or at coolant temperatures corresponding to a reactor vessel metal temperature less than RT_{NDT} + 50°F, whichever is greater. RT_{NDT} is the highest adjusted reference temperature for weld or base metal in the beltline region at a distance one-fourth of the vessel section thickness from the vessel inside surface, as determined by Regulatory Guide 1.99, Revision 2. Although expected soon, use of Code Case N-514 has not yet been formally approved by the NRC. In the interim, an exemption to the regulations must be granted by the NRC before Code Case N-514 can be used in the determination of the LTOPS setpoint(s) and enable temperature.

3.4 Enable Temperature for LTOPS

The enable temperature is the temperature below which the LTOPS system is required to be operable. ~~an exemption to the regulations must be granted by the NRC before Code Case N-514 can be used in the determination of the COMS setpoints and enable temperature.~~

~~3.4 Enable Temperature for COMS~~

~~The enable temperature is the temperature below which the COMS system is required to be operable.~~ The definition of the enabling temperature currently approved and supported by the NRC is described in Branch Technical Position RSB 5-2[18]. This position defines the enable temperature for LTOP systems as the water temperature corresponding to a metal temperature of at least RT_{NDT} + 90°F at the beltline location (1/4t or 3/4t) that is controlling in the Appendix G limit calculations. This definition is mostly based on material properties and fracture mechanics. ~~This definition is also supported by Westinghouse and is mostly based on material properties and fracture mechanics,~~ with the understanding that material temperatures of RT_{NDT} + 90°F at the critical location will be well up the transition curve from brittle to ductile properties, and therefore brittle fracture of the vessel is not expected.

The ASME Code Case N-514 supports an enable temperature of RT_{NDT} + 50°F or 200°F, whichever is greater as described in Section 3.3. This definition is also supported by Westinghouse and can be used by requesting an exemption to the regulations or when ASME Code Case N-514 is formally approved by the NRC.

The RCS cold leg temperature limitation for starting an RCP is the same value as the LTOPS enable temperature to ensure that the basis of the heat injection transient is not violated. The Standard Technical Specifications (STS) prohibit starting an RCP when any RCS cold leg temperatures is less than or equal to the LTOPS enable temperature unless the secondary side water temperature of each steam generator is less than or equal to 50°F above each of the RCS cold leg temperatures.

Figure 3.1

Figure 3.2

Figure 3.3

* The maximum pressure limit is the minimum of the Appendix G limit, the PORV discharge piping structural analysis limit, or the RHR system limit

Figure 3.4

* The maximum pressure limit is the minimum of the Appendix G limit, the PORV discharge piping structural analysis limit, or the RHR system limit

~~The RCS cold leg temperature limitation for starting an RCP is the same value as the COMS enable temperature to ensure that the basis of the heat injection transient is not violated. The Standard Technical Specifications (STS) prohibit starting an RCP when any RCS cold leg temperatures is less than or equal to the COMS enable temperature unless the secondary side water temperature of each steam generator is less than or equal to 50°F above each of the RCS cold leg temperatures.~~

FIGURE 3.1

TYPICAL APPENDIX G
P/T CHARACTERISTICS

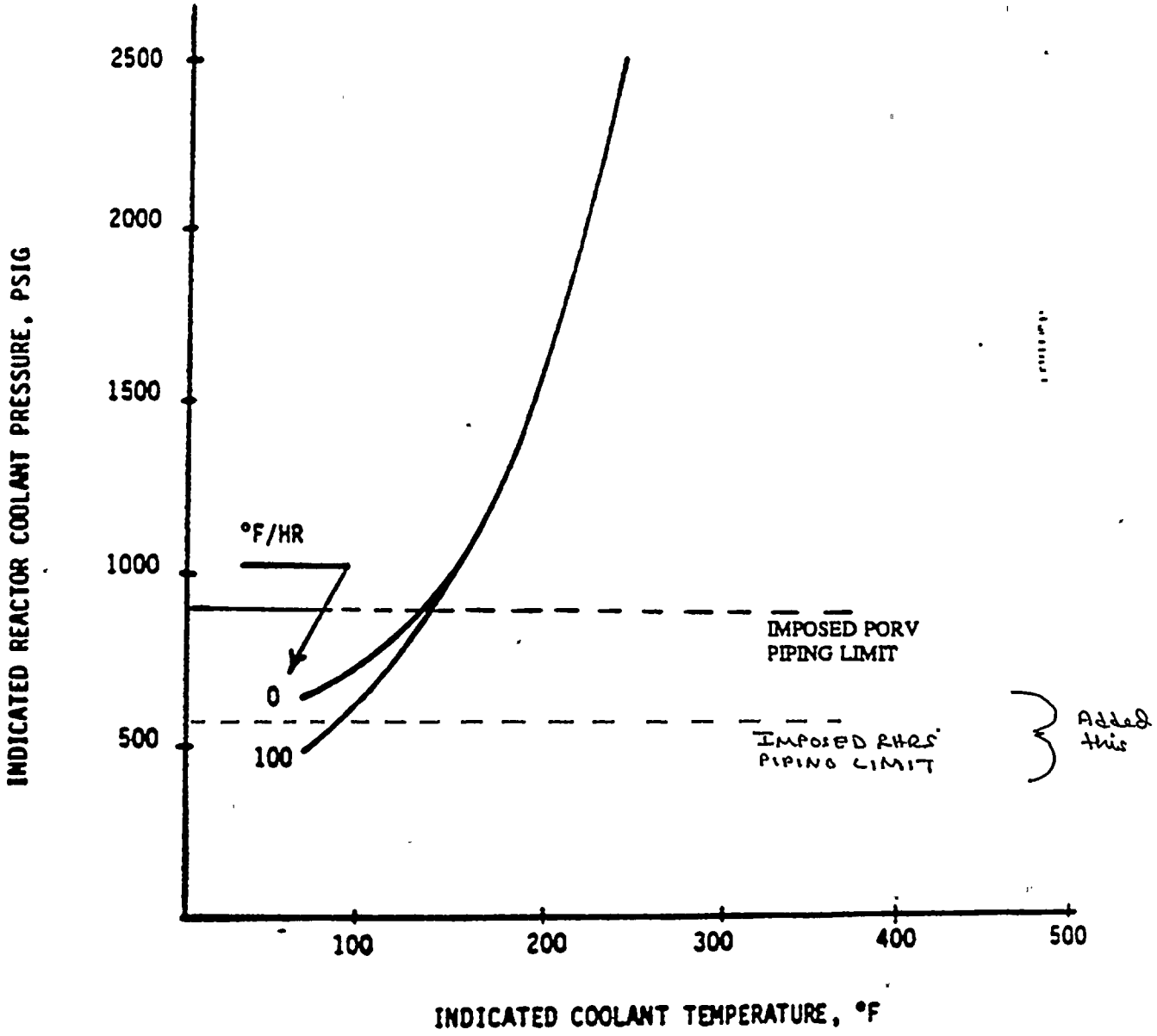

FIGURE 3.2

TYPICAL PRESSURE TRANSIENT

(1 RELIEF VALVE CYCLE)

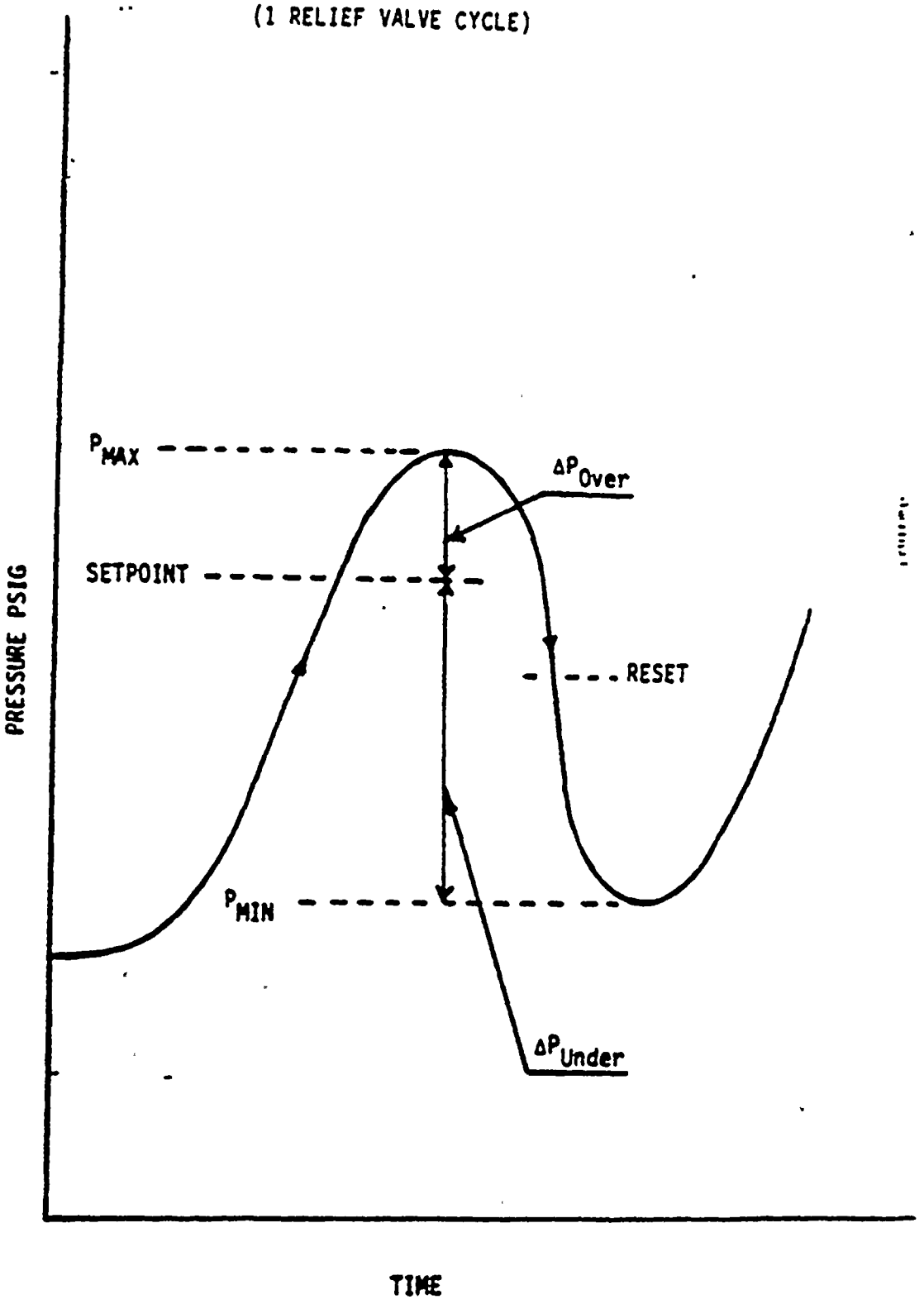

FIGURE 3.3

SETPOINT

DETERMINATION

(MASS INPUT)

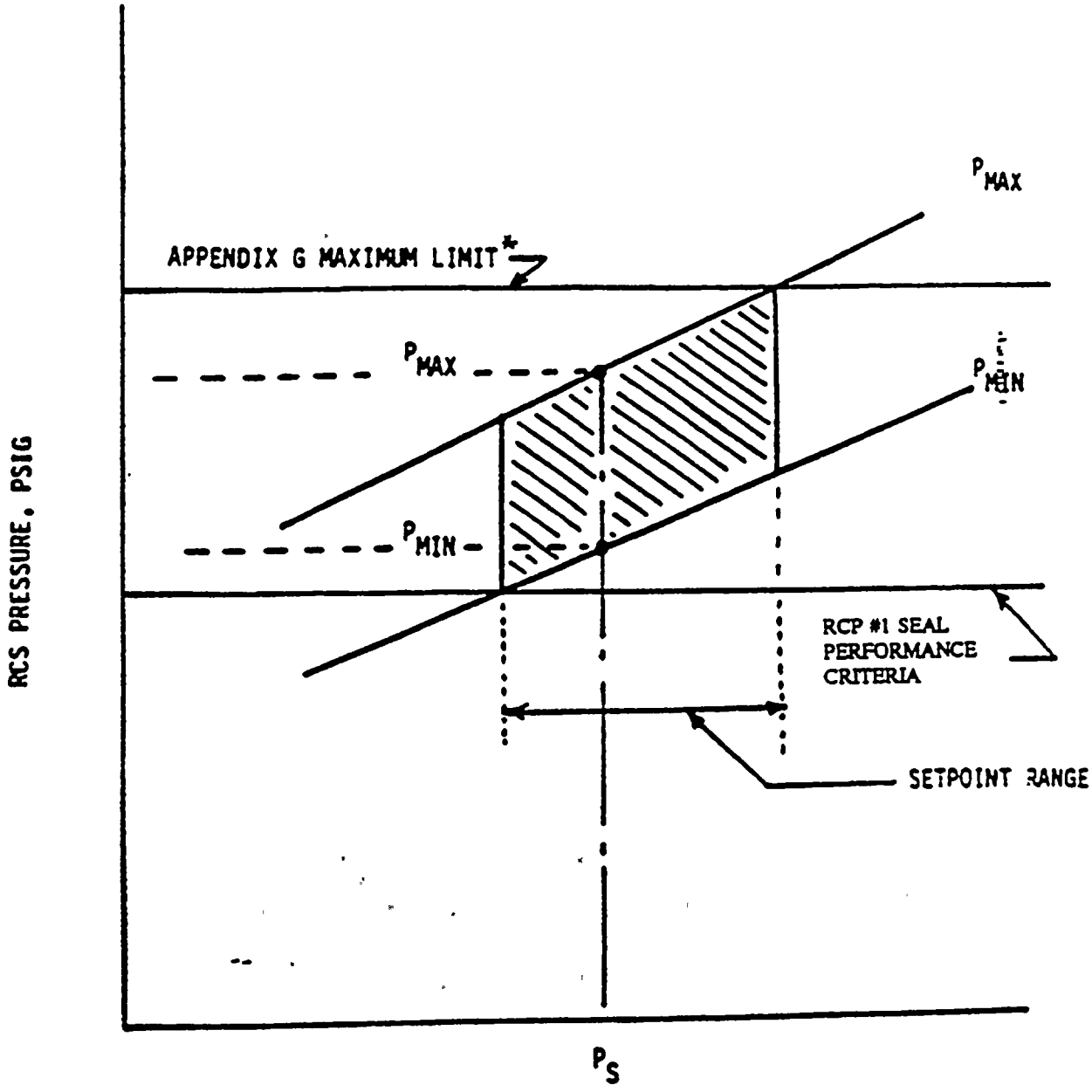

* The maximum pressure limit is the minimum of the Appendix G limit or the PORV discharge piping structural analysis limit, or the RHR system limit.

FIGURE 3.4

SETPOINT
DETERMINATION
(HEAT INPUT)

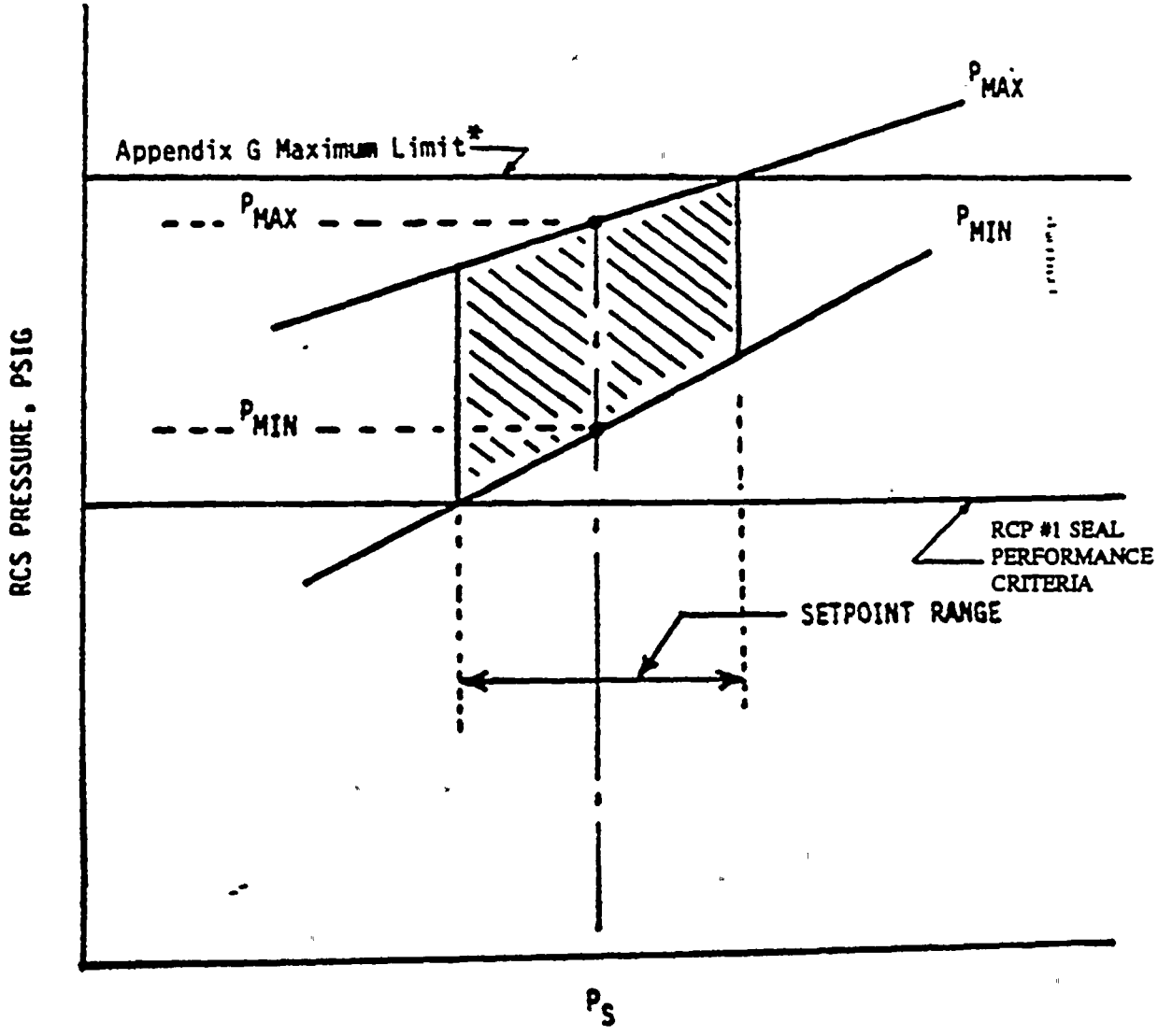

* The maximum pressure limit is the minimum of the Appendix G limit or the PORV discharge piping structural analysis limit, or the RHR system limit

4.0 REFERENCES

1. NUREG 1431, "Standard Technical Specifications for Westinghouse Pressurized Water Reactors", Revision 0, September, 1992.

2. U.S. Nuclear Regulatory Commission, "Removal of Cycle-Specific Parameter Limits from Technical Specifications", Generic Letter 88-16, October, 1988.

3. U.S. Nuclear Regulatory Commission, Radiation Embrittlement of Reactor Vessel Materials, Regulatory Guide 1.99, Revision 2, May, 1988.

4. Code of Federal Regulations, Title 10, Part 50, "Fracture Toughness Requirements for Light-Water Nuclear Power Reactors", Appendix G, Fracture Toughness Requirements.

5. ASME Boiler and Pressure Vessel Code, Section XI, "Rules for Inservice Inspection of Nuclear Power Plant Components", Appendix G, Fracture Toughness Criteria For Protection Against Failure.

6. R. G. Soltesz, R. K. Disney, J. Jedruch, and S. L. Ziegler, Nuclear Rocket Shielding Methods, Modification, Updating and Input Data Preparation. Vol. 5--Two-Dimensional Discrete Ordinates Transport Technique, WANL-PR(LL)-034, Vol. 5, August 1970.

7. ORNL RSIC Data Library Collection DLC-76 SAILOR Coupled Self-Shielded, 47 Neutron, 20 Gamma-Ray, P3, Cross Section Library for Light Water Reactors.

8. ASME Boiler and Pressure Vessel Code, Section III, "Rules for Construction of Nuclear Power Plant Components", Division 1, Subsection NB: Class 1 Components.

9. Branch Technical Position MTEB 5-2, "Fracture Toughness Requirements", NUREG-0800 Standard Review Plan 5.3.2, Pressure-Temperature Limits, July 1981, Rev. 1.

10. ASTM E-208, Standard Test Method for Conducting Drop-Weight Test to Determine Nil-Ductility Transition Temperature of Ferritic Steels, ASTM Standards, Section 3, American Society for Testing and Materials.

11. B&W Owners Group Report BAW-2202, "Fracture Toughness Characterization of WF-70 Weld Material", B&W Owners Group Materials Committee, September 1993.

12. Letter, Clyde Y. Shiraki, Nuclear Regulatory Commission, to D. L. Farrar, Commonwealth Edison Company, "Exemption from the Requirement to Determine the Unirradiated Reference Temperature in Accordance with the Method Specified in 10 CFR 50.61(b) (2) (i) (TAC NOS. M84546 and M84547)", Docket Nos. 50-295 and 50-304, February 22, 1994.

13. Code of Federal Regulations, Title 10, Part 50, "Fracture Toughness Requirements for Light-Water Nuclear Power Reactors", Appendix H, Reactor Vessel Material Surveillance Program Requirements.

14. Timoshenko, S. P. and Goodier, J. N., Theory of Elasticity, Third Edition, McGraw-Hill Book Co., New York, 1970.

15. ASME Boiler and Pressure Vessel Code, Section XI, "Rules for Inservice Inspection of Nuclear Power Plant Components", Appendix A, Analysis of Flaws, Article A-3000, Method For K_I Determination.

16. WRC Bulletin No. 175, "PVRC Recommendations on Toughness Requirements for Ferritic Materials", Welding Research Council, New York, August 1972.

17. ASME Boiler and Pressure Vessel Code Case N-514, Section XI, Division 1, "Low Temperature Overpressure Protection", Approval date: February 12, 1992.

18. Branch Technical Position RSB 5-2, "Overpressurization Protection of Pressurized Water Reactors While Operating at Low Temperatures", NUREG-0800 Standard Review Plan 5.2.2, Overpressure Protection, November 1988, Rev. 2.

19. BWNT, "RELAPS/MOD2, An Advanced Computer Program for Light-Water Reactor LOCA and Non-LOCA Transient Analysis," BAW-10164P-A.